

**INVESTIGATION OF *Pavonia urens* AS A POTENTIAL BIOSORBENT IN
HEAVY METAL REMOVAL THROUGH COMPLEXATION**

BY

SALINA RUTTO

**A THESIS SUBMITTED IN PARTIAL FULFILLMENT OF THE
REQUIREMENT FOR THE AWARD OF MASTER OF SCIENCE DEGREE
IN CHEMISTRY, IN THE DEPARTMENT OF CHEMISTRY AND
BIOCHEMISTRY, SCHOOL OF SCIENCE, UNIVERSITY OF ELDORET,
KENYA**

SEPTEMBER, 2023

DECLARATION

Declaration by Candidate

This thesis is my original work and has not been presented for award of degree in any other University or elsewhere. No part or whole of this thesis may be reproduced without the prior written permission of the author and/or University of Eldoret

Salina Rutto

SC/PGC/037/13

Date

Declaration by Supervisors

This thesis has been submitted for examination with our approval as university supervisors

Prof. Kituyi Lusweti

Date

Department of Chemistry and Biochemistry

University of Eldoret, Kenya

Dr. Martin Wetungu

Date

Department of Chemistry and Biochemistry

University of Eldoret, Kenya

Dr. Ayabei Kiplagat

Date

Department of Chemistry and Biochemistry

University of Eldoret, Kenya

DEDICATION

I dedicate this work to my parents and family.

TABLE OF CONTENTS

DECLARATION	ii
DEDICATION	iii
TABLE OF CONTENTS	iv
LIST OF FIGURES	vii
LIST OF TABLES	ix
LIST OF SCHEMES.....	x
LIST OF ABBREVIATIONS.....	xi
ABSTRACT.....	xiii
CHAPTER ONE	1
INTRODUCTION.....	1
1.1 Background Information.....	1
1.2 Statement of the Problem.....	3
1.3 Justification of the Study	3
1.4 Objectives	5
1.4.1 General objectives.....	5
1.4.2 Specific objectives	5
1.5 Research Questions	5
CHAPTER TWO	6
LITERATURE REVIEW	6
2.1 Sources of heavy metals.....	6
2.2 Harmful effects of heavy metals	6
2.2.1 Selected heavy metals (Zn, Cu and Ni) and their toxicity	7
2.3 Heavy metals pollutants.....	8
2.4 Conventional techniques for removal of heavy metals.....	9
2.5 Removal of heavy metals by plants	10
2.5.1 Phytoremediation	10
2.5.2 Phytoextraction	12
2.5.3 Biosorption.....	14
2.6 Genus <i>Pavonia</i>	17
2.6.1 Ethnomedicinal uses of genus <i>Pavonia</i>	17
2.6.2 Phytochemical Analysis and Biological Activities of Genus <i>Pavonia</i>	18

2.7 <i>Pavonia urens</i>	23
2.7.1 Physical characteristics	23
2.8 Complexation by coordination of heavy metals and functional groups	24
CHAPTER THREE	33
MATERIALS AND METHODS	33
3.1 Materials	33
3.1.1 Reagents/chemicals.....	33
3.1.2 Instrumentation	33
The equipment used for analysis included:.....	33
3.2 Methods.....	33
3.2.1 Plant collection and identification	33
3.2.2 Summary of experimental procedure.....	34
3.2.3 Sample processing	35
3.3 Solvent Extraction.....	35
3.4 Spectroscopic Analysis of the Fractions	36
3.5 Preparation of Metal Aqueous Solution.....	37
3.6 Analysis of complex formation using UV-VIS spectroscopy.....	37
3.7 Biosorption studies using Atomic Absorption Spectrometer.....	38
CHAPTER FOUR.....	42
RESULTS AND DISCUSSION	42
4.1 Fractionation of crude extracts of <i>Pavonia urens</i>	42
4.2 Spectroscopic Analysis of the fractions.....	42
4.2.1 GC- MS.....	42
4.3 UV- VIS analysis of complex formation between heavy metals with <i>Pavonia urens</i> compounds	52
4.4 Biosorption of heavy metals by <i>Pavonia urens</i> using atomic absorption spectroscopy.....	58
4.4.1 Effect on contact time	58
4.4.2 Influence of temperature	61
4.4.3 Adsorption isotherm.....	63
4.4.4 Biosorption thermodynamics	68

CHAPTER FIVE	71
CONCLUSION AND RECOMMENDATION	71
5.1 Conclusions.....	71
5.2 Recommendations.....	72
5.2.1 Recommendation from the study	72
5.2.2 Recommendations for further study.....	72
REFERENCES.....	73
APPENDICES	95
Appendix I: GC-MS Analysis of Fraction 1A	95
Appendix II: GC-MS Analysis of Fraction 2A.....	96
Appendix III: GC-MS Analysis of Fraction3A	97
Appendix IV: GC-MS analysis of Fraction 4A	98
Appendix V: Metal uptake.....	99
Appendix VI: Temperature on adsorption of (a) copper (b) nickel and (c) zinc on <i>Pavonia urens</i> leaves	99
Appendix VII: Adsorption equilibrium isotherms of Langmuir of Cu (II), Ni (II) and Zn (II) ions on <i>Pavonia urens</i>	100
Appendix VIII: Experimental data's adsorption equilibrium isotherms	100
Appendix IX: Adsorption equilibrium isotherms of Langmuir of Cu (II), Ni (II) and Zn (II) ions on <i>Pavonia urens</i>	101
Appendix X: Adsorption equilibrium isotherms of Freundlich.....	101
Appendix XI: Isotherm of Temkin for biosorption of Cu (II), Ni (II) and Zn (II) ions onto <i>Pavonia urens</i> leaves	102
Appendix XII: Similarity Report	103

LIST OF FIGURES

Figure 2.1: The terpenoids from <i>Pavonia genus</i> plants	19
Figure 2.2: The triterpenoids and phenolic compounds from <i>Pavonia multiflora</i> plant	20
Figure 2.3: The volatile oils and sesquiterpenes alcohol found from <i>Pavonia Odorata</i> plant.....	21
Figure 2.4: The anti-oxidative compounds from <i>Pavonia Sepioides</i> plant	22
Figure 2.5: Picture of <i>Pavonia urens</i> plant	23
Figure 3.1: The map of the site where the plant material was collected.....	34
Figure 3.2: Extraction and characterization of crude extract fractions	35
Figure 4.1: Fraction 1A chromatogram	43
Figure 4.2: Fraction 2A chromatogram	44
Figure 4.3: Fraction 3A chromatogram	46
Figure 4.4: Fraction 4A chromatogram	48
Figure 4.5: The proposed compounds present (fractions (1A, 2A, 3A and 4A) in <i>Pavonia urens</i> and possible metal complex structures	51
Figure 4.6: UV/VIS absorption of plant material and Cu^{2+} , Ni^{2+} , Zn^{2+} ions at $c=4 \times 10^{-3} \text{ mol dm}^{-3}$	52
Figure 4.7: UV/VIS absorption spectra of plant material and their copper complexes in a 1:1 ratio $c=4 \times 10^{-3} \text{ mol dm}^{-3}$	56
Figure 4.8: UV/VIS Absorption spectra of plant material and Nickel complexes in a 1:1 ratio $c=4 \times 10^{-3} \text{ mol dm}^{-3}$	57
Figure 4.9: Effects of contact time on metal absorption.....	59

Figure 4.10: Temperature's impact on adsorption of copper (a) nickel (b) and zinc(c) on <i>Pavonia urens</i> leaves	62
Figure 4.11: Data from experimental adsorption equilibrium isotherms.....	63
Figure 4.12: Adsorption equilibrium isotherms of Langmuir for Cu (II), Ni (II) and Zn (II) ions on <i>Pavonia urens</i>	64
Figure 4.13: Adsorption equilibrium isotherms of Freundlich	65
Figure 4.14: Isotherm for Biosorption of Temkin Cu (II), Ni (II) and Zn (II) ions onto <i>Pavonia urens</i> leaves.	66
Figure 4.15: Plot of $\ln K_1$ vs $1/T$ for estimation of thermodynamic parameters.....	69

LIST OF TABLES

Table 2.1: Heavy metals effect on human health.....	8
Table 2. 2: Ethnomedicinal uses of genus <i>Pavonia</i>	18
Table 2.3: Nomenclature of <i>Pavonia urens</i>	24
Table 4.1: Chemical composition of Fraction 1A.....	43
Table 4.2: Chemical composition of fraction 2A.....	45
Table 4.3: Chemical composition of fraction 3A.....	47
Table 4.4: Chemical composition of fractions 4A	48
Table 4.5: Constants of the adsorption isotherm of Cu (II), Ni (II) and Zn (II) on to <i>Pavonia urens</i> leaves	67
Table 4.6: Thermodynamic parameters for adsorption of Cu (II), Ni (II) and Zn (II) on to <i>Pavonia urens</i> leaves	69

LIST OF SCHEMES

Scheme 2.1: Proposed interaction of p-morpholinomethylcalix [4] arene with divalent metal ion, M^{2+}	26
Scheme 2.2: Possible metal complex structure.....	27
Scheme 2.3: Proposed interaction of selective receptors with copper ions	28
Scheme 2.4: Theanine and the suggested Ce (III)-complex formation structure	29
Scheme 2.5: Catechin and the predicted Ce (III)-complex formation structure	29S
Scheme 2.6: Caffeine and the suggested Ce (III)-complex formation structure.....	30
Scheme 2.7: The suggested structure of the Ce (III)-complex formation and theaflavin	30
Scheme 2.8: Quercetin and its possible chelating sites of quercetin with metal ion ...	31

LIST OF ABBREVIATIONS

AIDS	-Acquired Immune Deficiency Syndrome
ATM	-African Traditional Medicine
CC	-Column chromatography
CDC	-Centre for Disease Control
DCM	-Dichloromethane
DMF	- Dimethylformamide
ERK	-Extracellular Signal Regulated Kinases
HB1 _{AC}	-Glaciated Hemoglobin
HCl	-Hydrochloric acid
HIV	-Human Immunodeficiency Virus
IDA	-International Diabetic Association
Kg	-Kilograms
LMCT	-Ligand to metal charge transfer
MeOH	-Methanol
MEPO	-Methanol Extract <i>Pavonia Odorata</i>
mL	-Milliliter
<i>P. urens</i>	- <i>Pavonia urens</i>
PKA	-Protein Kinase A
PPAR	-Peroxisome Proliferation Activated Receptor
ppm	- Parts per million
TLC	-Thin layer chromatography
TMS	-Tetramethyl silane
TNF	-Tumor Necrosis Factor

TZA-Thiazolidine dione

UV-VIS -Ultra-violet - visible spectroscopy

WHO-World Health Organization

Cu -Copper

Zn- Zinc

Ni-Nickel

SDG-Sustainable Development Goal

FT-IR-Fourier Transformed Infra-red spectroscopy

GC-MS-Gas Chromatogram-mass spectroscopy

ABSTRACT

Metal ion-related environmental pollution poses a possible risk to human life. This is a result of various chemical wastes being released into the environment after being treated in an affordable and effective manner. Several herbs have been reported for use in heavy metals removal in wastewater. This study aimed at investigating the phytochemicals present and demonstrating the possible use of *Pavonia urens* leaves as adsorbent material through formation of a complex with selected metals zinc (Zn), copper (Cu) and nickel (Ni) from aquatic environment. The plant was collected from Uasin Gishu County and air dried before crushing. The ground powder was soaked in organic solvents (hexane, ethyl acetate, and acetone) of increasing polarity each for 48 hours followed by filtration and drying. The Four fractions obtained were labelled 1A, 2A, 3A and 4A. The GC-Mass spectrometer (MS) identified compounds with functional groups hydroxyl (OH), amine (-NH), and (-COOH). The ability of *Pavoniaurens* to complex with bimetallic ions in aqueous solution was also investigated using UV-VIS spectrometry. The interaction of these ions with functional groups revealed by UV-VIS analysis showed higher complexation for copper ions and zinc was the least. Plant material containing known concentration of the given metal ions was prepared for analysis at a fixed pH of 6, temperature of 298 K and 300 K, dosage of plant material 1 g and agitation speed at 125 rpm. One gram (1 g) of plant material was introduced to every 100 mL solution. Change in concentration was noted at intervals of 20 minutes using Atomic Absorption Spectrometer (AAS) until the rate of biosorption was constant. With regard to contact time and temperature, the biosorption of Cu (II), Ni (II), and Zn (II) ions on *Pavonia urens* leaves in a batch system was examined. The first step of the biosorption, which was rapid, happened in two stages, with Zn being the least biosorbed while Cu was the most. Compared to the Freundlich and Temkin isotherms, the Langmuir isotherm more closely matched the experimental results. The adsorption reactions were demonstrated to be spontaneous because $\Delta G^0 < 0$, feasible and exothermic ($\Delta H^0 < 0$). *P. urens* contains bioactive species and is a viable alternative as an economical, environmentally friendly biosorbent that may successfully complex with metal pollutants in aqueous solution. As a result, *P. urens* merits exploration in the search for key chemicals in drug discovery as well as for use as an adsorbent.

CHAPTER ONE

INTRODUCTION

1.1 Background Information

A number of toxic substances, mainly metals are found in the environment, such as in water, soils, and rocks, and are also discharged into the surrounding from anthropogenic resources, largely through commercial and industrial activities (Bhagure and Mirgane, 2011; Jaishankar *et al.*, 2014; Masindi and Muedi, 2018). These anthropogenic activities include, but not limited to, farming, urbanization, the discharge of untreated sewage into aquatic environments, and industrial effluents (Bobade and Eshtiagi, 2015; Kahlon *et al.*, 2018; Häder *et al.*, 2020).

Heavy metals, comprising of elements with atomic weight greater than 5g/cm^3 are toxic or poisonous even at low concentrations (Jarup, 2003; Tchounwou *et al.*, 2012). Heavy metals that are frequently found in the environment include copper (Cu), iron (Fe), zinc (Zn), lead (Pb), aluminum (Al), manganese (Mn), cadmium (Cd), arsenic (As), mercury (Hg), chromium (Cr), nickel (Ni), and silver (Ag) (Vetrimurugan *et al.*, 2017; Goyal *et al.*, 2020; Karahan *et al.*, 2020). Trace levels of Zn, Fe, Cu, Mg, and Mn are important in animal and plant life (Chanda *et al.*, 2015; Shukla *et al.*, 2018). Because of their diverse valency, reactivity, ability to produce colorful solutions, strength, and complex creation, among other physical and chemical characteristics, heavy metals have a variety of purposes (Rioux, 2017; Madasamy *et al.*, 2019).

Heavy metals pose a serious hazard to human health since they can enter the body by food, water, or breathing and build up there through biomagnification (Jarup, 2003;

Chen *et al.*, 2009; Rehman *et al.*, 2018). As a result, remediation efforts are required to stop heavy metals from entering the food chain (Sarwar *et al.*, 2017; Yan *et al.*, 2020). Currently, a number of remediation strategies have been developed to reclaim soil contaminated with heavy metals (Hseuet *et al.*, 2010; Liu *et al.*, 2018; Vardhan *et al.*, 2019). These procedures include cementing, ion exchange, chemical precipitation, electro-dialysis, electrolytic extraction, land filling, soil cleansing, solidification, and electric field application (Zvinowanda *et al.*, 2009; Dhaliwal *et al.*, 2020; Rajendran *et al.*, 2022). However, when pollutants are present at low amounts, they are costly and ineffective (Yan *et al.*, 2020).

Plants are used in a technique called phytoremediation to either absorb or remove contaminants from soil or to reduce their bioavailability (Petruzzelli *et al.*, 2013; Parmar and Singh, 2015; Muthusaravanan *et al.*, 2018). Plants can absorb ionic substances from the soil at low quantities via their roots (Arao *et al.*, 2010). Several plant materials have strong coordination bonding capabilities for ions of heavy metal (Gardea-Torresdey *et al.*, 2000). These plants have hydroxyl, carboxylate, and amino groups in their cell walls, which have a strong affinity for ions from heavy metals (Park *et al.*, 2005; Kwon *et al.*, 2007). Heavy metals can be bound to these groups by way of complexing the metal ions in solution with an electron pair (Paul *et al.*, 2017). These methods are cheaper and more efficient than chemical or physical methods, and they reduce chemical and biological sludge. Complex formation and metal recovery is also possible (Gopalakrishnan *et al.*, 2010).

Adsorption via complex formation has been demonstrated to be a more cost-efficient approach for removing metals from aqueous solutions (Wong, 2003). Although activated carbon is the most extensively used adsorbent, its high cost makes it

unsuitable for usage in developing nations (Sajidu *et al.*, 2006). Literature search reveals no known reported work that has been done on complexing metals such as zinc, copper, and nickel with *Pavoniaurens*. The possibility of using *Pavonia urens*, which can be used to compound with heavy metals, as a biosorption option was investigated. Heavy metals are agents that directly or indirectly cause diseases, according to studies, in addition to being pollutants.

1.2 Statement of the Problem

Heavy metal accumulation in soil, water, and air is a global environmental hazard caused by industrialization, urbanization, and mining (Islam *et al.*, 2018; Asgari *et al.*, 2019; Ukaogo *et al.*, 2020). According to reports, heavy metals can lead to physical and mental impairments, decreased IQ, organ dysfunction, neurological illnesses, respiratory infections, gastrointestinal problems, complications for pregnant women, cancer, and even death (Iannitti *et al.*, 2010; Tchounwou *et al.*, 2012; Jaishankar *et al.*, 2014; Vigneri *et al.*, 2017; Fatima *et al.*, 2020). These contaminants damage the immune system, making the body more prone to infections. The majority of research in Kenya has only focused on heavy metal levels in water, soil, air, and food (Akenga *et al.*, 2020; Githaiga, *et al.*, 2021). The removal of heavy metals from contaminated water, soil, and air has, nevertheless, received relatively little study attention. Conventional physical or chemical repair procedures are not cost-effective or eco-friendly, necessitating new alternatives (Aransiola *et al.*, 2019; Yan *et al.*, 2020).

1.3 Justification of the Study

Plants, like *Cannabis sativa* (Ćaćić, *et al.*, 2019), *Nicotiana tabacum* (Evangelou *et al.*, 2007), *Zea mays* (Xiaomei *et al.*, 2005) and *Helianthus annuus* (Zhao *et al.*, 2019),

were demonstrated to successfully phytoextract heavy metal ions in polluted soil. In Kenya, few plant species have been used to remove heavy metals such as bamboo (Bosire, 2014), *Eichhornia crassipes* (Ndeda and Manohar, 2014; Matindi *et al.*, 2022).

Air, water, soil, and occupational pollution threaten human growth (Zhang *et al.*, 2011; Landrigan *et al.*, 2019). The Sustainable Development Goals (SDG) of the United Nations place a heavy emphasis on eliminating environmental pollution (Leal-Filho *et al.*, 2019). SDG 3.9 aims to "significantly reduce the number of fatalities and diseases caused by hazardous chemicals and air, water, and soil pollution and contamination" by 2030 (Zhao *et al.*, 2020). Pollution is also addressed by Sustainable Development Goals 2.4 focuses on enhancing soil quality, SDG 9.4 on clean industrial processes and technology, SDGs 14 and 15 relating to the preservation of water and land, SDGs 12 on ethical production and consumption, and SDG 11 on sustainable urban and rural areas. A clean, safe, and sustainable environment for its residents is what Kenya Vision 2030 aims to achieve by the year 2030. These goals can be achieved through reclaiming of polluted areas. Many methods exist to clean up the environment, but most are expensive and difficult to get optimal results. Complexation is now utilized to remove inert metals and metal contaminants in contaminated water since it is environmentally safe and economically effective. Therefore, there is a need for an effective, affordable, and eco-friendly option to take heavy metals out of polluted sites as an absorbent. The *Pavonia urens* plant was employed in this study because it is commonly used in Kenya's North Rift region to cure diabetes and clean dishes.

1.4 Objectives

1.4.1 General objectives

To investigate *Pavonia urens* as a potential biosorbent in heavy metal removal through complexation

1.4.2 Specific objectives

- (i) To extract and fractionate phytochemicals from the leaves of *Pavonia urens* using different solvents.
- (ii) To characterize the phytochemicals fractions from *Pavonia urens* using GC-MS.
- (iii) To assess complex formation between selected heavy metals (Cu^{2+} , Zn^{2+} and Ni^{2+}) and *Pavonia urens* leaves by analyzing UV-VIS spectroscopy absorption profiles.
- (iv) To demonstrate biosorption capacity of *Pavonia urens* leaves on selected metals (Cu^{2+} , Ni^{2+} and Zn^{2+}).

1.5 Research Questions

- i. Does *Pavonia urens* plant contain phytochemicals?
- ii. What are the structures and functional groups present in fractions obtained from *Pavonia urens* plant leaves?
- iii. Can complexes form between functional groups in *Pavonia urens* plant leaves with heavy metals?
- iv. Is *Pavonia Urens* efficient in removal of heavy metal contaminants from waste water?

CHAPTER TWO

LITERATURE REVIEW

2.1 Sources of heavy metals

According to Gill (2014), a heavy metal is "a metal with a density greater than 5 g/cm³ (that is, a specific gravity greater than 5)". It can also be defined as metallic components that are much denser than water (Sonone *et al.*, 2020). Sources of metals in the land, water, and air, are both natural and man-made (Bradl, 2005). In latest years, ecological and global public health concerns have grown about metal pollution (Tchounwou *et al.*, 2012). Human exposure has grown because of their increased use in industrial, agricultural, residential, and technical applications (Ali *et al.*, 2019).

Among the natural activities that might cause the release of metals from their endemic atmospheres into various environmental sections are volcanic eruptions, the weathering of rocks that contain metal, sea-salt sprays, forest fires, and natural weathering processes (Sonone, *et al.*, 2020; Abdullah-Al-Mamun, 2021). In addition to other forms, heavy metals can also be found in organic molecules, hydroxides, oxides, sulfides, phosphates, and silicates (Porter *et al.*, 2004; Masindi and Muedi, 2018).

2.2 Harmful effects of heavy metals

Heavy metal pollution is a worldwide issue. Plant quality and yield are impacted by pollution of soil with heavy metals, which also changes the size, makeup, and activity of the microbial population (Singh and Kalamdhad, 2011). Heavy metals contribute to soil pollution (He *et al.*, 2015) and harm soil biochemical and biological characteristics. It impacts soil enzymatic activity through altering the enzyme-producing microbial population (Burns *et al.*, 2013). It also disrupts essential

microbial processes and diminishes soil micro-organism population and activity. Long-term heavy metal effects can improve bacterial community tolerance and fungal tolerance, which can help restore damaged environments (Shuaib *et al.*, 2021).

In plants, heavy metals can cause chlorosis, sluggish plant development, yield depression, and reduced nutrient uptake, metabolic abnormalities, and reduced nitrogen fixation in leguminous plants (Kaur and Nayyar, 2013). As the lead (Pb) level increased, the seed germination was increasingly delayed. This may be due to prolonged incubation of the seeds, which neutralized the harmful effects of lead via leaching, chelation, metal binding, or accumulation by microbes. Since heavy metals can easily infiltrate the food chain of an aquatic ecosystem, they are a significant source of pollution in aquatic habitats. Since the majority of heavy metals have extremely harmful effects on a variety of aquatic life, they pose a significant threat to aquatic environments (Valavanidis and Vlachogianni, 2010).

2.2.1 Selected heavy metals (Zn, Cu and Ni) and their toxicity

Heavy metals are of global concern particularly because of their effects on human health. Table 2.1, lists some of the effects on the human health.

Table 2.1: Effects of heavy metals on human health

Pollutants	Major sources	Effects on human health
Zinc	Refineries, brass manufacture, plating, plumbing	Zinc fumes have corrosive effects on skin, cause damage to nervous membrane (Rahimzadeh <i>et al.</i> , 2020)
Nickel	Smelting operations, incinerations of waste and sewage	Oxidative damage to proteins and DNA. Contact dermatitis, asthma, respiratory tract, cancer (Zhou <i>et al.</i> , 2020)
Copper	Electroplating, polishing, operations	Bone health, immune function, cardiovascular risk, alterations in cholesterol metabolism (Kiris & Baltas, 2021)

2.3 Heavy metals pollutants

The term "heavy metals" describes atoms with a large atomic weight that are dangerous at incredibly tiny dosages (Jarup, 2003; Tchounwou *et al.*, 2012). As a result of their interactions with a contaminated environment, humans are exposed to heavy metals in a variety of ways (Khan *et al.*, 2015).

Numerous inorganic pollutants pollute the biosphere, that is, air, water, and soil, causing serious health concerns. A wide range of heavy metals are created as a result

of industrial and home processes, including copper, chromium, nickel, mercury, and zinc (Abdel-GhANI *et al.*, 2017).

Bioaccumulation accumulates these elements in the food chain. Ineffective at low metal concentrations, traditional metal extraction technologies are prohibitively expensive (Hokkanen *et al.*, 2013). Nickel is emitted during smelting, operations, battery manufacturing, and thermal power plants (Rathna *et al.*, 2019). Electroplating, paint manufacturing, wire drawing, copper polishing, and printing are all processes that create copper. Copper is essential for the creation of enzymes, as well as tissue and bone formation (Zofkova *et al.*, 2017).

2.4 Conventional techniques for removal of heavy metals

The conventional processes for extracting metal include chemical precipitation, lime coagulation, ion exchange, reverse osmosis, and solvent extraction (Gunatilake, 2015; Ziarati *et al.*, 2020) all used to remove metal ions. It works by applying a pressure greater than the dissolved solid's osmotic pressure. This method's flaw is its high cost (Liakos *et al.*, 2015).

In electrodialysis, semi-permeable ion selective membranes are used. A voltage connecting two electrodes moves cations and anions. Scattered cation and anion porous membranes form salt cells. Metal hydroxides form and clog the membrane (Sao *et al.*, 2016).

Ultrafiltration is a pressure-driven membrane technique that removes heavy metals. The main disadvantage is sludge build-up. Electrostatic forces exchange metal ions from dilute liquids for ions held on the exchange resin. A high cost and

incomplete ion removal are downsides of this approach. Metals are coagulated with alum, lime, iron salts, and other organic polymers (Din *et al.*, 2021).

The main downside is the large amount of dangerous sludge generated (Cielik, *et al.*, 2015). In phytoremediation, plants remediate contaminated soil, sediment, and water. Disadvantages include long metal removal times and difficulty renewing plants for biosorption (Qasemet *et al.*, 2021). To solve the issues associated with each method, it is necessary to have a low-cost treatment system that can get rid of heavy metals from aqueous effluents (Priya and Arulmozhi, 2012). However, these traditional methods for removing heavy metals from wastewaters frequently are too expensive, inefficient at low metal concentrations, ineffective at removing all of the heavy metals, and they use a lot of energy (Dev *et al.*, 2020). Some of these processes produce hazardous sludge, and disposing makes treatment approaches less technologically and economically viable (Celebi *et al.*, 2020). To have a successful management of toxic heavy metal removal, the search for new technologies has focused emphasis on biosorption, based on the metal-binding abilities of diverse biological materials.

2.5 Removal of heavy metals by plants

2.5.1 Phytoremediation

Detoxification of heavy metals is essential for phytoremediation in which plants can avoid or tolerate heavy metal poisoning (Dalvi and Bhalerao, 2013). By these two methods, plants keep heavy metal concentrations below toxicity thresholds. There are several, phytoremediation cleaning methods available for metal-contaminated soils:

Phytostabilization, which involves using plants to reduce the bioavailability of metals in soil, phytoextraction, which involves removing plants that use soil to remove heavy

metals, phytovolatilization, which involves taking soil-borne heavy metals and releasing them as volatile chemicals, using plants grown in hydroponic systems to filter polluted water, and rhizodegradation are some other examples. Plants' intake of heavy metals is influenced by a number of variables (Tangahu *et al.*, 2011).

Plant species alter chemical absorption. Success of phytoextraction depends on identifying types of plants that hyperaccumulate the production of heavy metals in significant biomass quantities (Jabeen *et al.*, 2009). Agronomic methods (pH correction, chelators, fertilisers) promote remediation (Rathore *et al.*, 2019). Soil pH, organic matter, and phosphorus determine how much metals plants absorb. Soil pH is altered with lime to minimise lead uptake by plants. It can store or metabolize pollutants in plant tissue (Tangahu *et al.*, 2011).

Phytoremediation uses hyper-accumulator plants to extract and concentrate heavy metals (Hamadouche, 2012; Mojiri *et al.*, 2013). Hyper-accumulator plants may store metals 100 times more than regular plants (Khan *et al.*, 2000; Muszynska and Hanus-Fajerska, 2015). These hyper-accumulator species have powerful metal sequestration mechanisms and, sometimes, larger internal metal needs (Mehes-Smith *et al.*, 2013; Kosakivska *et al.*, 2021). It removes heavy metals from a location while maintaining biological activity and soil structure, and bio-recovering metals (Mabhungu *et al.*, 2019).

Another phytoremediation technique involves root-exuded plant enzymes degrading soil pollutants. Increased root diameter and reduced root extension are morphological adaptations to drought (Prakash, 2021). Environment affects the metal uptake. Temperature impacts growth and root length. Field and greenhouse root structures

differ (Shtangeeva, 2010). Understanding mass balance analyses and pollutant metabolism in plants is crucial to showing phytoremediation's applicability (Mwegoha, 2008). The metal's water bioavailability, which is based on its retention time, and interactions with other substances and elements, determines how readily plants may absorb it. When metals are incorporated into soil, the metal's ionic and plant-available form are altered by soil pH, redox potential, and organic matter.

Plants can lower soil pH and oxygenate sediment, which influences metal availability. Heavy metal bioavailability is increased by Chelating agents and micronutrients which are examples of physical substances that decay gradually. Energy crops can better absorb heavy metals by increasing their bioavailability through these chelating agents and micronutrients as well as by encouraging the microbial population around the plant to be more capable of absorbing metal ions (Olaniran *et al.*, 2013). Faster uptake of metal ions will reduce remediation costs. Synthetic chelating agents enhance leaching risk. Chelating compounds in heavy-metal-contaminated soils may enhance leaching. Since heavy metal bioavailability declines above pH 5.5–6, alkaline soils may require a chelating agent (Awa and Hadibarata, 2020).

2.5.2 Phytoextraction

The Greek word "phyto" (plants) combine with the Latin verb "remedium" (to remedy) form the term phytoremediation, which refers to a developing approach for cleaning contaminated environments (Parmar and Singh, 2015). Phytoremediation (or phytotechnologies) is a group of plant-based technologies used to remove pollutants from soil, water, and sediments (Oleksińska, 2015).

Despite being thought of as a revolutionary tactic, phytoremediation, is actually a very old idea., as the Romans reputedly utilized Eucalyptus trees to de-water the waterlogged soils more than two centuries ago (Safford and Vallejo, 2019).

Phytoextraction is a cost-effective, environmentally benign, and cheap method for remediating hazardous metals (Ahmadpour *et al.*, 2012). Phytoextraction uses plants to clean polluted areas. Heavy-metal hyperaccumulating plants are utilized in phytoextraction their shoots may store huge amounts of heavy metals. Phytoextraction can clean soil, sludge, silt, groundwater, surface water, and storm water. Phytoextraction stabilizes and improves soil, prevents pollutant dispersion, and removes heavy metals into plant biomass (Wei *et al.*, 2008). Metal output per area per time is crucial for phytoextraction. This demands great biomass output, quick development, and strong metal buildup in plant tissue, especially above-ground for easy harvesting. Some plants collect and tolerate 100 times more metals than others in their above-ground tissues. (Hyper-)bio indicator plants only do so when metals in the soil solution are bioavailable, other plants species collect metals (Van der Ent *et al.*, 2013).

Several plants species such as *Helianthus annuus* (Alaboudi *et al.*, 2018), *Eucalyptus camaldulensis* (Ebrahimi, 2014), *Cannabis sativa* (Todde *et al.*, 2022), *Nicotiana tabacum* (Novakova *et al.*, 2018) and *Thlapsi caerulensis* (Cristaldi *et al.*, 2020), have been identified to successfully use phytoextraction to remove heavy metals from polluted soil.

Ndeda and Manohar (2014),examined the heavy metals' bioconcentration factor and translocation capacity in Nairobi Dam, Kenya. In both the dry and wet seasons,

Eichhornia crassipes exhibited the highest levels of bioconcentration and translocation.

The study recommends using *Eichhornia crassipes* to remove heavy metals from contaminated freshwater bodies. Kimenyu *et al.* (2009) indicated that *C. bengalensis* has a higher potential for the removal of Cu, Pb, and Cd metals than *Zea mays* and *Amaranthus hybridus*. Orao (2020), demonstrated that *Datura stramonium* and *Ricinus communis* exhibited bioconcentration factor and translocation factor; as a result, these plants are suited for phytoextraction. Oluoch (2018) studied *Cyperus Alternifolius*, *Cyperus Dives* and *Canna Indica* at Flamingo Farm Constructed Wetland, Naivasha Sub-County. These results shows that the studied plants can be used for phytoremediation of Arsenic, Cadmium, and Lead.

2.5.3 Biosorption

Chemicals are removed from solutions through the physicochemical procedure of biosorption, which involves the surface adsorption of a biological substance. In order to eliminate metal ions from aqueous solutions, a variety of waste biomaterials, microorganisms, bacteria, fungi, yeast, and algae have been utilized. Agricultural wastes contain lignocellulosic chemicals as well as they could serve as a source for biosorbents because they contain other polar functional groups such alcohols, aldehydes, carboxylic, ketones, phenolic, thiol, and ether groups (Younas *et al.*, 2021). These groups can complex the metal ions in solution and bind heavy metals by giving a pair of electrons (Demirbas, 2008).

In a study, a biocarbon derived from the healing plant *Tagetes spp.* (Asteraceae) was used in an effort to create an environmentally friendly technology (Singanan and

Peters,2013). The impacts of pH, contact time, starting metal ions concentration, and biocarbon dosage, are key factors in the biosorption of heavy metals (Wiśniewska *et al.*, 2021).

The percentages of Pb (II) and Cr (III) ions removed from synthetic wastewater were 94.8 and 95.4, respectively (Każmierczak *et al.*, 2021; Debnath *et al.*, 2021). These results were seen at an equilibrium period of 150 minutes and an optimal dosage of 2.5g bio- carbon. The most important factors affecting the removal of heavy metal ions from wastewater are the pH of the synthetic wastewater and the dosage of biosorbent. The main mechanisms include ionic interactions and poor surface adsorption on the biosorbent material (Singanan and Peters, 2013).

There have already been numerous studies that mention *M. oleifera's* capacity to remove heavy metals. Using unaltered *M. oleifera* seeds, some studies have reported removing 92 percent of the lead, while others have reported removing 81 percent of the lead (Sajidu *et al.*, 2005; Aziz *et al.*, 2015). In another study, the elimination of zinc by *M. oleifera* biomass has been observed to be 90 % (Bhatti *et al.*, 2007). Additionally, the ability of *M. oleifera* parts like the husk, seeds, and pods to biosorbently remove lead from contaminated water has been determined and literature has, respectively, shown efficiencies of 98.3, 99.4, and 96.6 % (Tavares *et al.*, 2017). In another study, chemically altered *M. oleifera* leaves have been utilized for lead removal, which produced 91 % efficiency (Reddy *et al.*, 2010). There has also been use of unaltered *M. oleifera* leaves to successfully remove lead from contaminated water, with a reported removal effectiveness of 98.6 % at a high lead concentration

(160 ppm) (Imran *et al.*, 2019). Positively charged heavy metals have a strong attraction for these sorbents (Kwon *et al.*, 2007; Park *et al.*, 2005).

Pavonia urens tree, is readily available practically everywhere, and is used in washing utensils (Kamau, 2018). The significant properties of *P. urens* leaves were analyzed in this current study and used in the adsorption process for the cleanup of heavy metals.

The removal of heavy metals from wastewater is very effective when done through biosorption, which uses non-growing biomass. Another study examined how well Periyakulam-2 (PKM-2) type *Moringa Oleifera* leaves (MOLs) could absorb Pb (II) and Zn (II) ions from an aqueous solution (Jayan *et al.*, 2021). To obtain maximum metal removal effectiveness of lead and zinc metals using the PKM-2 MOL biosorbent, a series of factors, including the metal ion starting concentration, adsorbent dose, and pH, were optimized using the response surface methodology (Alara *et al.*, 2017).

Different isotherms and kinetic models were used to investigate the adsorption findings.

Langmuir's isotherm was found to have the best fit and greatest adsorption capacity for lead and zinc, respectively, at 51.71 and 38.50 mg/g (Hafshejani *et al.*, 2015; Mwandira *et al.*, 2020). The kinetics of lead and zinc metal adsorption were found to be consistent with the pseudo-second-order model (Zhou *et al.*, 2020). Thermodynamic parameters confirmed ($\Delta G^\circ < 0$, $\Delta H^\circ < 0$ and $\Delta S^\circ > 0$), demonstrated the exothermic, spontaneous, and adsorption-friendly physisorption was the sorption process (Ofudje *et al.*, 2021). The findings of this investigation revealed that the PKM-2 type MOL is a potential choice for an environmentally friendly, low-

cost biosorbent capable of effectively removing Cd, lead and zinc metals from aqueous solutions.

2.6 Genus *Pavonia*

Pavonia includes perennials, prostrate plants, erect shrubs, and small trees (Githitho, 2021). In disturbed areas like roadside ditches and abandoned croplands this *Pavonia* species develops as a shrub (Lopes *et al.*, 2016).

2.6.1 Ethnomedicinal uses of genus *Pavonia*

Genus *Pavonia* have previously been put to many uses. The different parts have traditionally been used for some particular purposes as shown in the Table 2.2.

Table 2. 2: Ethnomedicinal uses of genus *Pavonia*

Part	Ethnos medicinal Use of genus	Reference
<i>Pavonia</i>		
<i>Pavonia urens</i> : stem, bark, leaves and roots	Making baskets, roofing, fuel, cattle feed, cleaning hands and utensils, wiping infant faecal matter. Leaves to pat eyes in case of weak eye sight, dressings on fractures and dislocations, antidiarrheal, nausea and vomiting, antipyretic and as oxytocic.	(Githitho, 2021; Sarvalingam <i>et al.</i> , 2017)
<i>Pavonia zeylanica</i> : leaves	Anthelmintic, anti-inflammatory, analgesic and antipyretic drug	(Githitho, 2021)
<i>Pavonia odorata</i>	Diuretic diaphoretic, demulcent, anti-inflammatory, antipyretic and astringent.	(Kashima, Paladino & Margetts, 2014)
<i>Pavonia senegalensis</i> L.	Antidiarrheal, soft and tissue infections, Induction of labor and contraception.	(Adebisi & Alebiosu, 2014)

2.6.2 Phytochemical Analysis and Biological Activities of Genus *Pavonia*

Pavonia Genus has been known to contain terpenoids (mostly), triterpenoids, and sesquiterpenes (Masoko and Makgapeetja, 2015). The terpenoids include citral (27), menthol (28), camphor (29), salvinorin-A (30), the cannabinoids (31), ginkgolide (32), and bilobalide (33), curcuminoids found in turmeric and mustard seed (Nayaket *al.*, 2021). Figure 2.1 shows some of the terpenoids found in pavonia plants.

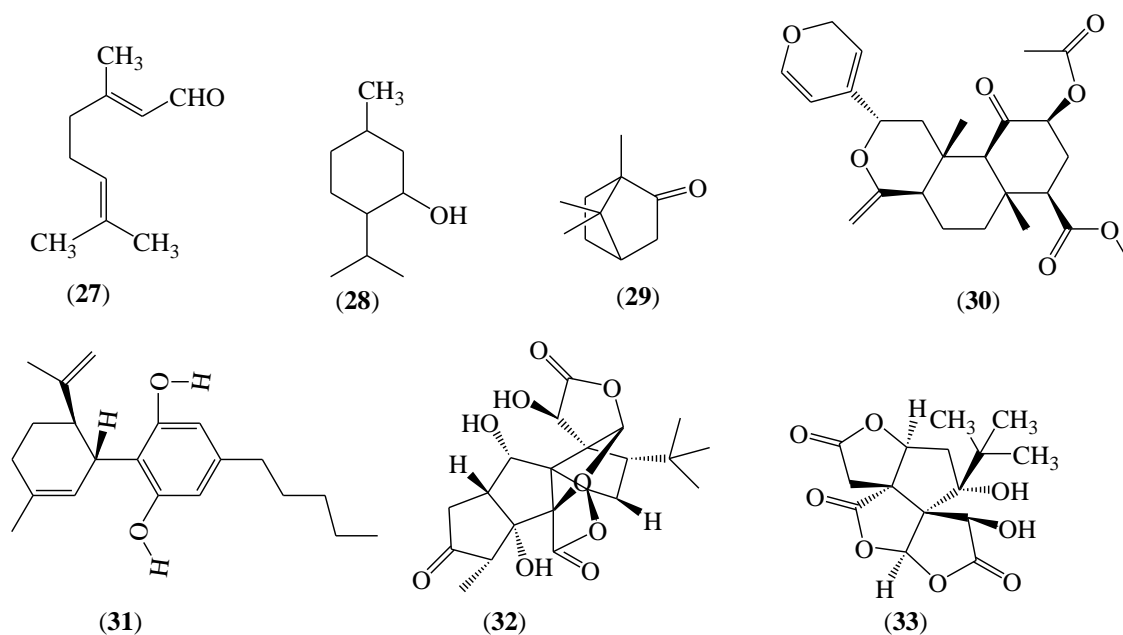
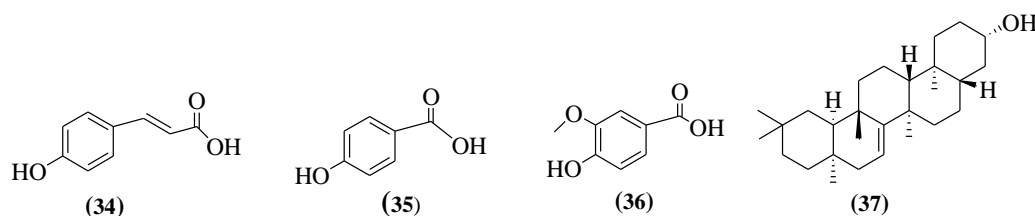


Figure 2.1: The terpenoids from *Pavonia* genus plants(Albuquerque *et al.*, 2022)

A phytochemical study of *Pavonia multiflora* ethanolic extract from the leaves led to isolation of esterified derivative of triterpenoids taraxerol p-methoxy benzoate, including four phenolic compounds; p-hydroxybenzoic acid (34), p-coumaric acid (35), vanillic acid (36) and ferulic acid (37) and five terpene derivatives; oliolide, vomifoliol (38), 4,5-dihydroblumenol A (39), 3-oxo- α -ionol(40) and blumenol C (41) (Lopes *et al.*, 2016). Figure 2.2 shows some of the terpenoids and phenolic compounds found in *p. multilora*.



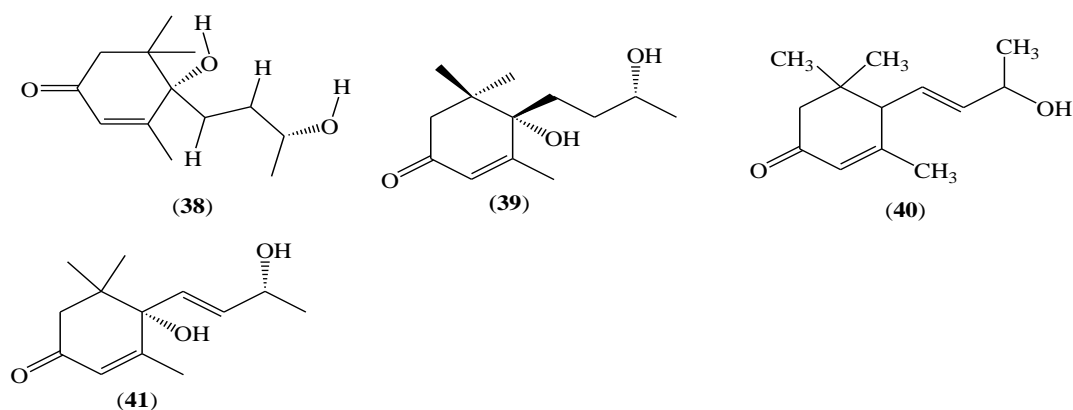
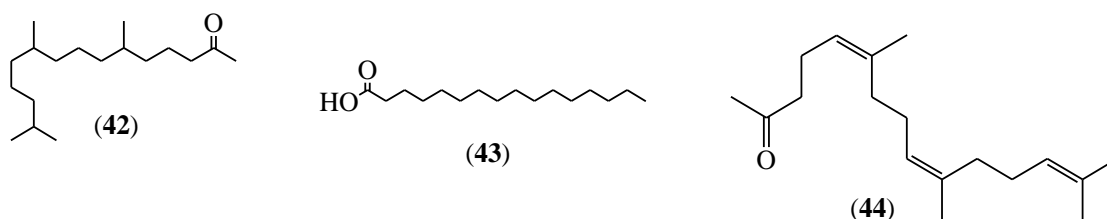


Figure 2.2: The triterpenoids and phenolic compounds from *Pavonia multiflora* plant(Mus *et al.*, 2022)

GC-MS analysis of volatile oils from *Pavonia odorata* aerial parts revealed ageratochromene (42), palmitic acid (43), hexahydro farnesyl acetone (44), -eudemon (45), and -caryophyllene oxide (46)-caryophyllene oxide's volatile oil aroma components were found (*E*)-pinocarveol (47), 3-butylpyridine (48) and 2-nonanone (49). Additionally, pavonenol,(50) (C₁₅H₂₄O) a sesquiterpene alcohol, was said to be present in *Pavonia odorata* (Masoko and Makgapeetja, 2015). Figure 2.3 shows some of the volatile oils and sesquiterpenes alcohol found in *Pavonia Odorata* plant.



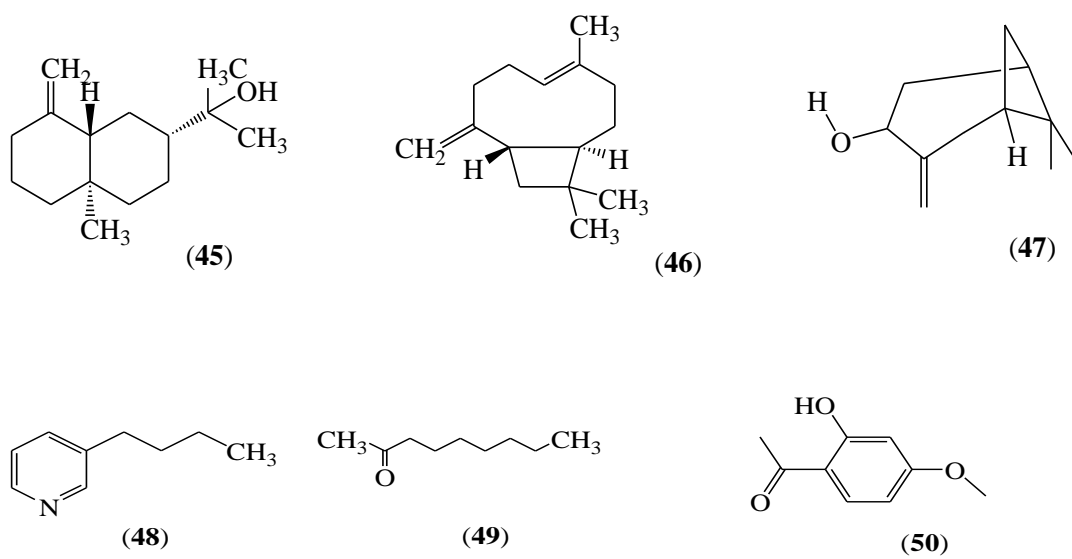


Figure 2.3: The volatile oils and sesquiterpenes alcohol found from *Pavonia Odorata* plant (Fahim *et al.*, 2017)

A study of the antioxidant activity of *Pavonia sepioides* revealed the presence of low molecular weight phenolic compounds such as salicylic acid(51), cinnamic acid(52), *p*-hydroxybenzoic acid (53), *p*-hydroxyphenylacetic acid (54), *p*-hydrocinnamic acid(55), vanillic acid(56), gentisic acid(57), *P*-cinnamic acid(58), protocatechilic acid(59), syringic acid(60), ferulic acid(61) and caffeic acid(62) (Gasca *et al.*, 2013). Figure 2.4 shows some of the anti-oxidative compounds from *Pavonia Sepioides* plant.

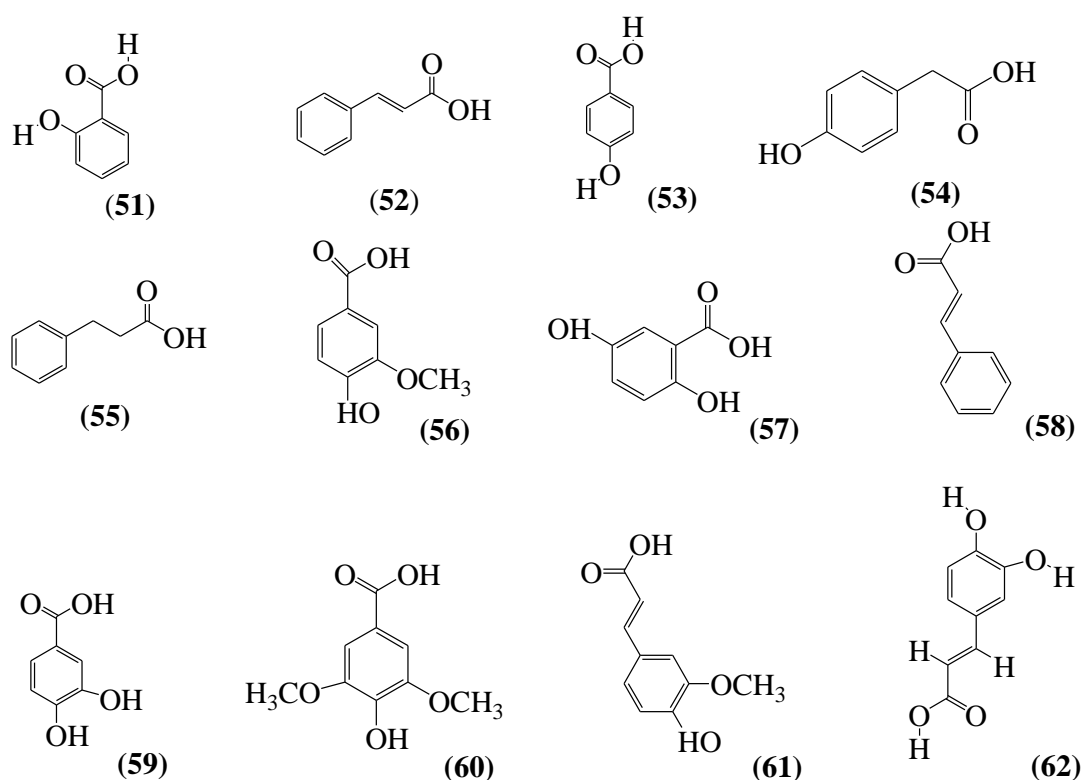


Figure 2.4: The anti-oxidative compounds from *Pavonia Sepioides* plant

(Gasca *et al.*, 2013)

Phytochemical investigation on *Pavonia zeylanica* demonstrated that the plant is a significant source of water-soluble polyphenols, including flavonoids (Shrivastava, 2010). To determine its pharmacological activity, an aqueous extract of *Pavonia zeylanica* leaves was tested on alloxan hyperglycemic rats. The main chemical elements of the extract were flavonoids and tannins (Shinde and Mulay, 2015).

The landmark finding that is very relevant for this work is that the structures of *Pavonia* have functional groups with lone pairs that have the potential to complex with heavy metals.

2.7 *Pavonia urens*

Figure 2.5 shows *pavonia urens* under study that belongs to genus *pavonia* and Malvaceae family.



Figure 2.5: *Pavonia urens* plant

2.7.1 Physical characteristics

A huge shrub-sized herb known as *Pavonia urens* has up to three large, variable; 3-5 lobed leaves 6–12 lines on the epicalyx bracts (de Boer *et al.*, 2005). Table 2.3 shows the nomenclature of *Pavonia urens* plant.

Table 2.3: Nomenclature of *Pavonia urens*

Group	<i>Dicot</i>
Family	<i>Malvaceae</i>
Genus	<i>Pavonia</i>
Species	<i>Pavonia urens</i>

Also called flora of Zimbabwe, stinging *Pavonia* (Sseruwagi *et al.*,2005). Other names;

Kalenjin-*motosiet*

Kikuyu- *maigoya*

Luhya- *Kiroga*

2.8 Complexation by coordination of heavy metals and functional groups

Complexation is the process by which two or more species become one. Between the metal ion and the ligands, mononuclear complexes occur. The polynuclear complex contains several metal ions, each with a positive charge. Desorption of adsorbed metal ions and regeneration of numerous bio sorbents are easy with the polynuclear complex. This is because the biomass cell wall contains functional groups such as amine, carboxyl, hydroxyl, phosphate, and sulfhydryl (Dey *et al.*, 2021).

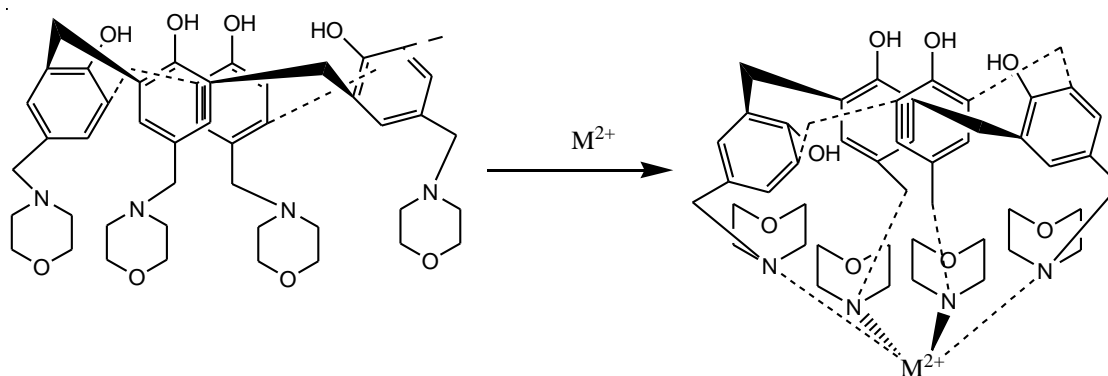
Thus, coordination complexation involves two electron transfers from ligand to metal ion (Khare *et al.*, 2021). This experiment investigated plant molecule coordination via a coordination complexation mechanism. Chemistry of metal ions involved reacting with ligands (neutral or negatively charged compounds). A metal complex or

coordination compound is the consequence (Dinu and Shkinev, 2020). The metal ions, ligand type, ligand combination, shape, and bond angle all affect the coordination compound's character (Liu *et al.*, 2014). Electron paramagnetic resonance (EPR), UV-visible and infrared (IR) studies can be used to analyse complex chemical synthesis in plants and metal ions with d-electron and their coordination modes (Zabizak *et al.*, 2021).

The ideal conditions for UV-VIS measurements on systems can be determined (Mocanu *et al.*, 2021). For instance, the spectroscopic research on complex formation in systems containing L-tartaric acid or L-malic acid and divalent metal ions of copper (II), cobalt (II), and nickel (II) has been done by (Zabizak *et al.*, 2021). They used UV-VIS spectroscopy to confirm metal ion coordination with plant ligand complexes. To test their hypothesis, they employed a shift in absorbance, toward shorter wavelengths. To them, differences in spectrum features are produced by oxygen in -hydroxy acid molecules bonding to copper (II).

There were no significant wavelength changes at maximum absorption to longer wavelengths in complexes with fully deprotonated acids in systems including cobalt (II) ions. Nickel (II) ions complexed with L-tartaric and L-malic acids showed a modest blue shift. Their results show that adding L-tartaric and L-malic acids to metal ions affects the internal coordination sphere due to complexation. The spectra show that adding copper, nickel, and cobalt salts to the ligand solution adds new bands. The bands show that plant ligands can interact with metal ions (Qureshi *et al.*, 2009). Cu^{2+} absorbs the most.

Complexation occurs in an environment where cation–lone pair interactions favour complication with more polarizable transition metal ions (Mocanu *et al.*, 2021). Reddy proposed that the strong red-shift in wavelength is attributed to the cation–lone pair interactions as proposed in Scheme 2.1.



Scheme 2.1: Proposed interaction of p-morpholinomethylcalix [4] arene with divalent metal ion, M^{2+}

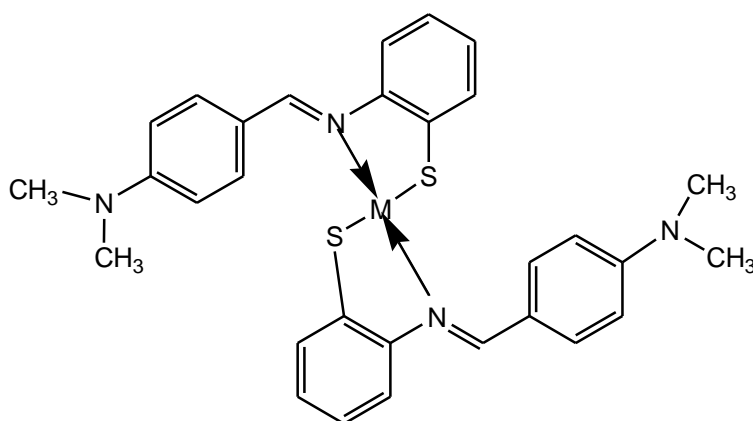
Its improved metal ion extraction capability may be due to its four nitrogen - containing binding sites aligning with the metal ion's square planar geometry, according to scheme 2.2. The delicate nature of the nitrogen-metal ion connection allows for better interaction (Qureshi *et al.*, 2009).

Lewis's acid is a metal ion that can accept electrons from Lewis's base ligands (Doddi *et al.*, 2019). The steric barrier caused by the arene's staggered conformation has changed the geometry of the arene with the metal ion (Bickelhaupt and Baerends, 2003).

The colorimetric chemosensor 1-(2-thiophenylimino)-4-(N-dimethyl) benzene (SL1) was synthesized and tested. In addition, it has azomethine ($>C=N-$) and thiol ($-SH$) the molecules that can create metal complexes. In a solution of water and

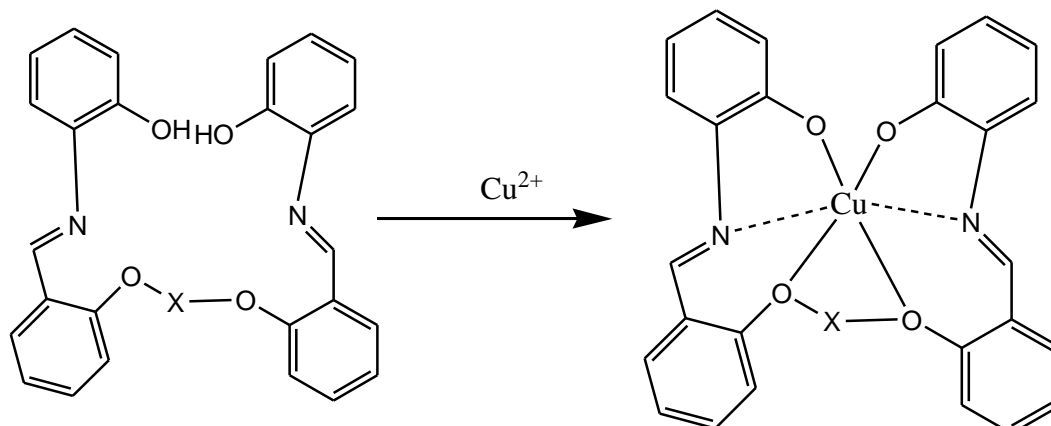
dimethylformamide, the sensing capabilities of Cu^{2+} , Ni^{2+} and Zn^{2+} metal ions were examined (DMF).

The Schiff base ligand showed colorimetric properties with metal ions, resulting in a different colour shift for each metal. This charge transfer occurred when the ligand was introduced to the metal ions, as shown by the strong red shift (69–288 nm) in the UV–vis spectra (LMCT). The UV–VIS spectra revealed a large red shift (69–288 nm) from the origin when the ligand was added to these metal ions, which could be attributed to charge transfer from the ligand to the metal (LMCT) (Alorabi *et al.*,2020) as proposed in the scheme 2.2.



Scheme 2.2: Possible metal complex structure

Another study tested the ability of cation receptors to perceive transition metal ions calorimetrically. An apparent colour change (from colourless to yellowish brown for Cu^{2+}) and UV–vis absorption spectrum shift occurs quickly when metal ions are introduced to these sensors' methanol solutions. Cu^{2+} ions boosted colour change and receptor binding ability more than other ions, according to ocular and UV–VIS spectral changes(Gupta *et al.*, 2013), as shown in the scheme 2.3.



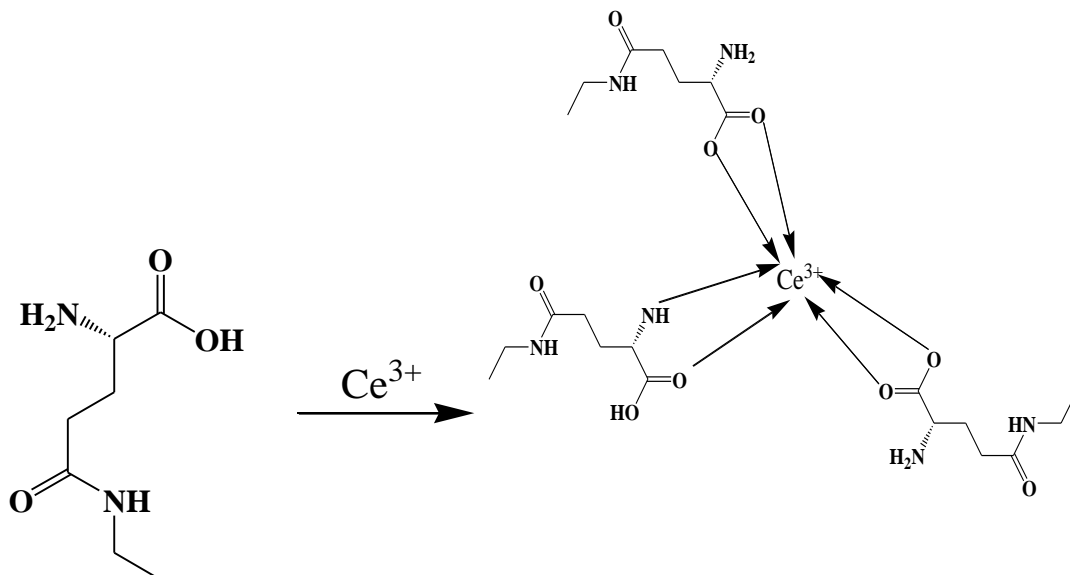
Scheme 2.3: Proposed interaction of selective receptors with copper ions

Prior to this, Drynan *et al.*, (2010), established the synthesis of Ce (III)-complexes from black tea extract solution, which was characterised by Fourier Transformed Infra-red spectroscopy (FT-IR). The studies showed that cerium cations and polyphenols worked together. A wide band at 3401 cm^{-1} was linked to polyphenol O-H and N-H stretching modes (Senthikumar and Sivakumar, 2014).

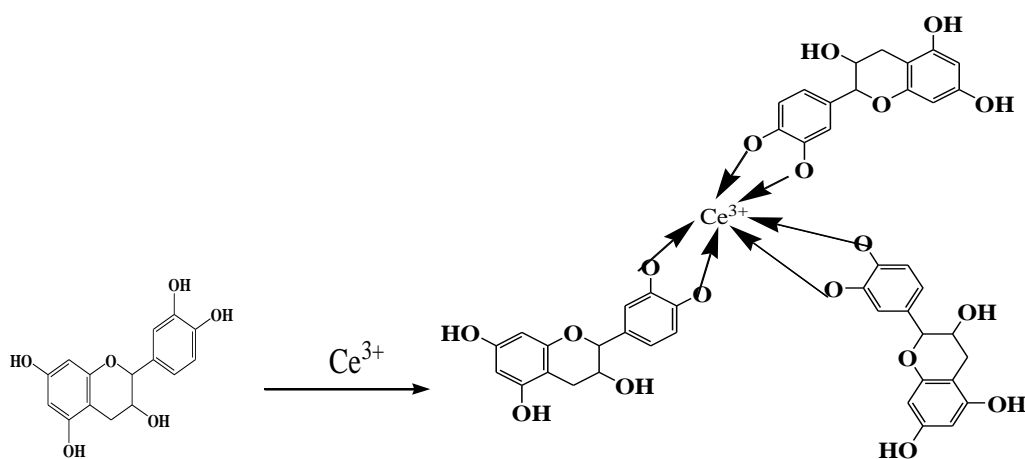
Significant bands at 3310.7 cm^{-1} and 1628 cm^{-1} , both related with hydroxyl (OH) functional groups were detected and found in aldehydes and phenols, and C=C bond stretching in aromatic ring compounds (Saif *et al.*, 2016). The C-O stretching in amino acids created another band at 1029 cm^{-1} (Dubey *et al.*, 2017). The FT-IR bands at 3388 cm^{-1} , 1636 cm^{-1} , and 1039 cm^{-1} are related to the O-H/N-H, C=C, and C-O-C strains, respectively (Cai *et al.*, 2015). These are the main functional groups in tea extract.

With metal cations, these functional groups form metal complexes (Wu *et al.*, 2010).

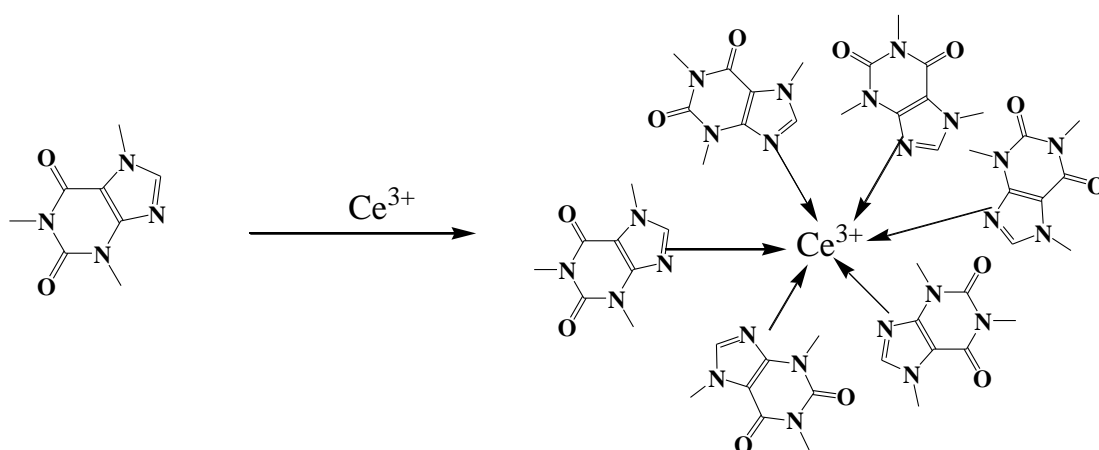
Theanine, catechin, caffeine, and theaflavine are all trivalent ions found in tea extract solution represented by Schemes 2.4-2.7



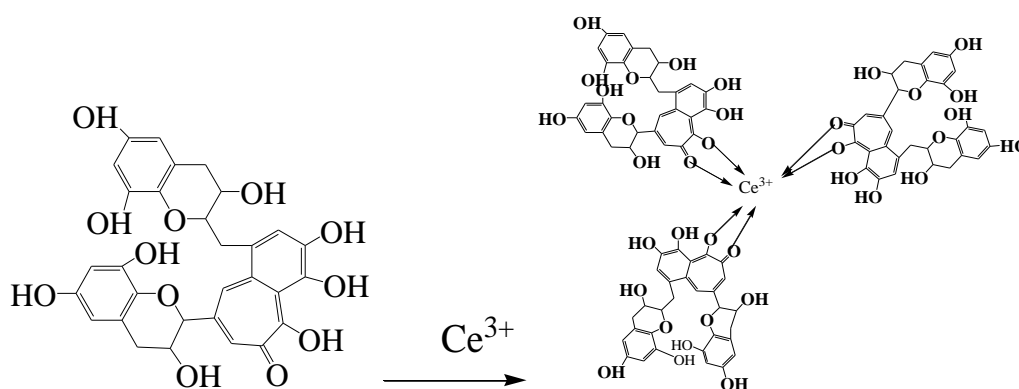
Scheme 2.4: Theanine and the suggested Ce (III)-complex formation structure



Scheme 2.5: Catechin and the predicted Ce (III)-complex formation structure



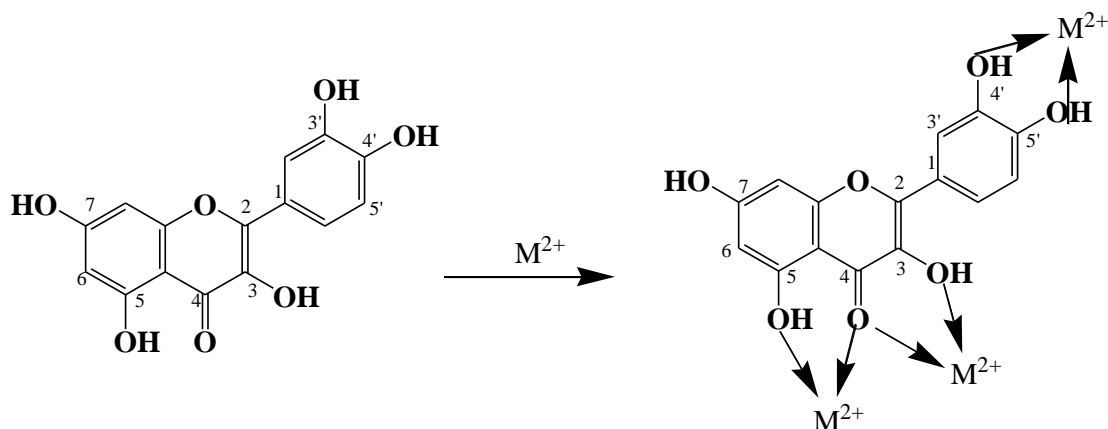
Scheme 2.6: Caffeine and the suggested Ce (III)-complex formation structure



Scheme 2.7: The suggested structure of the Ce (III)-complex formation and theaflavin

Another study found quercetin, a flavonoid, had hydroxyl, carbonyl, and ether groups (Corradini *et al.*,2011). The UV-VIS and FT-IR experiments looked at the binding sites and coordination characteristics of metal-quercetin complexes. The UV-VIS spectra of quercetin in methanol revealed absorption bands at 376 nm and 260 nm corresponding to $n \rightarrow \pi^*$ and $\pi \rightarrow \pi^*$ transitions. The metal quercetin compound showed a 376 nm absorption band transition, indicating a redshift (Zhang *et al.*,2019).From 1662 to 1653 cm^{-1} with the addition of metal ions, the FT-IR spectra shown. This change confirmed metal-oxygen cooperation (Alugaju *et al.*,2019).Peaks at 1541 and 1373

cm^{-1} are linked to binding site vibrational modes of the C-O group. Peaks at 1662 and 1274 cm^{-1} correspond to C=C and C-O-C bond stretching, slightly displaced due to metal complex production (Lakshmi *et al.*, 2019) as shown in the scheme 2.8.



Scheme 2.8: Quercetin and its possible chelating sites of quercetin with metal ion

The absorption spectra of phenols depend on steric effects, intra- and intermolecular H-bonding, and electron-withdrawing and electron-donating substituents in the benzene ring (Mathiyalagan and Mandal, 2020). A case at hand of quercetin scheme 2.8, showed the possible chelating sites at OH of C3, C5, C3' and C4' but not OH at C7. This is due to steric hindrance, which is greater at C7 than at C3, C5, C3' and C4'. The epoxy also plays a role of steric hindrance because of the bulkiness of the groups at the atoms. This may slow or prevent reactions at the atom (Grzelczak *et al.*, 2012). This is evident in scheme 2.1, where steric hindrance is responsible for the observed shape and geometry of the compound. Bulky groups exert substantial repulsion against the incoming reactant, resulting in steric strain (Pinter *et al.*, 2012).

In scheme 2.2, the amino group bonded to two methyl groups makes the compound stable and no reaction takes place through these groups because the methyl groups are bulky. They are larger than the hydrogen atom. Trans-orientation produces a more

stable product due to steric hindrance which causes limitations of the substituents. Unlike the case in scheme 2.1 the cis-molecule, the OH and epoxide the substituent repels each other because of molecule interactions (Mathiyalagan and Mandal, 2020). This is also evident in scheme 2.6. Complexation using *Pavonia urens* as a plant material provides an opportunity to explore adsorption of metal ions hence their removal from the environment.

CHAPTER THREE

MATERIALS AND METHODS

3.1 Materials

3.1.1 Reagents/chemicals

Sulphuric acid, acetic acid, ethanol, distilled water, n-hexane, concentrated hydrochloric acid, chloroform, acetone, ethyl acetate, NaOH, HNO₃ and methanol. The chemicals were purchased at Chemo-quip Kenya and were of analytical grade.

3.1.2 Instrumentation

The equipment used for analysis included:

GC-MS (Turbo mass model 20141128), UV-VIS spectrophotometer (Shimadzu, UK), Absorption Spectrophotometer Model SPECTRA AA – 200 (Varian, Australia).

3.2 Methods

3.2.1 Plant collection and identification

The plant material was collected in the environs of University of Eldoret, Uasin-Gishu county of Rift Valley region as shown in figure 3.1. The geographical coordinates of the collection area were 00 35⁰ 30⁰ North, 35⁰ 19⁰ 00⁰ East. Fresh plant was picked and taxonomically identified at the Department of Biological Sciences Herbarium, University of Eldoret. The voucher specimen HM 2020/01 was deposited appropriately for future references.

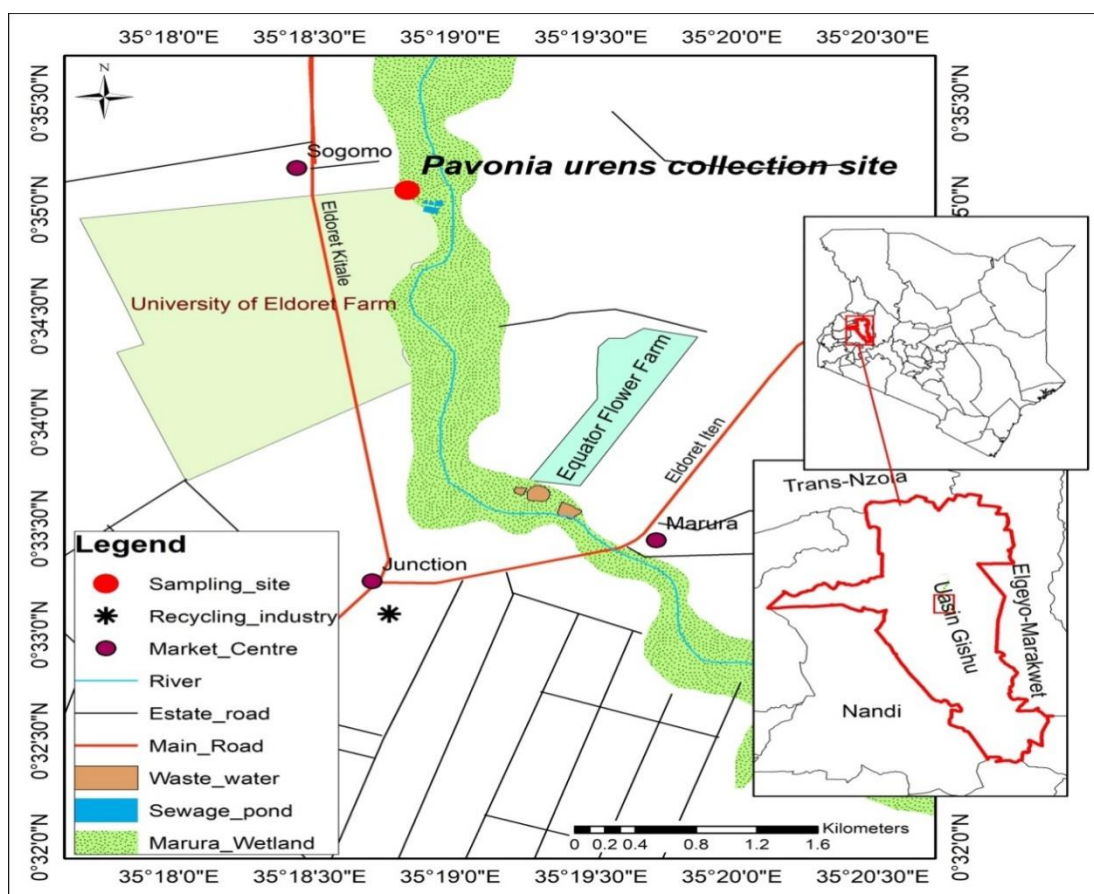


Figure 3.1: The map of the site where the plant material was collected (Achieng *et al.*, 2017)

3.2.2 Summary of experimental procedure

This is the schematic flow chart that was followed in extraction, fractionation and characterization of plant material fractions.

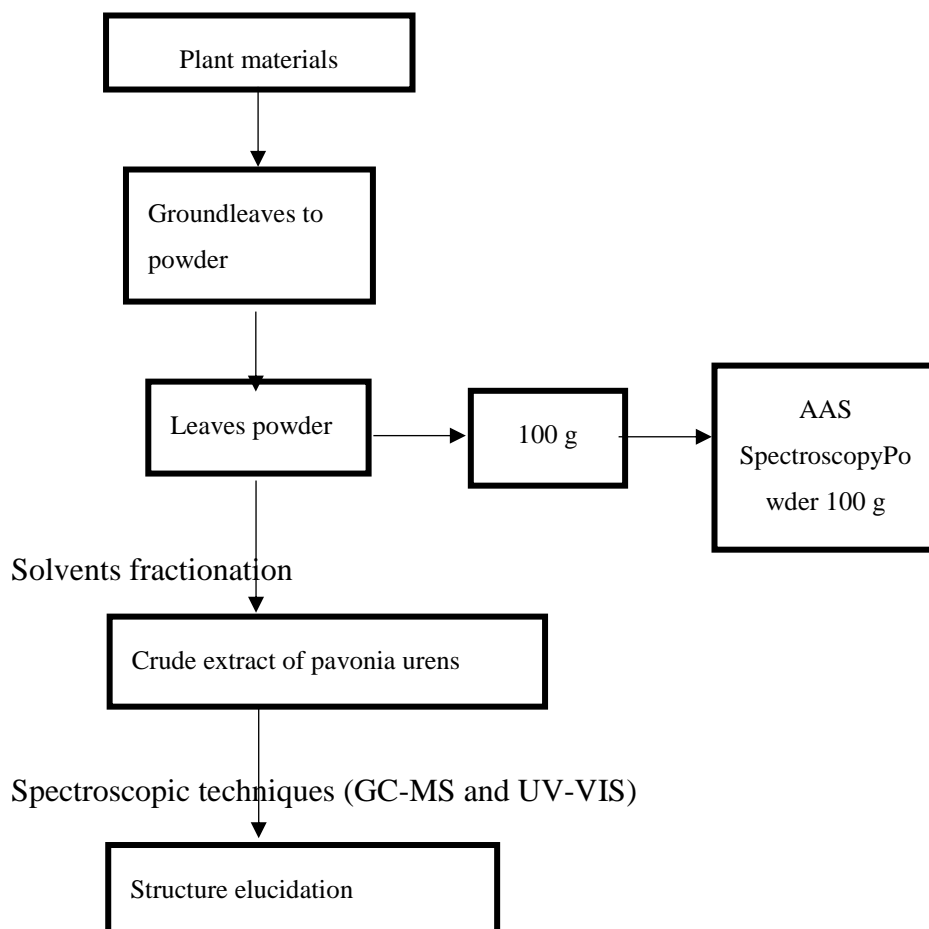


Figure 3.2: Extraction and characterization of crude extract fractions

3.2.3 Sample processing

The leaves of the plant were washed and weighed before air drying for 2 weeks to remove water completely. Its weight was taken again after grinding into fine powder so as to increase the surface area of the sample and enhance the contact between the solvent and the sample.

3.3 Solvent Extraction

Two kilogrammes of leaves plant material were ground into fine powder using an electric grinder, and then extracted for 72 hours using increasing polarity solvents starting with hexane, dichloromethane, ethyl acetate, acetone and methanol. The

extract was decanted and filtered with Whatman filter paper then concentrated and solvents were recovered on a rotator evaporator (Buchi Rotavapor R-205, England).

Percentage yield of *Pavonia urens* extracts was determined by using Equation 1.

$$\text{Percentage yield} = \frac{W_2 - W_1}{W_0} \times 100 \dots\dots\dots (\text{Equation 1})$$

where,

W_0 : The weight of the initial dried sample.

W_1 : The weight of the container alone

W_2 : Weight of the extract and container

3.4 Spectroscopic Analysis of the Fractions

The solvent fractions were subjected to spectroscopic analysis and compared with the spectral data reported in literature. The GC-MS analysis was performed on a Turbo mass model 20141128. Oven initial temperature was 200°C for 1 min, ramp 15 °C/minute to 300 °C. Carrier gas was He, solvent delay was 2.10 min, transfer temperature was 200 °C, source temperature was 180°C, and scan was 45 to 800Da, column measurements were 30.0m by 250µm. Identification was based on sample condition data.

The GC indicated the relative concentrations of various compounds which were eluted at different retention times. Mass spectrometer analyzed eluted compounds at different times identifying the structures and nature of the compounds.

For the UV- visible Spectrophotometer, dry fraction weighing 2 g of the fraction was mixed with 100 mL distilled water to dissolve it and 2 mL was placed in a cuvette in every analysis. The samples were scanned at the range of 220-500nm to detect its characteristic wavelength of absorption.

3.5 Preparation of Metal Aqueous Solution

Stock Zn (II) having concentrations 1000mg/L was prepared by dissolving 4.40 g of zinc sulphate in 100 mL and diluting quantitatively to 1000 mL. To this stock solution 100 ppm was prepared of which 2 mL in every analysis was used. A similar procedure was adopted for the preparation of copper chloride (2.70 g) and nickel chloride (4.10 g). The equation 2 was used;

$$q = \frac{(C_0 - C_c)V}{1000w} \dots \dots \dots \text{Equation 2(Ali \& Seng, 2018)}$$

where,

v-is the volume of the solution in mL

w- is the mass of the substance in g.

C_c- initial metal ion concentration (mg/l)

C_o-final metal ion concentration (mg/l)

3.6 Analysis of complex formation using UV-VIS spectroscopy

Two (2 g)ofthe dried plant material samples (that had already been prepared) were combined with 100 mL of distilled water, vigorously agitated for 10 minutes, and then filtered using Whatmann filter paper.

The samples were scanned at the range of 250-500 nm to detectcharacteristic wavelength. Other measurements included spectrum observation for free single metals and plant materials that is Zn (II) and plant material, Cu (II) and plant material and Ni (II) and plant material. Then the combinations of ions with plant materials followed.

Part 1: Analysis of plant with metal ions separately,

Zn^{2+} + plant

Cu^{2+} + plant

Ni^{2+} + plant

Part2: Analysis of:

(Cu^{2+} + plant) followed by Ni^{2+}

Ni^{2+} (Cu^{2+} + plant) followed by Zn^{2+}

Zn^{2+} (Cu^{2+} + plant) followed by Ni^{2+}

Part 3: Analysis of:

(Ni^{2+} + plant) followed by Zn^{2+}

(Ni^{2+} + plant) followed by Cu^{2+}

Cu^{2+} (Ni^{2+} + plant) followed by Zn^{2+}

3.7 Biosorption studies using Atomic Absorption Spectrometer

To change the pH to the necessary whole number value of 6, a diluted solution of 0.1 M HNO₃ and 0.1 M NaOH was used. Before measuring biosorption, the absorbance of known standard solutions of each metal ion was established in order to create calibration graphs. 1 g of *Pavonia Urens* was added to the contents of each plastic bottle, which had a pH of 6, and was periodically shaken before being allowed to settle before readings of absorbance were taken. To determine the concentration using AAS (SPECTRA A A-200, Varian, Australia), a 5 mL solution was extracted.

Over the course of 120 minutes, metal concentrations were assessed every 20 minutes. *Pavonia* performed mixed metal ion biosorption at pH 6. By deducting the leftover concentrations from the initial values and dividing by the initial metal concentration values for each metal (mg/L), the concentration of metal ions that were biosorped was

calculated. Equation 3 was used to compute absorption by comparing changes in concentration over time to changes based on maximum biosorption.

$$q_e = \frac{C_i - C_f}{C_i} \dots\dots\dots\text{equation 3, (Vijayaraghavan } et al., 2016)$$

where,

q_e = metal sorption capacity (mg/L)

C_i = initial metal ion concentration (mg/L)

C_f = final metal ion concentration (mg/L)

Adsorption equilibrium studies were used to look at the adsorption potential of *Pavonia urens* leaves. In this study, the concentration of metal ions in solution and the amount of Cu, Ni, and Zn ions absorbed by *Pavonia urens* leaves (q_e) were studied. Equations 4 and 5 were used to plot data that was fit to the Langmuir and Freundlich isotherms in order to study this adsorption behavior.

$$\frac{C_e}{q_e} = \frac{C_e}{q_{\max}} + \frac{1}{K_L q_{\max}} \dots\dots\dots\text{equation 4 (Medhi } et al., 2020)$$

where,

q_e = the quantity of absorbed metal per unit weight at equilibrium (mg/g)

C_e = the residual metal concentration (mg/L)

q_{\max} = the maximum quantity of metal (mg/g)

K_L = parameter that affects how well the binding sites bind to each other (L/mg).

The adsorption behavior on heterogeneous adsorbent surfaces was described by the Freundlich isotherm, which assumes that multilayer adsorption occurs on a heterogeneous surface. Equation 5 can be used to describe this isotherm.

$q_e = K_F(C_e)^{1/n}$ equation 5 (Daochalermwong *et al.*, 2020).

where,

q_e =the equilibrium adsorption capacity (mg/g)

C_e =the amount of metal in solution needed to reach equilibrium (mg/L)

K_F =the empirical Freundlich constants associated with the capacity

$1/n$ = intensity of adsorption.

According to the Temkin isotherm model, adsorbate-adsorbent interaction results in a linear decrease in adsorption energy with surface coverage. The Temkin isotherm has a linear form in equation 6.

$q_e = B \ln A + B \ln C_e$ (6) (Kausar *et al.*, 2013).

where,

C_e =concentration of the adsorbate at equilibrium mg/L

q_e =the metal adsorption concentration (mg/g)

$B = RT/bT$ where,

R is the ideal gas constant ($8.314 \text{ J mol}^{-1}\text{K}^{-1}$) and

T is the temperature in Kelvin

bT is the Temkin isotherm constant.

Thermodynamic parameters (ΔH° , ΔG° and ΔS°) were used to calculate the spontaneity of adsorption process. The equation below was employed.

$\Delta H^\circ = C_p \Delta T$ equation (7) (Mangum *et al.*, 2001)

where,

ΔH° is the change in enthalpy (kJ/mol),

C_p is the heat capacity constant for different metals J/Kg/K

ΔT is change in temperature (Kelvin).

The free energy change of the sorption reaction is given by the following equation.

$$\Delta G^\circ = -RT \ln K_L \dots \dots \dots \text{equation(8) (Aravindhnan } et al., 2007)$$

$\ln K_L = -\Delta G^\circ / RT$ $K_L = \text{antilog in natural}_{\log} \text{ of } -\Delta G / RT.$

where,

ΔG° is standard free energy change,

R is the universal gas constant (8.314 J/mol K),

T is the temperature in Kelvin.

$$K_L = \frac{C_A e}{C_e} \dots \dots \dots \text{equation(9) (Sari \& Tuzen, 2009) is the distribution}$$

coefficient

where,

C_e is the solution's equilibrium concentration, expressed in mg/L,

$C_A e$ is the solution's equilibrium concentration on the sorbent-adsorbent difference is $(C_f - C_i)$.

$$\Delta G^\circ = \Delta H^\circ - T \Delta S^\circ$$

where,

ΔS° , change in entropy ($\text{kJ mol}^{-1} \text{K}^{-1}$).

According to equation (10), the values of enthalpy ΔH° and entropy ΔS° were derived from the slope and intercept of the plot of $\ln K_L$ against $1/T$.

$$\ln K_L = \frac{\Delta S^\circ}{R} - \frac{\Delta H^\circ}{RT} \dots \dots \dots \text{equation (10) (Flores-Gamica } et al., 2013)$$

CHAPTER FOUR

RESULTS AND DISCUSSION

4.1 Fractionation of crude extracts of *Pavonia urens*

Medicinal plant analysis begins with extraction, it is necessary to take the desired chemical components out of plant materials in order to further separate and characterize them. There were fractionated crude extracts of *Pavonia urens*. The hexane, dichloromethane, ethyl acetate, acetone and methanol extracts were labeled as 1A, 2A, 3A and 4A respectively.

4.2 Spectroscopic Analysis of the fractions

4.2.1 GC- MS

Fractions; 1A – 4A were characterized by GC-MS. The results presented in GC-MS chromatogram reveals the presence of 15 peaks in Fraction 1A as seen in Figure4.1. NIST (National Institute of Standards Technology) library match characterized them into several different phytochemical constituents. Elution occurred between retention times (RT) ranging from 7.866 to 29.187 minutes. The details of each compound were tabulated in Table 4.1. n-tetracosanol-1 (40.73%) andhen eicosane(10.13%) predominantly occurred among the compounds characterized. Other compounds present in very less quantity in the fraction as presented in Table 4.1.and their structures are given in Appendix I.

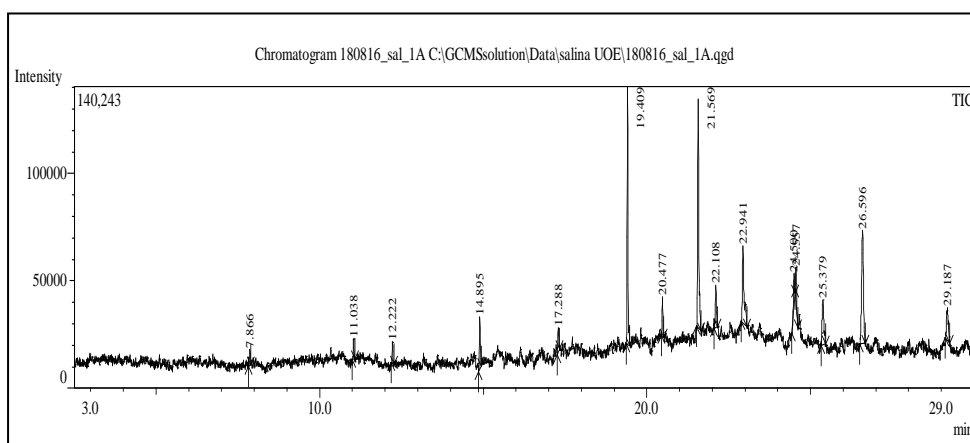


Figure 4.1: Fraction 1A chromatogram

N/B: Peak numbers correlate to compounds listed in Table 4.2 below.

Table 4.1: Chemical composition of Fraction 1A

S/N	Retention	Area		Height		Name
	time	Area	%	Height	%	
1	7.866	10616	0.9	7358	1.53	Nonanal
2	11.038	15385	1.31	9683	2.01	Undecanal
3	12.222	15351	1.31	9975	2.08	Tetradecane
4	14.895	41096	3.5	24155	5.03	Hexadecane
5	17.288	19972	1.7	11104	2.31	Heptadecane
6	19.409	221635	18.85	119837	24.93	n-Tetracosanol-1
7	20.477	31953	2.72	18255	3.8	Tetracosane
8	21.569	257304	21.88	106582	22.17	n-Tetracosanol-1
9	22.108	43364	3.69	19583	4.07	Heneicosanal
10	22.941	119050	10.13	36041	7.5	Heneicosane
11	24.5	31076	2.64	14707	3.06	Bacteriochlorophyll-c-stearyl
12	24.557	25710	2.19	14154	2.94	Heneicosane
13	25.379	77508	6.59	20940	4.36	Docosanal
14	26.596	209209	17.79	52828	10.99	Tetracosane
15	29.187	56469	4.8	15458	3.22	Tetracosane

The results presented for GC-MS chromatogram revealed the presence of 11 peaks in Fraction 2A and are shown in Figure 4.2. and Appendix II. NIST library match characterized them into several different phytochemical constituents. Elution occurred between retention times (RT) ranging from 14.596 to 28.375 minutes. The details of each compound are tabulated in Table 4.2. Squalene (70.01 %) and stetratriacontane (13.27 %), predominantly occurred among the compounds characterized. Other compounds were present in low fractions.

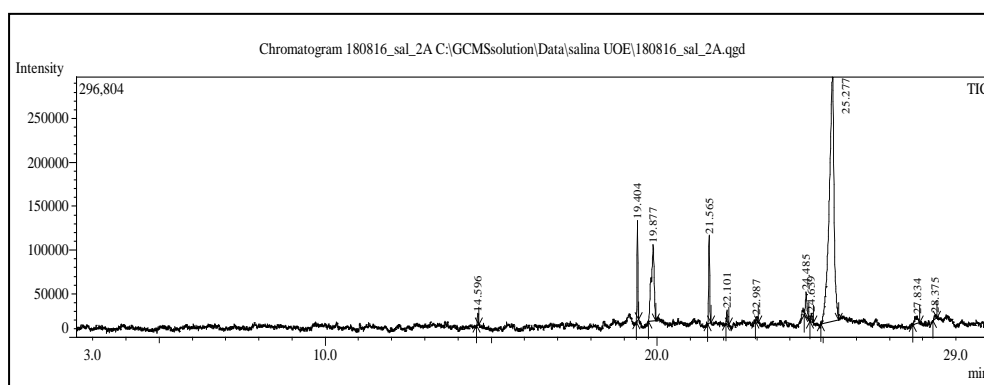


Figure 4.2: Fraction 2A chromatogram

N/B: Peak numbers correlate to compounds listed in Table 4.2.

Table 4.2: Chemical composition of fraction 2A

S/N	Retention		Area			Name
	time	Area	%	Height	Height %	
						2(4H)-Benzofuranone, 5,6,7,7a-
1	14.596	25597	0.63	13566	2.03	tetrahydro-4,4,7a-trimethyl-
2	19.404	199887	4.93	114316	17.14	n-Tetracosanol-1
3	19.877	538468	13.27	87300	13.09	Tetratriacontane
4	21.565	218815	5.39	101071	15.15	n-Tetracosanol-1
5	22.101	35323	0.87	15888	2.38	Eicosanal-
6	22.987	12595	0.31	5398	0.81	1,1'-Biphenyl, 2-(phenylmethyl)-
7	24.485	93703	2.31	27674	4.15	n-Tetracosanol-1
8	24.639	25340	0.62	9638	1.45	n-Tetracosanol-1
9	25.277	2841078	70.01	278236	41.72	Squalene
10	27.834	50623	1.25	8650	1.3	2-Bromotetradecane
11	28.375	16666	0.41	5190	0.78	Nonadecyl heptafluorobutyrate

The results presented in GC-MS chromatogram revealed the presence of 13 peaks in Fraction 3A and shown in Figure 4.3 and Appendix III. NIST library match characterized them into several different phytochemical constituents. Elution occurred between retention times (RT) ranging from 12.454 to 19.789 minutes. The details of each compound are tabulated in Table 4.3. Hexadecanoic acid (37.04 hexadecenoic acid methyl ester (18.14 %), and tetratriacontane (9.03 %), predominantly occurred among the compounds characterized. Other compounds were present in very low quantities in the fractions as presented in Table 4.3.

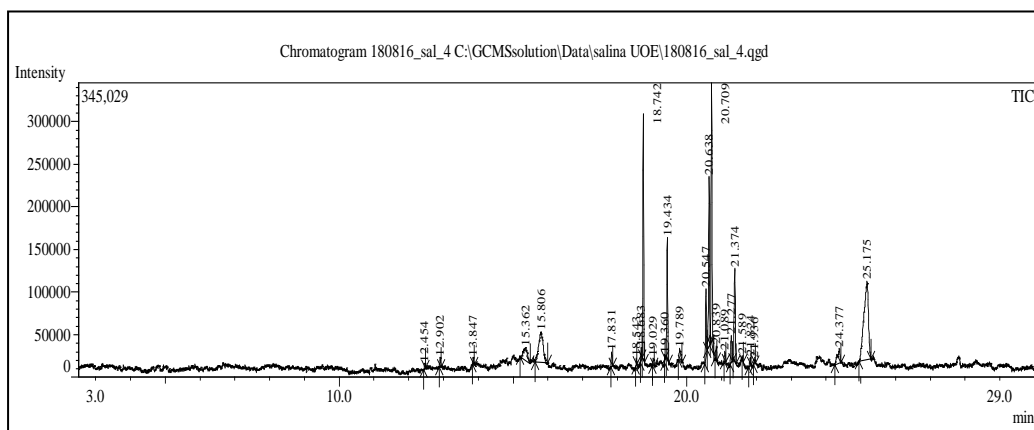


Figure 4.3: Fraction3A chromatogram

N/B: Peak numbers correlate to compounds listed in Table 4.4.

Table 4.3: Chemical composition of fraction 3A

S/N	Retention		Area		Height		Name
	time	Area	%	Height	%		
1	12.454	10815	0.81	6115	1.05	Benzene, 1,2-dimethoxy-4-propenyl-, (Z)-	
2	12.902	20253	1.51	11412	1.97	Nonanoic acid, 9-oxo-, methyl ester	
3	13.847	11952	0.89	8229	1.42	Nonanoic acid, 9-oxo-, ethyl ester	
4	15.362	121195	9.03	15856	2.73	Tetratriacontane	
5	15.806	314112	23.4	35954	6.2	Tetratriacontane	
6	17.831	28147	2.1	16466	2.84	2-Pentadecanone, 6,10,14-trimethyl- 7-Hexadecenoic acid, methyl ester,	
7	18.543	8484	0.63	8448	1.46	(Z)- 1,6,10,14,18,22-Hexacosahexaen-3-ol, 2,6,10,15,19,23-hexamethyl-, (all-E)- (.	
8	18.683	22294	1.66	14393	2.48	+/-)-	
9	18.742	497413	37.04	288780	49.81	Hexadecanoic acid, methyl ester Undec-10-ynoic acid, tridec-2-yn-1-yl	
10	19.029	17286	1.29	8893	1.53	ester	
11	19.36	6136	0.46	6954	1.2	Ethyl 9-hexadecenoate	
12	19.434	243517	18.14	143494	24.74	Hexadecanoic acid, ethyl ester	
13	19.789	40742	3.04	14920	2.57	Tetratetracontane	

The results of fraction 4A shown in GC-MS chromatogram revealed the presence of 9 peaks shown in Fraction 4A and shown in Figure 4.4 and Appendix IV. NIST library match characterized them into several different phytochemical constituents. Elution occurred between retention times (RT) ranging from 14.955 to 24.818 minutes. The details of each compound are tabulated in Table 4.4. Phytol (29.1 %) tetratriacontane

(15.59 %), and hexatriacontane (10.81%), predominantly occurred among the compounds characterized. Other compounds were present in very low quantities in the fraction as presented in Table 4.4

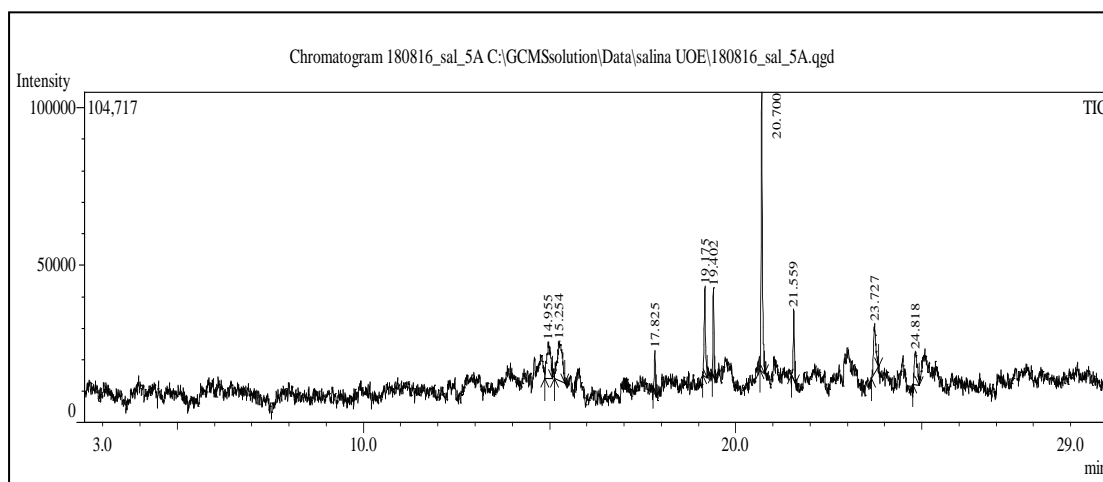


Figure 4.4: Fraction4A chromatogram

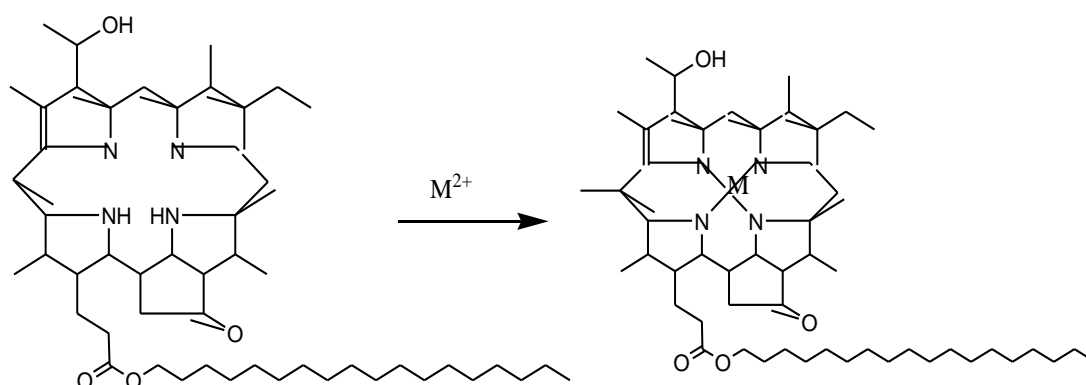
N/B: Peak numbers correlate to compounds listed in Table 4.5.

Table 4.4: Chemical composition of fractions 4A

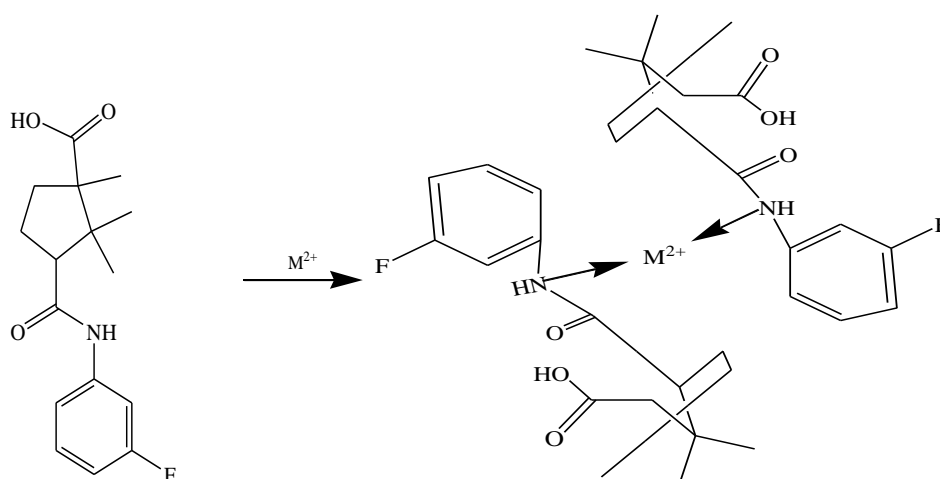
Retention						
S/N	time	Area	Area %	Height	Height %	Name
1	14.955	79971	10.89	11658	5.05	Hexatriacontane
2	15.254	114467	15.59	12459	5.39	Tetratriacontane
3	17.825	23760	3.24	13297	5.75	2-Pentadecanone,6,10,14-trimethyl-
4	19.175	73313	9.99	28466	12.32	1-(+)-Ascorbic acid 2,6-dihexadecanoate
5	19.402	52572	7.16	27975	12.11	9-Tricosene, (Z)-
6	20.7	213681	29.1	88332	38.22	Phytol
7	21.559	49245	6.71	22394	9.69	n-Tetracosanol-1
8	23.727	71790	9.78	16008	6.93	10-12-Pentacosadiynoic acid
9	24.818	55364	7.54	10479	4.54	10-12-Pentacosadiynoic acid

Mass fragmentation of fractions 1A – 4A revealed most of these compounds identified contained functional groups with O-H, C=O, C - N and N-H having lone pairs and thus displaying the potential to form complexes with metals (coordinate bond formation).

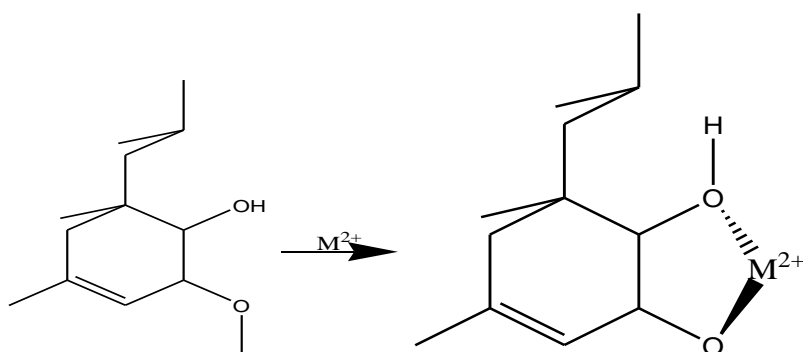
From the chemical, physical, and spectral evidences compared with the ones in literature, possible structures of fractions 1A – 4A with lone pairs can bind with metal ions. These fractions show a schematic view of proposed binding of metal ions with some structures of some compounds of *Pavonia urens*.



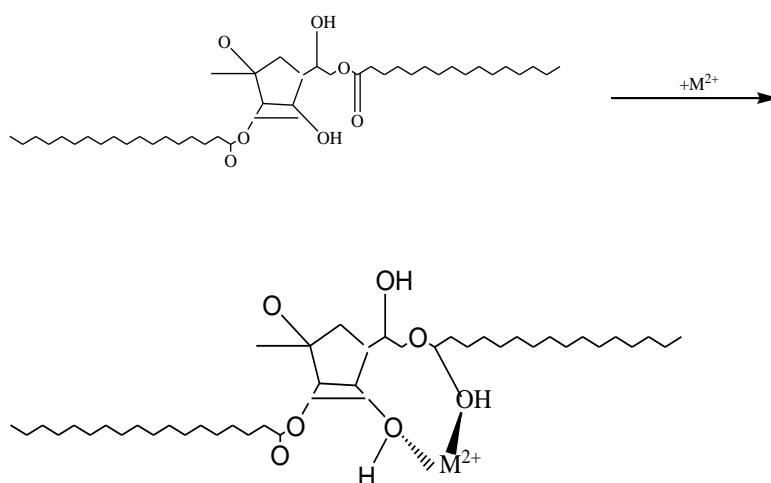
Fraction 1A: Bacteriochlorophyll-C-stearyl and proposed possible metal complex structure



Fraction2A: Cyclopentane carboxylic acid,3-(-fluorophylcarbonyl)-1,2,2-trimethyl and possible metal complex structure



Fraction 3A:Phenol,2-methoxy-4-methyl-6-(propenyl) and possible metal complex structure



Fraction 4A: Ascorbic acid 2,6-dihexadecanoate and possible metal complex structure

$M^{2+} = Cu^{2+}$ and Ni^{2+} ions

Figure 4.5: The proposed compounds present (fractions (1A,2A,3A and 4A) in *Pavonia urens* and possible metal complex structures

Substituents in the benzene ring that remove or donate electrons, the steric effects and inter-molecular, intra-molecular H-bonding affect the absorption spectrum of phenols (Mathiyalagan and Mandal, 2020). In fraction 1A, a complex formation of the metal ion with the amino group took place, other sites like the OH and C=O could not form due to steric hindrance. The epoxy also contributed to steric hindrance since the group is bulky. This could reduce or prevent reactions at the atom (Grzelczak *et al.*, 2012). This was evidenced in fractions 2A and 4A in which, steric hindrance is responsible for the observed shape and geometry of the compound. The steric barrier caused the complex compound change the conformation and geometry of the functional group with the metal ion (Bickelhaupt and Barends, 2003).

Bulky groups exert significant repulsion against the incoming reactant, resulting in steric strain. This effect slowed down the reaction by reducing the reactive centre's

accessibility (Pinter *et al.*,2012). In fraction 2A, the amine group formed a complex with the metal ion while in fraction 4A, formation of a complex with C=O and OH occurred. The nature of binding nitrogen and metal ion connection allowed for better ion-functional group interactions (Qureshi *et al.*, 2009). The epoxide repelled each other because of molecular interactions and steric hindrance (Mathiyalagan and Mandal, 2020). For fraction 3A, the complex was formed between the methoxy and hydroxyl group with the metal ion. The oxygen atom has two lone pairs of electrons while methyl groups are bulky but the methyl groups were hindered because of its size.

4.3 UV- VIS analysis of complex formation between heavy metals with *Pavonia urens* compounds

Spectroscopy confirmed the production of complex chemicals in metal ion systems. From the UV-VIS spectra, it was observed that there was a shift in wavelength of the plant material when metal ions were introduced as shown in Figure 4.7.

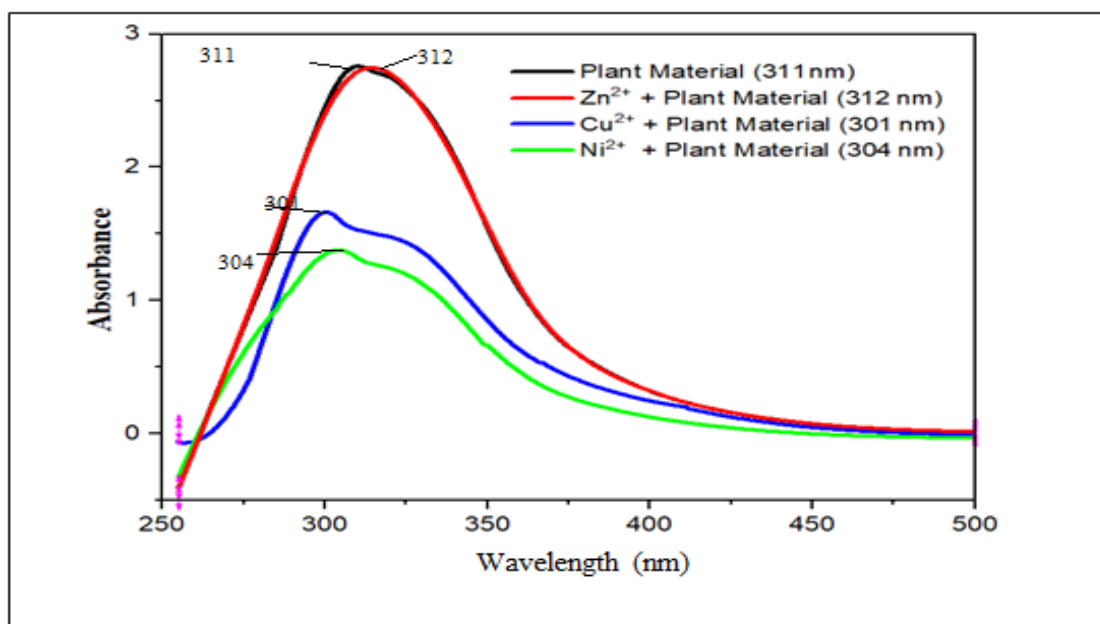


Figure 4.6: UV/VIS absorption of plant material and Cu^{2+} , Ni^{2+} , Zn^{2+} ions at $c=4 \times 10^{-3} \text{ mol dm}^{-3}$

When copper ions and nickel (II) ions were introduced separately, a shift to shorter wavelength from original 311 nm to 302 nm and 305 nm, respectively occurred. Therefore, there was a decrease in absorption frequencies in both cases. This bathometric shift occurred as a result of coordination. However, for zinc (II) ions, there was almost no observable shift from the original plant material spectrum. The change in shift of wavelength or frequency demonstrated coordinate bond formed through the lone pair from the functional groups in the plant cell with the metal ion. For example, functional group -OH, a bond formed can be illustrated as $M^{2+} \dots O-H$, where $M^{2+} \dots O$ shows interactions of different groups in plant material having O-atom with different metal ions. The O-H bond of the plant cell is affected by shifts of wavelength with lowering or increasing absorption bands. For instance, for strong coordinate bonds, $M^{2+} \dots O$ is strengthened, while the O-H is weakened leading to a shift to longer wavelength, that is lowering of stretching and vibrational energies. For weak coordinate bonds, $M^{2+} \dots O$ is weakened as the O-H bond is strengthened. This is accompanied by a shift to shorter wavelength that increased stretching and vibrational frequencies of O-H bond (Shoaib *et al.*, 2011).

Based on the spectra obtained in Figure 4.6 above, copper ions had the largest shift in wavelength range. Overall, the data show that the size of the metal ion's internal coordination sphere changes (Scerri, 2011).

Since *Pavonia urens* compounds are deprotonated, they can operate as coordination centers. In biological systems, these molecules can be partly or completely deprotonated, allowing complexes with metal ions such as copper (II) or nickel (II) to form (Zabizak *et al.*, 2021). The reason could be ligand-to-metal charge transfer

(LMCT). The coordination of deprotonated hydroxyl, carboxyl, and amine groups in plant material with metal ions caused the development of new peaks (Rasheed and Nabeel, 2019). The shift to shorter wavelength of different metals may be related to differences in metal ionic size and atomic number (Scerri,2011) and encouraging the transport of electron-generated charge within molecules donor (-OH) to the complex's metal ions.

Metal ion reduction was caused by charge transfer from oxygen O-H lone pairs to partially filled metal d-orbitals. The variation to longer shift across metals may be attributable to metal ionic size, these findings are supported with those of Alorabi *et al* (2020).

Zinc is a metallic element with an atomic number of 30 and an electronic structure. $1s^2 2s^2 2p^6 3d^{10}$. Therefore, the 3d orbitals are filled and there are no unpaired electrons for the transition. Thus, zinc compounds are colourless (Crabtree, 2009) since there is no d-d electronic transition. This confirms why there was no observable shift. In addition, the coordinate bond between the electron pair acceptor from plant material to say 4s orbital of Zn^{2+} is of higher energy because energy needed to lower these sets of orbitals is not achieved (Shoaib *et al.*,2011). However, charge transfer in Zn^{2+} may involve higher energy orbitals such as 4s. The possible binding mode is through the coordination of the nitrogen atoms (N) and the oxygen atoms (O) of the functional groups to form complexes with possible structures as shown in fractions 1A to 5A of Figure 4.5.

Pavonia urens compound complexes with metal ions have been established. In the complexes, monodentate binding to negatively charged oxygen donor atoms (phenolic and carboxylic functional groups) was observed, as well as a linear free energy relationship between metallic and complexation or bidentate modes (Ratié *et al.*, 2021). The lone pair in ligands (such as OH, C=O and N-H) is donated to the stable and lowest empty orbital of the metal to form coordinate bond.

The atomic radii of the first series transition metals decreased with atomic number. The increased nuclear charge attracts the electron cloud inward, reducing metallic/ionic size. Horsefall and Spiff (2005) argued that decreased ionic radius leads to more hydrolysis and less absorption. This confirms that absorption may be linked to the hydration sphere depletion prior to hydrolysis. Ionic size confirms there was high interaction of copper ions with the plant material. Therefore, copper, could have “displaced” zinc and formed bonds with plant material. Higher energy is needed to break the bond formed between the functional group O-H with copper than with zinc or nickel. Figure 4.7 shows UV/VIS absorption spectra of plant with Cu^{2+} .

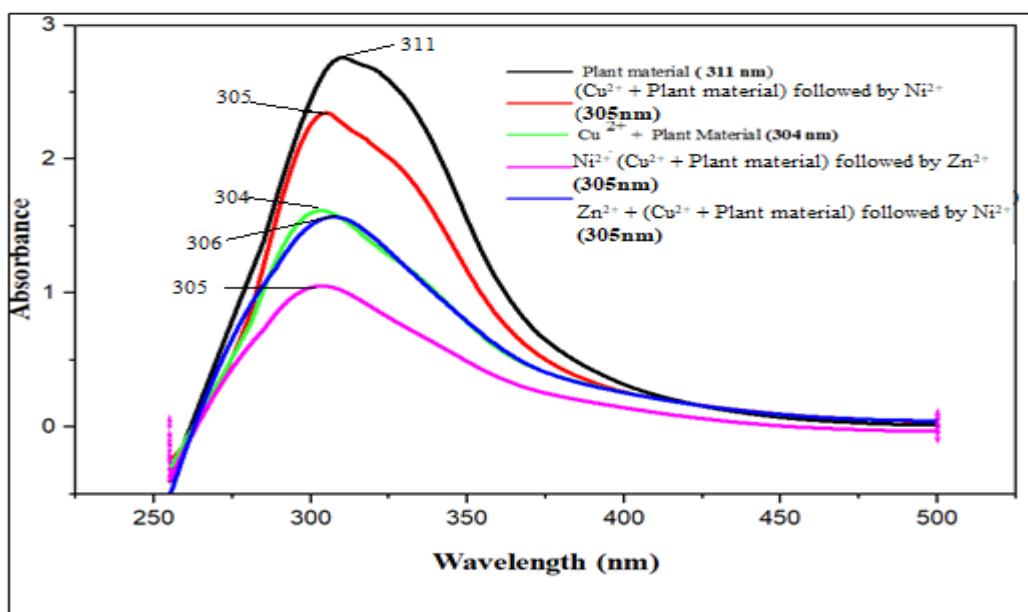


Figure 4.7: UV/VIS absorption spectra of plant material and their copper complexes in a 1:1 ratio $c=4 \times 10^{-3} \text{ mol dm}^{-3}$

When Cu (II) was added to the plant,(Figure 4.7), the absorption of metal ions was high as a result of interactions between metal ions and the active sites of bioactive groups of the plants cell. With the addition of nickel ions, for example, the metal ions compete for binding sites, causing overlapping of absorption bonds due to particle crowding. Due to its smaller ionic radius and higher hydration energy, Zn (II) could have, in general, easier access to plant pores than Cu (II) and Ni (II) (Shoaib *et al.*, 2011).

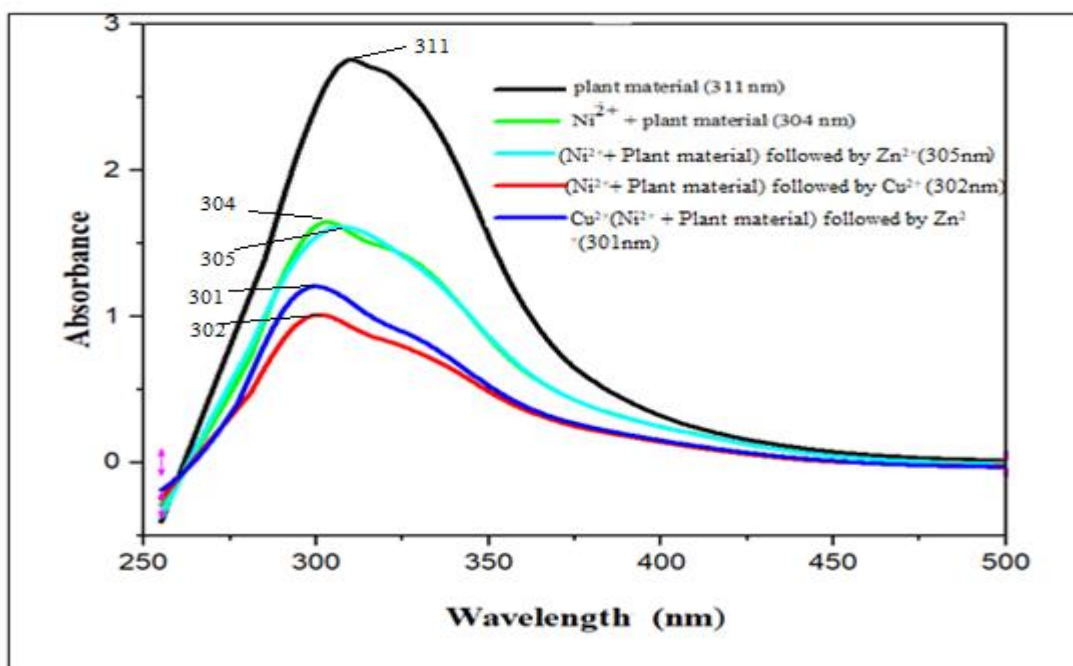


Figure 4.8: UV/VIS Absorption spectra of plant material and Nickel complexes in a 1:1 ratio $c=4 \times 10^{-3} \text{ mol dm}^{-3}$

In Figure 4.8, the UV-VIS spectra of nickel with plant material showed a shift to shorter wavelength from original 311 nm to 304 nm. The shift to lower wavelength or high stretching frequency formed a stronger bond with the functional group. This showed there were high interactions of nickel with the plant material. This could be maximum absorbance which was achieved because of increased accessibility to interchangeable locations or surface area. When zinc ions were introduced, there was not much observable change in wavelength although absorption slightly dropped implying the interaction was quite low or absent. Copper and nickel ions competed for active sites in plant material, which became saturated at a specific metal ion concentration and absorption, therefore dropped.

Figure 4.8, showed that there was a shift to different frequency levels after absorption. When a new metal was introduced, the peaks shifted to higher energies of shorter wavelength with functional group O-H and therefore increasing stretching and vibrational frequencies. In this regard with copper ions, there was a shift to shorter wavelength due to weak bond formation with the functional group. This was also seen with nickel ions. The metal ion adsorption on the surface of the plant material was typically established by this shifting of bands.

Complexes between *Pavonia urens* compounds and d-electron metal ions have been observed. Overall, the data showed that metal (II) ions had a higher propensity for coordination with the examined ligands in order of copper(II) >nickel(II)> zinc (II), showing metal complexes possessing a good absorption ability.

4.4 Biosorption of heavy metals by *Pavonia urens* using atomic absorption spectroscopy

4.4.1 Effect on contact time

Parameters remained constant were, pH at 6, dosage of biosorbent at 1 g and agitation speed at 125 rpm in all the experiments. For the various concentrations of Zn (II), Ni (II), and Cu (II), the impact of contact time on the biosorption process was examined over the time range of 0 to 120 min at the optimum dose.

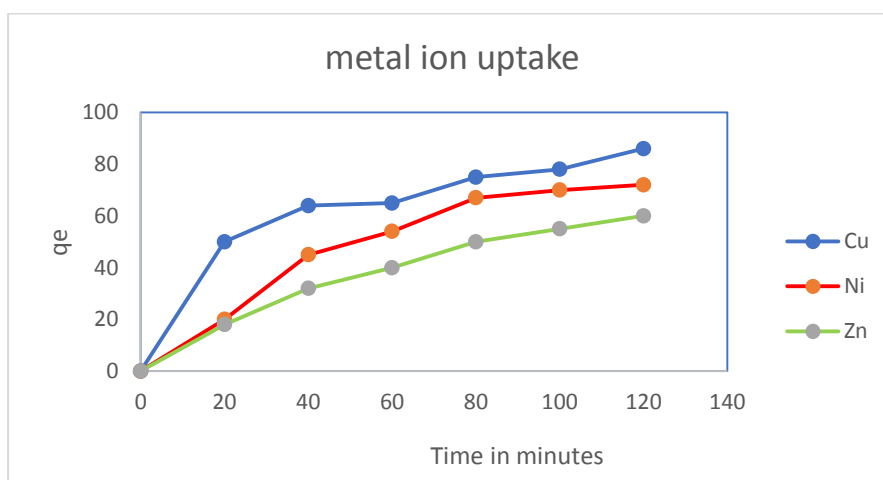


Figure 4.9: Effects of contact time on metal absorption

The gradient of metal biosorption was first steeper and then gradually decreased with time. *Pavonia urens* when used as an adsorbent, Figure 4.9 and Appendix V, it is shown that there was an evident increase in removal of bimetallic ions up to 40 min with further increase in contact time up to 120 minutes, where the increase in removal of metal was quite minimal. This was because there were initially an infinite number of active sites, and the second phase took place after the bulk of active sites had been occupied resulting in metal ion dispersion into the plant material's cells. These results are in agreement to those of Ayabei and Kituyi (2013). More so, the number of active sites per adsorbate, the adsorbate's particular interactions with each adsorbate, and the adsorbate's diffusion in each adsorbate medium should be considered. These findings are in agreement to those of Iftekhar, (2018).

The optimum condition of Cu (II) ions was obtained at the contact time of 40 min. The first 20 min displayed steeper gradient and, this could be attributed to the less hydration sphere of copper which is a fairly big ion. The ionic size confirms there was high interactions of copper and plant material (Horsefall and Spiff, 2005). The second

phase was from 60 min to 120 min whereby biosorption was gradual implying the active sites were saturated. This observation was similarly reported that the adsorption takes place in two phases using coffee husks as low-cost adsorbent (Arun *et al.*, 2018).

Nickel uptake by plant material was also in phases. The first phase up to 40 min was related to external surface biosorption where adsorption occurred instantaneously. The second phase was from 40 to 60 min where there was gradual biosorption. This observation can be seen in the biosorption experiment done using coir fibers (Shukla *et al.*, 2006; Kulkarni *et al.*, 2022). Nickel being a big ion is less hydrated and having lower hydrated radius made the ions to move faster (Shoaib *et al.*, 2011). The last phase was from 60 to 120 min which showed minimal absorption.

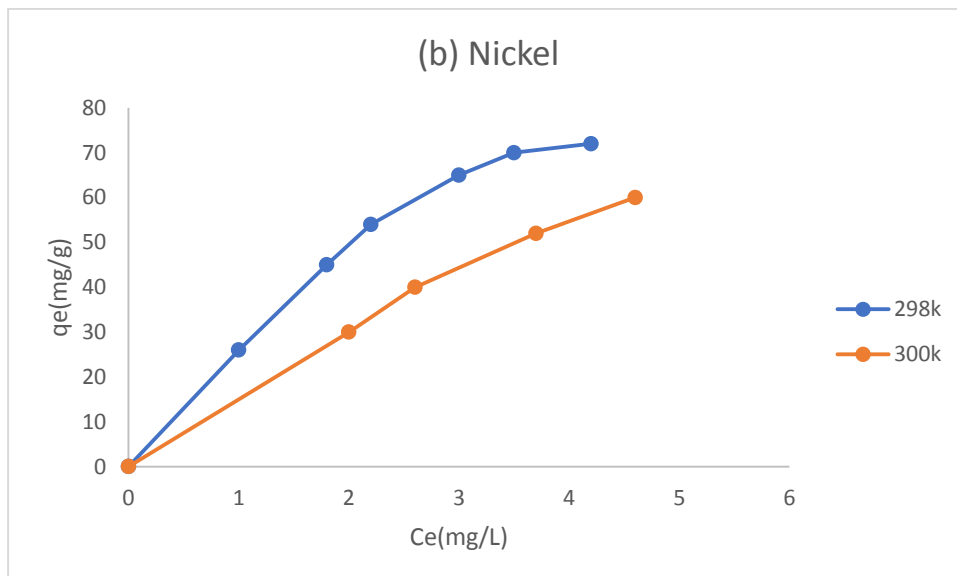
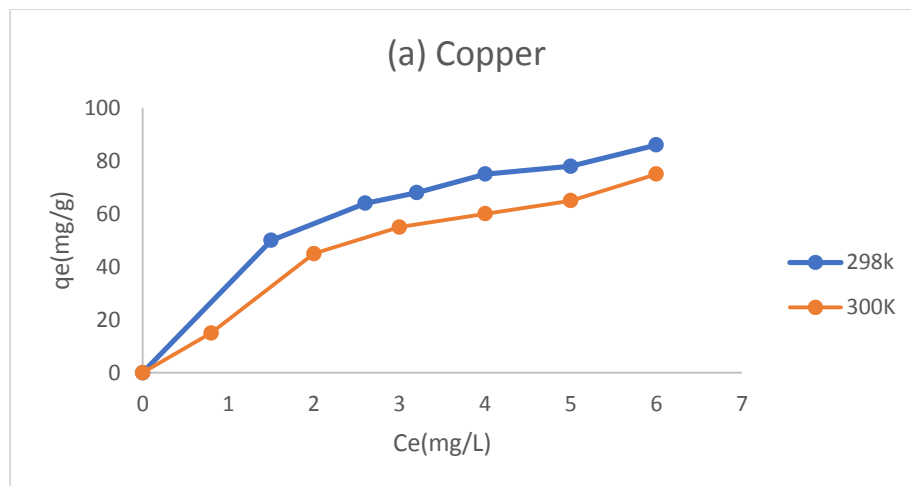
Zinc ions uptake from solution showed that biosorption was the equilibrium process in which the optimum biosorption reached after about 10 minutes. The biosorption remained almost constant from 10 to 120 minutes. However, adsorption slows down, because initially a high number of vacant surface sites may be available for adsorption and after sometime, the remaining free sites may be difficult to occupy due to interactions between the solute molecules of the solid and bulk phase (Bishnoi *et al.*, 2007). These results are in agreement with the results reported of low absorption of zinc metal using algae and plant biomass (Melcakova and Ruzovic, 2010).

It was also noted that all the metal ions absorption gradually increased with time but reached maximum adsorption efficiency where it remained constant. These results can perhaps be explained by the production of complexes by coordinate bond.

4.4.2 Influence of temperature

To assess its thermodynamic parameters and data, equilibrium studies at two different temperatures—298 and 300 K—at 125 rpm in a mechanical shaker were performed.

The results are shown in Figure 4.10 (a), (b) and (c). Appendix VI.



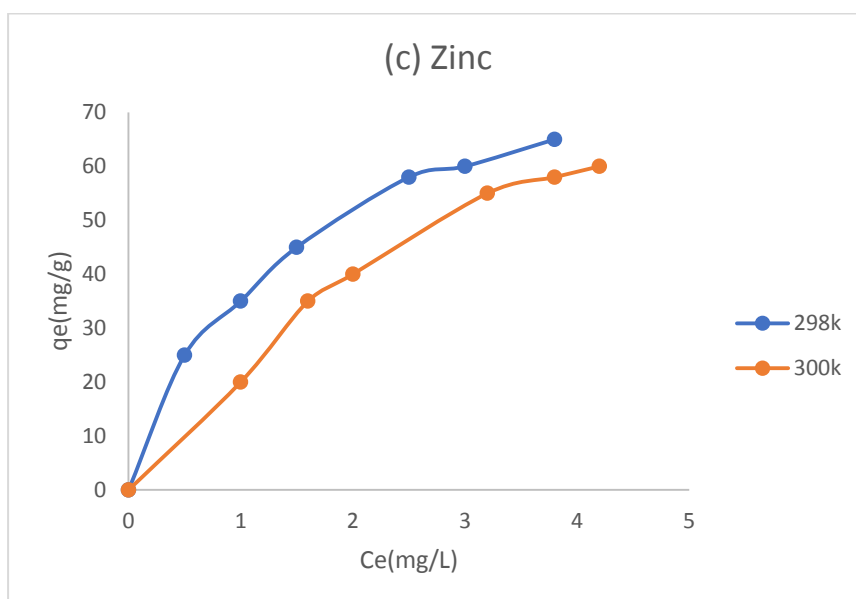


Figure 4.10: Temperature's impact on adsorption of copper (a) nickel (b) and zinc(c) on *Pavonia urens* leaves

From Figure 4.10, it was observed that the amount of Cu (II), Ni (II) and Zn (II) ions absorption decreased with a rise in temperature since the biosorption process diminish with higher temperatures. In regard to copper ions at 298 K the absorption increases and at 300 K absorption was lower than of 298 K but increases until it reached a limit where absorption was gradual. For nickel ions absorption at 298 K was gradual to the maximum point where as for 300 K it was lower while zinc ion absorption was gradual for 298 K and at 300 K was lower. These findings are in agreement to those of Manirethan (2018) but with less intensity, and physical functional groups interactions occurred. These results were similar to those of Piccin, (2009).

The physical connections between metal ions and functional groups reduced when hydrogen and coordination bond interactions were weakened at high temperatures, hence higher absorption capacities at 298 K than at 300 K. A similar effect was observed for adsorption of Congo Red by chitosan hydro beads (Chattejee *et al.*,

2007). Due to a combination of factors, the adsorption capacity decreases as the temperature rises. This demonstrated that an exothermic mechanism governed the physio- sorption of functional groups in *Pavonia urens* leaves. A similar finding was observed for adsorption of Indigo carmine dye by chitosan (Anjos *et al.*, 2002).

4.4.3 Adsorption isotherm

The adsorption behavior was described using the Langmuir isotherm model. The sorption process generated a monolayer at the surface, and the surface has a finite number of identical sites, according to this concept. Equation 4 on Page 30, can be used to define this isotherm. Graphs illustrating the Langmuir isotherm for the metal ions Cu (II), Ni (II), and Zn (II) are shown in Figure 4.11 and Appendix VII.

Experimental data

The Figure 4.11 and Appendix H, show the equilibrium data for copper, nickel and zinc ions adsorption. This plot q_e vs C_e .

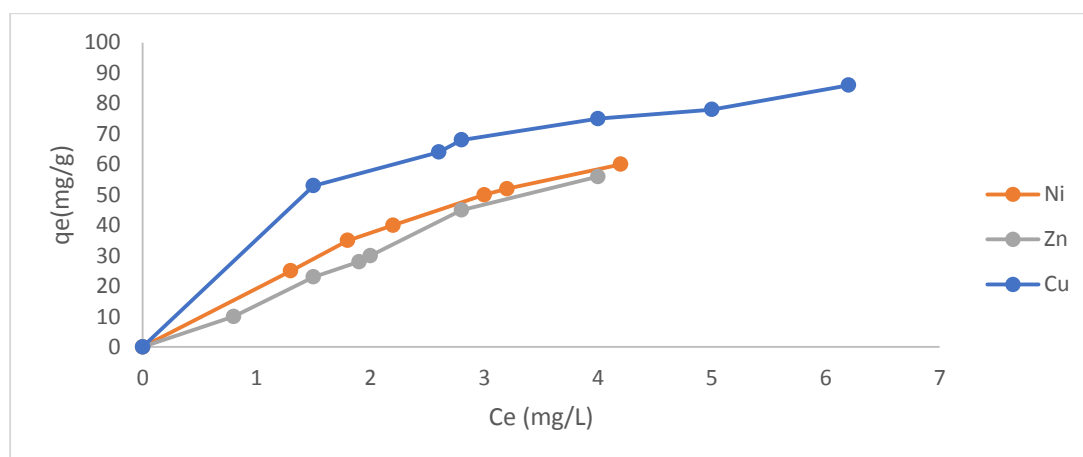


Figure 4.11: Data from experimental adsorption equilibrium isotherms

From the Figure 4.11, it was observed that copper ions were absorbed faster than nickel and zinc ions, that the adsorption process took place in two phases, the first of

which was rapid and the second of which was gradual. This was owing to the fact that there were an endless number of active sites. The second step took place when the majority of the active sites were occupied and entailed the diffusion of the metal ions into the plant material's cells. Zinc, ions was the least adsorbed, in order of copper (II) > nickel (II) > zinc (II), showing *Pavonia urens* possessing a good absorption ability.

(a) The Langmuir model plot

The values of Langmuir parameters q_{max} and K_L were calculated from the slope and intercept of linear plot C_e / q_e vs C_e as illustrated in Figure 4.12 and Appendix VIII

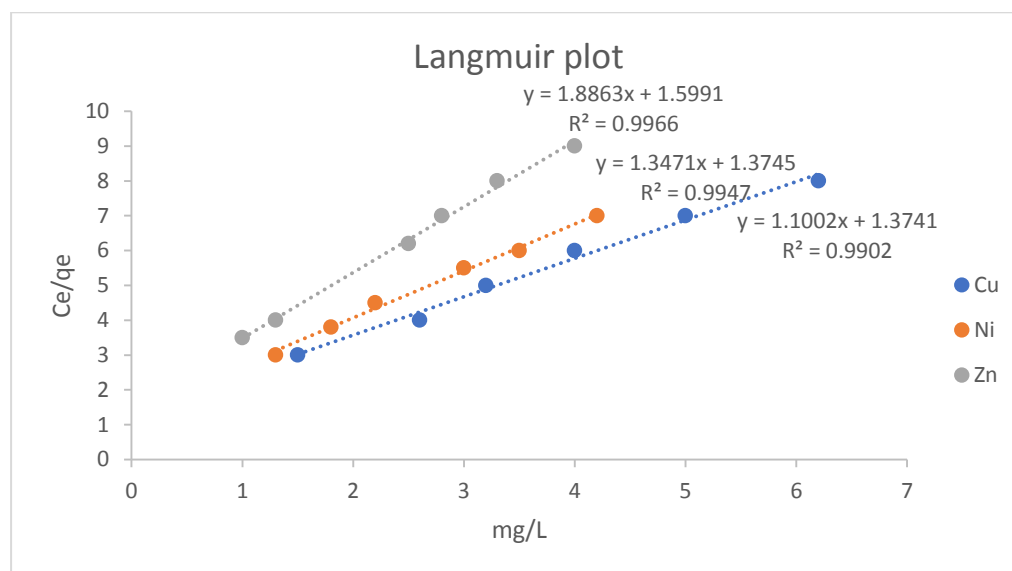


Figure 4.12: Adsorption equilibrium isotherms of Langmuir for Cu (II), Ni (II) and Zn (II) ions on *Pavonia urens*

The regression coefficient (R^2) of the model plays a big role in model fitting. The value of R^2 indicates the type of Langmuir isotherm (Ho *et al.*, 2002). The values of R^2 in Table 4.5, are observed to be less than one in all cases, indicating favourable adsorption of metals copper, nickel and zinc by *Pavonia urens*. These findings are in agreement to those of Aman, (2018). The slope and intercept of the linear plot of

C_e/q_e vs C_e displayed in were used to derive the values of the Langmuir parameters q_{\max} and K_L . Figure 4. 12. Constant values that have been examined are provided in Table 4.5.

This examines the likelihood of a heterogeneous distribution of active sites and interactions between compounds that have been adsorbed.

(b) Freundlich plot

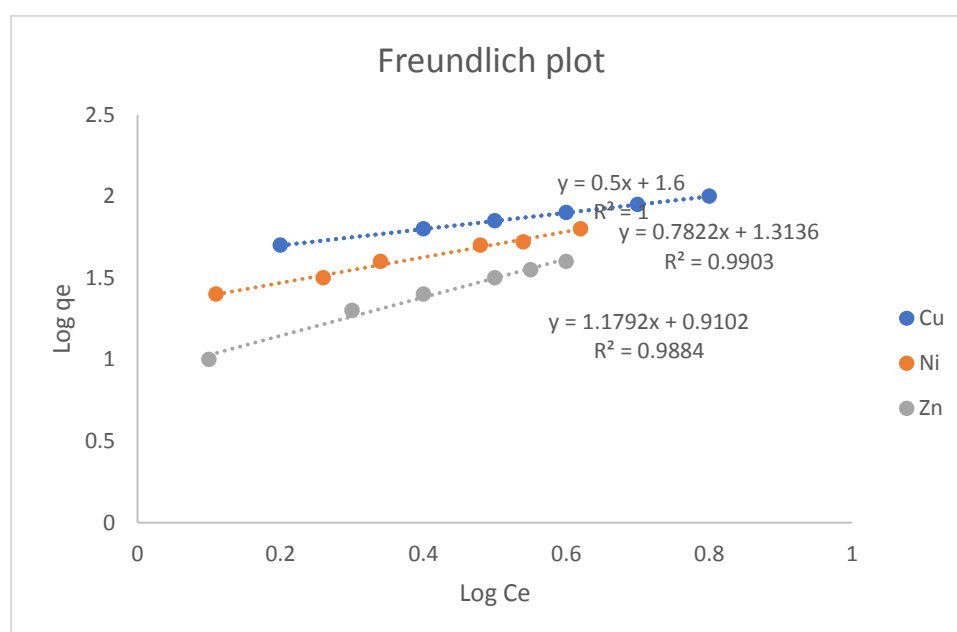


Figure 4.13: Adsorption equilibrium isotherms of Freundlich

The Freundlich isotherm model plots [$\log(q_e)$ vs $\log(C_e)$] were drawn using experimental data and illustrated in Figure 4.13 and Appendix IX; and the Constant K_F and $n/1$ can be determined from the linear plot and using equation 5. The evaluated constants are given in Table 4.5. All of the metal ions' n values are reported to be larger than 1, suggesting favorable adsorption, and the sorption process is physical adsorption. This effect is similar to those of Ngabura, (2018).

(c) Temkin plot

The Temkin isotherm model states that the interaction between the adsorbate and the adsorbent causes the adsorption energy to drop linearly with surface coverage. The equation 6 on Page 31, is a linear representation of the Temkin isotherm. The heat of sorption is represented by B, while A is the equilibrium binding constant. The values of A and B are given in Table 4.5 and data in Appendix X and Figure 4.14.

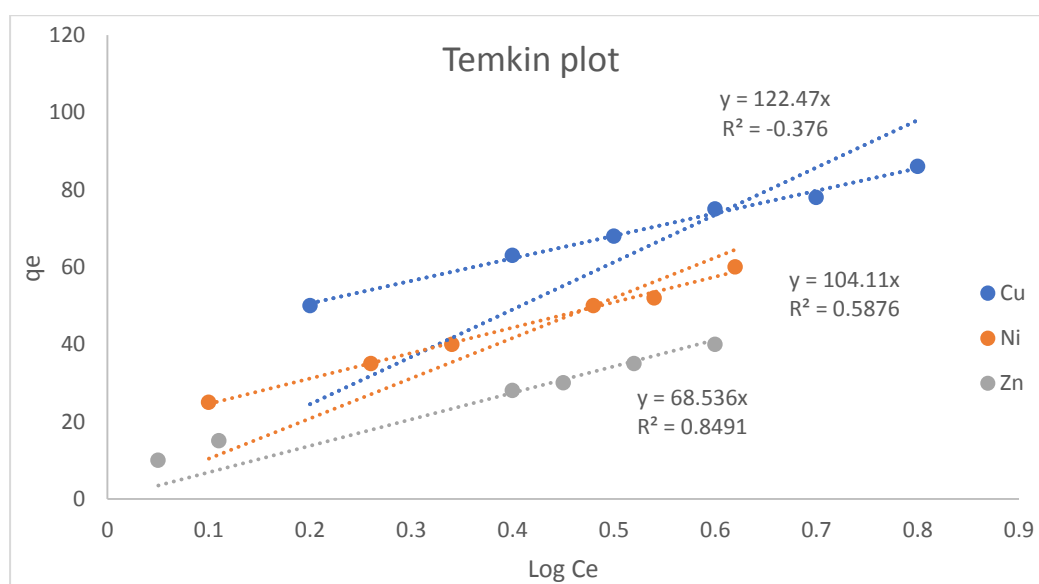


Figure 4.14: Isotherm for Biosorption of Temkin Cu (II), Ni (II) and Zn (II) ions onto *Pavonia urens* leaves.

Table 4.5: Constants of the adsorption isotherm of Cu (II), Ni (II) and Zn (II) on to *Pavonia urens* leaves

Metals	Cu (II)	Ni (II)	Zn (II)
Langmuir parameters			
q_{\max}	2.85	1.75	1.06
K_L	0.08	0.2	1.20
R^2	0.9902	0.9947	0.9966
Freundlich parameters			
$K_F(\text{mg/g}) (\text{L/mg})^{1/n}$	0.62	0.680	0.805
n	1.98	2.35	3.80
R^2	1	0.9903	0.9884
Temkin parameters			
B (mg/g)	0.58	0.45	0.22
A	0.8	2.3	5.2
R^2	0.9636	0.9726	0.979

Based on Table 4.5 and R^2 values of the sorption of Cu (II), Ni (II), and Zn (II), the Langmuir isotherm fits the experimental equilibrium adsorption data better than the Freundlich and Temkin isotherms. It can also be seen from Table 4.5, that the Langmuir constant " q_{\max} " was 2.85, 1.75 and 1.06 and K_L was 0.08, 0.2 and 1.2 for Cu (II), Ni (II), Zn (II). The positive sorption was shown by the regression coefficient (R^2) values being less than one and greater than zero for Cu (II), Ni (II) and Zn (II) ions on to *Pavonia urens* leaves.

The Freundlich constant K_F indicates the sorption capacity of the sorbent and the corresponding values of K_F 0.62, 0.68 and 0.82 mg/g for Cu (II), Ni (II) and Zn (II). It could be observed from the Table 4.5, that since the regression coefficient was 1 for Cu (II) implying a linear relationship and thus the Freundlich isotherm was not followed.

However, n was high, suggesting that the adsorption on the adsorbate was favourable. Furthermore, the respective values of ' n ' at equilibrium were 1.98, 2.35, and 3.8 for Cu (II), Ni (II), and Zn (II) ions, these values of ' n ' were between 1 and 10 indicating favorable adsorption for the Freundlich mechanism.

By this mechanism, the order of absorption was copper (II) > nickel (II) > zinc (II). Temkin isotherm favours all the metal ions. As a result, the Freundlich model's adsorption mechanism suggested that the adsorption sites on the adsorbent of *Pavonia urens* leaves are heterogeneous, with interaction between adjacent sites. These findings are similar to those of Ngabura, (2018) and Mwandira, (2020).

4.4.4 Biosorption thermodynamics

Thermodynamic parameters ΔH° , ΔG° and ΔS° were used for calculating the spontaneity of adsorption. Equations 7 and 8 in chapter three were employed. The free energy change indicates how spontaneous the adsorption process is, with a higher (-) negative value indicating a more energetically advantageous adsorption (Joshi *et al.*, 2020). The value of free energy ΔG° , ΔH° and ΔS° calculated from the slope and intercept of the plot of $\ln K_L$ against $1/T$ as given in equation (9) in chapter three. The value of ΔH° and ΔS° are tabulated in Table 4.6. The specific heat capacity of copper, nickel, and zinc are 0.4 J/gK, 0.44J/gK and 0.387 J/gk respectively.

Table 4.6: Thermodynamic parameters for adsorption of Cu (II), Ni (II) and Zn (II) on to *Pavonia urens* leaves

Heavy metals	T (K)	ΔG° (kJ/mol)	ΔH° (kJ/mol)	ΔS° (J/mol K)
Cu	298	-2.150	-10.21	-24.77
	300	-2.950		
Ni	298	-1.920	-13.4	-33.55
	300	-2.487		
Zn	298	-2.32	-16.05	-45.05
	300	-3.525		

From Table 4.6, negative ΔG° values revealed clearly the spontaneous character of the adsorption process and limited biosorption feasibility at extremely high temperatures.

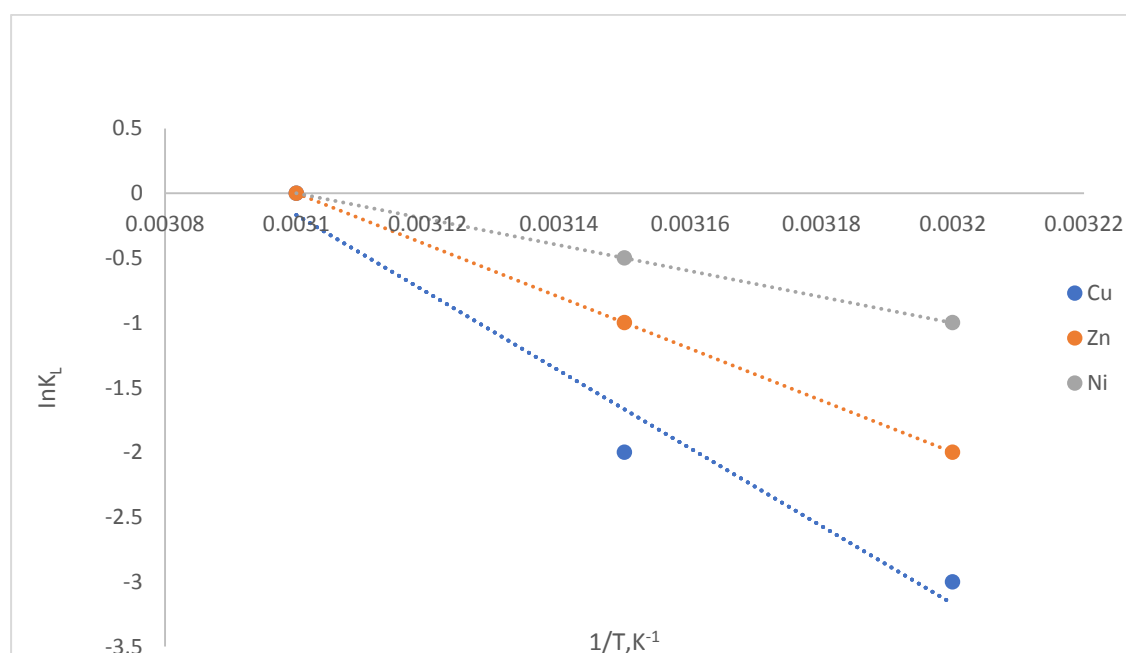


Figure 4.15: Plot of $\ln K_L$ vs $1/T$ for estimation of thermodynamic parameters

The exothermic nature of the adsorption was suggested by the negative values of ΔH° . Therefore, the adsorption process is spontaneous since both ΔH° and ΔG° are negative. The temperatures involved are low. ΔG° values are negative, involved charge transfer from sorbent surface to the metal ion to form coordination bond. The lower free energy values imply that the adsorption process is feasible. The change in entropy ΔS° values that are negative suggests that the sorption is enthalpy-governed rather than entropy-governed. It demonstrated that the freedom of metal ions is not too restricted at the adsorbent surface. These results are in agreement to those of Jayan, (2021).

CHAPTER FIVE

CONCLUSION AND RECOMMENDATION

5.1 Conclusions

Solvent extraction of the *Pavonia urens* leaves using hexane, dichloromethane, ethyl acetate and methanol resulted in four fractions labelled 1A, 2A, 3A and 4A. The major compounds identified in fractions were as Bacteriochlorophyll-C-stearyl (fraction 1A), cyclopentane carboxylic acid,3-(3-fluorophylcarbonyl)-1,2,2-trimethyl (fraction 2A),phenol,2-methoxy-4-methyl-6-(propenyl) (fraction 3A) and ascorbic acid 2,6-dihexadecanoate (fraction 4A).

Spectroscopy confirmed the production of complex chemicals in metal ion systems. There was a shift in wavelength of the plant material when metal ions were introduced. When copper and nickel (II) ions were introduced separately a blue-shift of wavelength was observed. In addition, there was decrease in absorption in both cases showing a shift of wavelength through coordination.

Pavonia urens demonstrated high efficiency for biosorption of metals from aqueous solutions. In this study, *p. urens* was able to remove 60 % of (Zn (II), 72% of Ni (II) and 86% of Cu (II) ions from aqueous solution.

The experimental data were represented using the Langmuir, Freundlich, and Temkin adsorption models, with the Langmuir isotherm model fitting the data well. The elimination of Cu (II), Ni (II), and Zn (II) from aqueous solution of *Pavonia urens* appeared to be spontaneous and exothermic, according to thermodynamic study.

This study revealed that the leaves of *Pavonia urens* could offer a potential adsorbent for an effective, cheap, available and ecofriendly method as a result of complexation

process with functional groups such as hydroxyl, amino, and carboxyl groups found in cell of plant material.

5.2 Recommendations

5.2.1 Recommendation from the study

Pavonia urens being an efficient biosorbant can be used to remove heavy metals from sewerage effluents

5.2.2 Recommendations for further study

1. Further work should be carried out to isolate other compounds which may be more bioactive.
2. The crude extracts and pure compounds should be evaluated for other biological activities such as anticancer and antimicrobial activities.
3. Further work should be carried out on biosorption of heavy metals pollutants and washing abilities using the plant material.

REFERENCES

- Abdel-GhANI, N. T., El-Chaghaby, G.A., Rawash, E.S.A., and Lima, E.C. (2017). 'Adsorption of Coomassie Brilliant Blue R-250 Dye onto Novel Activated Carbon Prepared from Nigella Sativa l. Waste: Equilibrium, Kinetics and Thermodynamics Running Title: Adsorption of Brilliant Blue Dye onto Nigella Sativa l. Waste Activated Carbon'. *Journal of the Chilean Chemical Society***62**(2):3505–11.
- Abdullah-Al-Mamun, M. (2021). Ecological and health risk assessments of fishes in industrial contaminated water of Bangladesh, Bangladesh University of Engineering and Technology, 2021.
- Achieng', A. O., Raburu, P. O., Kipkorir, E. C., Ngodhe, S. O., Obiero, K. O., and Ani-Sabwa, J. (2017). Assessment of water quality using multivariate techniques in River Sosiani, Kenya. *Environmental monitoring and assessment*, **189**, 1-13.
- Adebisi, I.M., and Alebiosu, O.C. (2014). 'A survey of herbal abortifacients and Contraceptives in Sokoto, North-West Nigeria.' *Age (Yrs)***21**(30):31–40.
- adsorbents: a critical review. *Chemosphere***204**,413–430.
- Ahmadpour, P., Ahmadpour, F., Mahmud, T. M. M., Abdu, A., Soleimani, M., and Tayefeh, F. H. (2012). Phytoremediation of heavy metals: A green technology. *African Journal of Biotechnology*, **11**(76), 14036-14043.
- Akenga, T., Ayabei, K., Kerich, E., Sudoi, V., and Kuya, C. (2020). Evaluation of levels of selected heavy metals in kales, soils and water collected from irrigated farms along river Moiben, Uasin-Gishu County, Kenya. *Journal of Geoscience and Environment Protection*, **8**(02), 144.
- Akenga, T., Sudoi, V., Machuka, W., and Kerich, E. (2016). Heavy Metal Concentrations in Agricultural Farms in Homa Hills Homa Bay County, Kenya
- Alaboudi, K. A., Ahmed, B., and Brodie, G. (2018). Phytoremediation of Pb and Cd contaminated soils by using sunflower (*Helianthus annuus*) plant. *Annals of agricultural sciences*, **63**(1), 123-127.

- Alara, O. R., Abdul Mudalip, S. K., and Olalere, O. A. (2017). Optimization of mangiferin extracted from *Phaleria macrocarpa* fruits using response surface methodology. *J. Appl. Res. Med. Aroma*, **5**, 82–87.
- Ali, E. N., and Seng, H. T. (2018). Heavy metals (Fe, Cu, and Cr) removal from wastewater by *Moringa oleifera* press cake. MATEC Web of Conferences, EDP Sciences
- Ali, H., Khan, E., and Ilahi, I. (2019). Environmental chemistry and ecotoxicology of hazardous heavy metals: environmental persistence, toxicity, and bioaccumulation. *Journal of chemistry*, 2019
- Alorabi, A. Q., Hassan, M. S., and Azizi, M. (2020). Fe₃O₄-CuO-activated carbon composite as an efficient adsorbent for bromophenol blue dye removal from aqueous solutions. *Arabian Journal of Chemistry*, **13**(11), 8080-8091.
- Albuquerque, J. B. L. D., Silva, C. M. D., Fernandes, D. A., Souza, V. D., and Souza, V. D. (2022). *Pavonia Cav.* Species (Malvaceae sensu lato) as source of new drugs: A review. *Química Nova*, **45**, 977-993.
- Alugoju, P., Narsimulu, D., Bhanu, J.U., Satyanarayana, N., and Periyasamy, L. (2019). Role of quercetin and caloric restriction on the biomolecular composition of aged rat cerebral cortex: An FTIR study. *Spectrochemical Acta Part A: Molecular and Biomolecular Spectroscopy* **220**, 117-128.
- Aman, A., Ahmed, D., Asad, N., Masih, R., and Rahman, H. M. (2018). Rose biomass as a potential biosorbent to remove chromium, mercury and zinc from contaminated waters. *International Journal of Environmental Studies*, **75**(5), 774-787.
- Anjos, F. S., Vieira, E. F., and Cestari, A. R. (2002). Interaction of indigo carmine dye with chitosan evaluated by adsorption and thermochemical data. *Journal of Colloid and Interface Science*, **325** (2), 243-246.
- Aransiola, S. A., Ijah, U. J. J., Peter, A. O., and Bala, J. D. (2019). Microbial-aided phytoremediation of heavy metals contaminated soil.
- Arao, T., Ishikawa, S., Murakami, M., Abe, K., Maejima, Y., and Makino, T. (2010). Heavy metal contamination of agricultural soil and countermeasures in Japan. *Paddy and water Environment*, **8**(3), 247-257.

- Aravindhan, R., Rao, J. R., and Nair, B. U. (2007). "Removal of basic yellow dye from aqueous solution by sorption on green alga *Caulerpa scalpelliformis*", *J. Hazard. Mater.*, **142**, 68–76.
- Arun, J., Sushma, R., Darshan, B. S., and Pandimadevi, M. (2018). Chemically enhanced coffee husks as biosorbents for the removal of copper and nickel ions from aqueous solutions: study on kinetic parameters. *Desalination and Water Treatment*, **121**, 291-304.
- Asgari L, B., Khadem M, N., Maghsoodi, M, R., Ghorbanpour, M., and Kariman, K. (2019). Phytoextraction of heavy metals from contaminated soil, water and atmosphere using ornamental plants: mechanisms and efficiency improvement strategies. *Environmental Science and Pollution Research*, **26**(9), 8468-8484.
- Awa, S. H., and Hadibarata, T. (2020). Removal of heavy metals in contaminated soil by phytoremediation mechanism: a review. *Water, Air, & Soil Pollution*, **231**(2), 1-15.
- Ayabei, K., and Kituyi, L. (2013). Comparative study of rates of biosorption for Beads. *ACS Omega***5**, 17215–17222
- Aziz, H., Gaspers, S., Mackenzie, S., Mattei, N., Narodytska, N., and Walsh, T. (2015). Equilibria under the probabilistic serial rule. binding mechanism, equilibrium and kinetics. *Colloids and Surfaces A: Physicochemical and Engineering Aspects*, **299**(1-3), 146-152.
- Bhagure, G. R., and Mirgane, S. R. (2011). Heavy metal concentrations in groundwaters and soils of Thane Region of Maharashtra, India. *Environmental monitoring and assessment*, **173**(1), 643-652.
- Bhatti, H. N., Mumtaz, B., Hanif, M. A., and Nadeem, R. (2007). Removal of Zn (II) ions from aqueous solution using *Moringa oleifera* Lam. (horseradish tree) biomass. *Process Biochem.* **42**, 547–553.
- Bickelhaupt, F. M., and Baerends, E. J. (2003). The case for steric repulsion causing the staggered conformation of ethane. *Angewandte Chemie*, **115**(35), 4315-4320.
- Bishnoi, N. R., Kumar, R., Kumar, S., and Rani, S. (2007). Biosorption of Cr (III) from aqueous solution using algal biomass *spirogyra* spp. *Journal of Hazardous Materials*, **145**(1-2), 142-147.

- Bobade, V., and Eshtiagi, N. (2015). Heavy metals removal from wastewater by adsorption process: A review. In *Asia Pacific Confederation of Chemical Engineering Congress*.
- Bosire, G. O. (2014). *Rehabilitation and phytoremediation of heavy metal polluted riverine wetlands using bamboo for Phytoextraction in Kibera* (Doctoral dissertation, Kenyatta University).
- Bradl, H. B. (2005). Sources and origins of heavy metals. In *Interface science and technology* (Vol. 6, pp. 1-27).
- Burns, R. G., DeForest, J. L., Marxsen, J., Sinsabaugh, R. L., Stromberger, M. E., Wallenstein, M. D., and Zoppini, A. (2013). Soil enzymes in a changing environment: current knowledge and future directions. *Soil Biology and Biochemistry*, **58**, 216-234.
- Ćaćić, M., Perčin, A., Zgorelec, Ž., and Kisić, I. (2019). Evaluation of heavy metals accumulation potential of hemp (*Cannabis sativa* L.). *Journal of Central European Agriculture*, **20**(2), 700-711.
- Cai, X. X., Hong, Y. X., Wang, S. Y., Zhao, L. N., and Rao, P. F. (2015). Purification and enzymatic characteristics of a novel polyphenol oxidase from lotus seed (*Nelumbo nucifera* Gaertn.). *International Journal of Food Science & Technology*, **50**(4), 1026-1032.
- Çelebi, H., Gök, G., and Gök, O. (2020). Adsorption capability of brewed tea waste in waters containing toxic lead (II), cadmium (II), nickel (II), and zinc (II) heavy metal ions. *Scientific reports*, **10**(1), 1-12
- Chanda, S., Paul, B. N., Ghosh, K., and Giri, S. S. (2015). Dietary essentiality of trace minerals in aquaculture-A Review. *Agricultural Reviews*, **36**(2), 100-112.
- Chatterjee, S., Chatterjee, B. P., and Guha, A. K. (2007). Adsorptive removal of Congo red, a carcinogenic textile dye by chitosan hydrobeads: *Chemical Engineering*, **1**(4), 884-890.
- Chen, H., Gu, X., Su, I. H., Bottino, R., Contreras, J. L., Tarakhovsky, A., and Kim, S. K. (2009). Polycomb protein Ezh2 regulates pancreatic β -cell Ink4a/Arf expression and regeneration in diabetes mellitus. *Genes & development*, **23**(8), 975-985.

- Cieřlik, B.M., Namieřnik, J., and Konieczka, P. (2015). 'Review of Sewage Sludge Management: Standards, Regulations and Analytical Methods'. *Journal of Cleaner Production* **90**:1–15.
- Corradini, E., Foglia, P., Giansanti, P., Gubbiotti, R., Samperi, R., and Lagana, A. (2011). Flavonoids: chemical properties and analytical methodologies of identification and quantitation in foods and plants. *Natural product research*, **25**(5), 469-495.
- Crabtree, R. H. (2009). *The organometallic chemistry of the transition metals*. John Wiley & Sons.
- Cristaldi, A., Copat, C., Conti, G. O., Zuccarello, P., Grasso, A., and Ferrante, M. (2020). Phytoremediation. In *The Handbook of Environmental Remediation* (pp. 268-298).
- Dalvi, A. A., and Bhalerao, S. A. (2013). Response of plants towards heavy metal toxicity: an overview of avoidance, tolerance and uptake mechanism. *Ann Plant Sci*, **2**(9), 362-368.
- Daochalermwong, A., Chanka, N., Songsrirote, K., Dittanet, P., Niamnuy, C., and Seubsai, A. (2020). Removal of heavy metal ions using modified celluloses prepared from pineapple leaf fiber. *Acs Omega*, **5**(10), 5285-5296.
- de Boer, H. J., Kool, A., Broberg, A., Mziray, W. R., Hedberg, I., and Levenfors, J. J. (2005). Anti-fungal and anti-bacterial activity of some herbal remedies from Tanzania. *Journal of ethnopharmacology*, **96**(3), 461-469.
- Debnath, B., Haldar, D., and Purkait, M. K. (2021). Potential and sustainable utilization of tea waste: A review on present status and future trends. *Journal of Environmental Chemical Engineering*, **9**(5), 106179.
- Demirbas, A. (2008). Heavy metal adsorption onto agro-based waste materials: a review. *Journal of hazardous materials*, **157**(2-3), 220-229.
- Dev, S., Khamkhash, A., Ghosh, T., and Aggarwal, S. (2020). Adsorptive removal of Se (IV) by Citrus peels: Effect of adsorbent entrapment in calcium alginate beads. *ACS omega*, **5**(28), 17215-17222.
- Dey, S., Haripavan, N., Basha, S.R., and Babu, G.V. (2021). 'Removal of Ammonia and Nitrates from Contaminated Water by Using Solid Waste Bio-Adsorbents'. *Current Research in Chemical Biology* 100005.

- Dhaliwal, S. S., Singh, J., Taneja, P. K., and Mandal, A. (2020). Remediation techniques for removal of heavy metals from the soil contaminated through different sources: a review. *Environmental Science and Pollution Research*, **27**(2), 1319-1333.
- Din, N.A.S., Lim, S.J., Maskat, M.Y., Abd Mutalib, S., and Zaini, N.A.M. (2021). 'Lactic Acid Separation and Recovery from Fermentation Broth by Ion-Exchange Resin: A Review'. *Bioresources and Bioprocessing***8**(1):1–23.
- Dinu, M. I., and Shkinev, V. M. (2020). Complexation of metal ions with organic substances of humus nature: methods of study and structural features of ligands, and distribution of elements between species. *Geochemistry International*, **58**(2), 200-211.
- Doddi, A., Peters, M., and Tamm, M. (2019). N-heterocyclic carbene adducts of main group elements and their use as ligands in transition metal chemistry. *Chemical reviews*, **119**(12), 6994-7112.
- Drynan, J. W., Clifford, M. N., Obuchowicz, J., and Kuhnert, N. (2010). The chemistry of low molecular weight black tea polyphenols. *Natural Product Reports*, **27**(3), 417-462.
- Dsikowitzky, L., Mengesha, M., Dadebo, E., de Carvalho, C. E. V., and Sindern, S. (2013). Assessment of heavy metals in water samples and tissues of edible fish species from Awassa and Koka Rift Valley Lakes, Ethiopia. *Environmental monitoring and assessment*, **185** (4), 3117-3131.
- Dubey, S. P., Sillanpaa, M., and Varma, R. S. (2017). Reduction of hexavalent chromium using *Sorbaria sorbifolia* aqueous leaf extract. *Appl. Sci.* **7**.
- Ebrahimi, M. (2014). Effect of EDTA and DTPA on phytoremediation of Pb-Zn contaminated soils by *Eucalyptus camaldulensis* Dehnh and Effect on Treatment Time. *Desert*, **19**(1), 65-73.
- Emmy K., Akenga, T., Ayabei Kiplagat, Vincent Sudoi, Cyrus Kuya,(2019). Investigation of Selected Heavy Metal Ions in Irrigation Water, Soil and Managu (*Solanum Nigrum*) from Homahills, Homabay County, Kenya, *Journal of Health and Environmental Research*.

- Evangelou, M. W., Bauer, U., Ebel, M., and Schaeffer, A. (2007). The influence of EDDS and EDTA on the uptake of heavy metals of Cd and Cu from soil with tobacco *Nicotiana tabacum*. *Chemosphere*, **68**(2), 345-353.
- Fahim, M., Shrivastava, B., Shrivastava, A. K., Ibrahim, M., Parveen, R., and Ahmad, S. (2017). Review on extraction methods, antioxidant and antimicrobial properties of volatile oils. *Ann. Phytomed*, **6**(2), 5-46.
- Fatima, S., Muzammal, M., Rehman, A., Rustam, S. A., Shehzadi, Z., Mehmood, A., and Waqar, M. (2020). Water pollution on heavy metals and its effects on fishes. *International Journal of Fisheries and Aquatic Studies*, **8**(3), 6-14.
- Flores-Garnica, J. G., Morales-Barrera, L., Pineda-Camacho G., Cristiani- Urbina, E. (2013). "Biosorption of Ni (II) from aqueous solutions by *Litchi chinensis* seeds", *Bioresource Technol.*, **136**, 635-643.
- Gardea-Torresdey, J. L., Tiemann, K.J., Armendariz, V., Bess-Oberto, L., Chianelli, R.R., Rios, J., Parsons, M., and Gamez, G. (2000). 'Characterization of Cr (VI) Binding and Reduction to Cr (III) by the Agricultural Byproducts of *Avena Monida* (Oat) Biomass'. *Journal of Hazardous Materials* **80**(1-3):175-88.
- Gasca, C. A., Fabio, A. C., Laura, T., Jaume, B., and Carles, C. (2013). 'Chemical Composition and Antioxidant Activity of the Ethanol Extract and Purified Fractions of *Cadillo (Pavonia Sepioides)*'. *Free Radicals and Antioxidants. Geoscience and Environment Protection*, **8**(02), 144.
- Gill, M. (2014). Heavy metal stress in plants: a review. *Int J Adv Res*, **2**(6), 1043-1055.
- Githaiga, K. B., Njuguna, S. M., Gituru, R. W., and Yan, X. (2021). Water quality assessment, multivariate analysis and human health risks of heavy metals in eight major lakes in Kenya. *Journal of Environmental Management*, **297**, 113410.
- Githitho, A. N. (2021). 'Annotated Checklist of the Plants of Arabuko-Sokoke Forest, Coastal Kenya'. *Journal of East African Natural History* **110**(1):13-74.
- Gopalakrishnan, K., Manivannan, V., and Jeyadoss, T. (2010). Comparative study on biosorption of Zn (II), Cu (II) and Cr (VI) from textile dye effluent using sawdust and neem leaves powder. *E-Journal of Chemistry*, **7**(S1), S504-S510.

- Goyal, D., Yadav, A., Prasad, M., Singh, T.B., Shrivastav, P., Ali, A., Dantu, P.K., and Mishra, S. (2020). Effect of heavy metals on plant growth: an overview. *Contaminants in agriculture*, pp.79-101.
- Grzelczak, M., Sánchez-Iglesias, A., Mezerji, H. H., Bals, S., Pérez-Juste, J., and Liz-Marzán, L. M. (2012). Steric hindrance induces crosslike self-assembly of gold nanodumbbells. *Nano letters*, **12**(8), 4380-4384.
- Gunatilake, S. K. (2015). 'Methods of Removing Heavy Metals from Industrial Wastewater'. *Methods* **1**(1):14.
- Gupta, K., Singh, R. P., Pandey, A., and Pandey, A. (2013). Photocatalytic antibacterial performance of TiO₂ and Ag-doped TiO₂ against *S. aureus*, *P. aeruginosa* and *E. coli*. *Beilstein journal of nanotechnology*, **4**(1), 345-351.
- Häder, D. P., Banaszak, A. T., Villafañe, V. E., Narvarte, M. A., González, R. A., and Helbling, E. W. (2020). Anthropogenic pollution of aquatic ecosystems: Emerging problems with global implications. *Science of the Total environment*, **713**, 136586.
- Hafshejani, L. D., Nasab, S. B., Gholami, R. M., Moradzadeh, M., Izadpanah, Z., Hafshejani, S. D., and Bhatnagar, A. (2015). Removal of Zinc and Lead from aqueous solution by nanostructured cedar leaf ash as biosorbent. *J. Mol. Liq.* **211**, 448–456.
- Hamadouche, N. A. (2012). Phytoremediation potential of *Raphanus sativus* L. for lead contaminated soil. *Acta Biologica Szegediensis*, **56**(1), 43-49.
- He, Z., Shentu, J., Yang, X., Baligar, V. C., Zhang, T., and Stoffella, P. J. (2015). Heavy metal contamination of soils: sources, indicators and assessment.
- Ho, Y. S., Huang, C. T., and Huang, H. W. (2002). "Equilibrium sorption isotherm for metal ions on tree fern", *Process Biochem.*, **37**, 1421–1430.
- Hokkanen, S., Repo, A., and Sillanpää, M. (2013). Removal of heavy metals from aqueous solutions by succinic anhydride modified mercerized nanocellulose. *Chemical engineering journal*, **223**, 40-47.
- Horsefall, M., and Spiff, I.A. (2005). Equilibrium Sorption Study of Al³⁺, Co²⁺ and Ag⁺ in Aqueous solutions by fluted pumpkin (*Telfairia Occidentalis* HOOK f). *Waste Biomass. Acta Chim. Slov.*, **52**: 174-181.

- Hseu, Z. Y., Su, S. W., Lai, H. Y., Guo, H. Y., Chen, T. C., and Chen, Z. S. (2010). Remediation techniques and heavy metal uptake by different rice varieties in metal-contaminated soils of Taiwan: new aspects for food safety regulation and sustainable agriculture. *Soil Science & Plant Nutrition*, **56**(1), 31-52.
- Iannitti, T., Capone, S., Gatti, A., Capitani, F., Cetta, F., and Palmieri, B. (2010). Intracellular heavy metal nanoparticle storage: progressive accumulation within lymph nodes with transformation from chronic inflammation to malignancy. *International Journal of Nanomedicine*, **5**, 955.
- Iftekhhar, S., Ramasamy, D.L., Srivastava, V., Asif, M.B., and Sillanpää, M. (2018). irrigated farms along river Moiben, Uasin-Gishu County, Kenya. *Journal of Imran, M., Rauf, A., Abu-Izneid, T., Nadeem, M., Shariati, M. A., Khan, I. A., ... and Mubarak, M. S. (2019). Luteolin, a flavonoid, as an anticancer agent: A review. Biomedicine & Pharmacotherapy*, **112**, 108612.
- Islam, M. M., Karim, M., Zheng, X., and Li, X. (2018). Heavy metal and metalloid pollution of soil, water and foods in bangladesh: a critical review. *International journal of environmental research and public health*, **15**(12), 2825.
- Jabeen, R., Ahmad, A., and Iqbal, M. (2009). Phytoremediation of heavy metals: physiological and molecular mechanisms. *The Botanical Review*, **75**(4), 339-364.
- Jaishankar, M., Staten, T., Anbalagan, N., Mathew, B. B., and Beeregowda, K. N. (2014). Toxicity, mechanism and health effects of some heavy metals. *Interdisciplinary toxicology*, **7**(2), 60-72.
- Jarup, L. (2003). Hazards of heavy metal contamination. *British medical bulletin*, **68**(1), 167-182.
- Jayan, N., Bhatlu, M. L. D., and Akbar, S. T. (2021). Central composite design for adsorption of Pb (II) and Zn (II) metals on PKM-2 Moringa oleifera leaves. *ACS omega*, **6**(39), 25277-25298.
- Joshi, S., Kataria, N., Garg, V. K., and Kadirvelu, K. (2020) Pb²⁺ and Cd²⁺ recovery from water using residual tea waste and SiO₂ TW nanocomposites. *Chemosphere*, **257**, 127277.

- Kahlon, S. K., Sharma, G., Julka, J. M., Kumar, A., Sharma, S., and Stadler, F. J. (2018). Impact of heavy metals and nanoparticles on aquatic biota. *Environmental chemistry letters*, **16**(3), 919-946.
- Kamau, L. K. (2018). 'Study of Extent of Use, Efficacy and Acute Toxic Effects of Selected Antidiabetic Plants in Nyeri and Narok Counties, Kenya'.
- Karahan, F., Ozyigit, I. I., Saracoglu, I. A., Yalcin, I. E., Ozyigit, A. H., and Ilcim, A. (2020). Heavy metal levels and mineral nutrient status in different parts of various medicinal plants collected from eastern Mediterranean region of Turkey. *Biological Trace Element Research*, **197**(1), 316-329.
- Kashima, Y., Paladino, A., and Margetts, E. A. (2014). Environmentalist identity and environmental striving. *Journal of environmental psychology*, **38**, 64-75.
- Kaur, N., and Nayyar, H. (2013). Heavy metal toxicity to food legumes: effects, antioxidative defense and tolerance mechanisms. *Journal of Food Legumes*, **26**(3and4), 1-18.
- Kausar, A., Nawaz, H. and Mackinnon, G., (2013). "Equilibrium, kinetic and thermodynamic studies on the removal of U (VI) by low-cost agricultural waste", *Colloids Surfaces B Bio interfaces* **111**, 124-133.
- Kaźmierczak, B., Molenda, J., and Swat, M. (2021). The adsorption of chromium (III) ions from water solutions on biocarbons obtained from plant waste. *Environmental Technology & Innovation*, **23**, 101737.
- Kenya.
- Khan, A., Khan, S., Khan, M. A., Qamar, Z., and Waqas, M. (2015). The uptake and bioaccumulation of heavy metals by food plants, their effects on plants nutrients, and associated health risk: a review. *Environmental science and pollution research*, **22**(18), 13772-13799.
- Khan, A. S., and Zhang, H. (2000). Mechanically alloyed nanocrystalline iron and copper mixture: behavior and constitutive modeling over a wide range of strain rates. *International journal of Plasticity*, **16**(12), 1477-1492.
- Khare, E., Holten-Andersen, A., and Buehler, M. J. (2021). Transition-metal coordinate bonds for bioinspired macromolecules with tunable mechanical properties. *Nature Reviews Materials*, **6**(5), 421-436.

- Kimenyu, P. N., Oyaró, N., Chacha, J. S., and Tsanuo, M. K. (2009). The potential of *Commelina bengalensis*, *Amaranthus hybridus*, *Zea mays* for phytoremediation of heavy metals from contaminated soils.
- Kırıs, E., and Baltas, H. (2021). Assessing pollution levels and health effects of heavy metals in sediments around Cayeli copper mine area, Rize, Turkey. *Environmental Forensics*, **22**(3-4), 372-384.
- Kosakivska, I. V., Babenko, L. M., Romanenko, K. O., Korotka, I. Y., and Potters, G. (2021). Molecular mechanisms of plant adaptive responses to heavy metals stress. *Cell Biology International*, **45**(2), 258-272.
- Kulkarni, R. M., Dhanyashree, J. K., Varma, E., and Sirivibha, S. P. (2022). Batch and continuous packed bed column studies on biosorption of nickel (II) by sugarcane bagasse. *Results in Chemistry*, **4**, 100328.
- Kwon, D. Y., Jin, S.J., Sang, M. H., Ji, E. L., So, R. S., Hye, R. P., and Sunnines, P. (2007). 'Long-Term Consumption of Fermented Soybean-Derived Chungkookjang Enhances Insulinotropic Action Unlike Soybeans in 90% Pancreatectomized Diabetic Rats'. *European Journal of Nutrition* **46**(1):44–52. doi: 10.1007/s00394-006-0630-y.
- Lakshmi, B.A., Bae, J. A., and Kim, S. (2019). Facile design and spectroscopic characterization of novel bioinspired Quercetin-conjugated tetracids (dimethyl sulfoxide) dichlororuthenium (II) complex for enhanced anticancer properties. *Inorganica Chimica Acta*, **495**, <https://doi.org/10.1021/cr400460s>.
- Lalah, J. O., Ochieng, E. Z., and Wandiga, S. O. (2008). Sources of heavy metal input into Winam Gulf, Kenya. *Bulletin of Environmental Contamination and Toxicology*, **81**(3), 277-284.
- Landrigan, P. J., Fuller, R., Fisher, S., Suk, W. A., Sly, P., Chiles, T. C., and Bose-O'Reilly, S. (2019). Pollution and children's health. *Science of the Total Environment*, **650**, 2389-2394.
- layer on the activated biocarbons surface—electrokinetic and stability studies.
- Leal-Filho, W., Tripathi, S. K., Andrade-Guerra, J. D., Giné-Garriga, R., Orlovic-Lovren, V., and Willats, J. (2019). Using the sustainable development goals towards a better understanding of sustainability challenges. *International Journal of Sustainable Development & World Ecology*, **26**(2), 179-190.

- Liakos, D. G., Manuel, S., Manoj, K. K., Jan, M. M., and Frank, N. (2015). 'Exploring the Accuracy Limits of Local Pair Natural Orbital Coupled-Cluster Theory'. *Journal of Chemical Theory and Computation***11**(4):1525–39.
- Liu, G. C., Chen, N. L., Zhang, J. W., Qu, Y., Lin, H. Y., and Gao, X. J. (2014). Effects of Metal Ions and N-Donor Ligands with Different Coordination Characters on the Construction of d10 Metal-organic Complexes with Selective Photocatalytic Activities. *Zeitschrift für Naturforschung B*, **69**(6), 681-690.
- Liu, L., Li, W., Song, W., and Guo, M. (2018). Remediation techniques for heavy metal-contaminated soils: Principles and applicability. *Science of the Total Environment*, **633**, 206-219.
- Lopes, L. G., Gabriela, L. T., Luciana, D. T., José, R. S., Keyller, B.B., Paulo, C.V., Thiago A. M. V., and Warley, S. B. (2016). 'Taraxerol 4-Methoxybenzoate, an in Vitro Inhibitor of Photosynthesis Isolated from *Pavonia Multiflora* A. St-Hil. (Malvaceae)'. *Chemistry & Biodiversity***13**(3):284–92.
- Mabhungu, L., Adam, E., and Newete, S. W. (2019). Monitoring of Phyto remediating Wetland Macrophytes Using Remote Sensing: The Case of Common Reed (*Phragmites Australis* (Cav.) Trin. Ex Steud.) And The Giant Reed (*Arundo Donax* L.). A. *Applied Ecology and Environmental Research*, **17**(4), 7957-7972.
- Madasamy, K., Kumaraguru, S., Sankar, V., Mannathan, S., and Kathiresan, M. (2019). A Zn based metal organic framework as a heterogeneous catalyst for C–C bond formation reactions. *New Journal of Chemistry*, **43**(9), 3793-3800.
- Mangum, B. W., Furukawa, G. T., Kreider, K. G., Meyer, C. W., Ripple, D. C., Strouse, G. F., and Saunders, R. D. (2001). The Kelvin and temperature measurements. *Journal of Research of the National Institute of Standards and Technology*, **106**(1), 105.
- Manirethan, V., Raval, K., Rajan, R., Thaira, H., and Balakrishnan, R. M. (2018). Kinetic and thermodynamic studies on the adsorption of heavy metals from aqueous solution by melanin nano pigment obtained from marine source: *Pseudomonas stutzeri*. *J. Environ. Manage.* **214**, 315–324.

- Masindi, V., and Muedi, K. L. (2018). Environmental contamination by heavy metals. *Heavy metals*, **10**, 115-132.
- Masoko, P., and Makgapeetja, D. M. (2015). 'Antibacterial, Antifungal and Antioxidant Activity of Olea Africana against Pathogenic Yeast and Nosocomial Pathogens'. *BMC Complementary and Alternative Medicine* **15**(1). doi: 10.1186/s12906-015-0941-8.
- Matindi, C. N., Njogu, P. M., Kinyua, R., and Nemoto, Y. (2022). Analysis of heavy metal content in water hyacinth (*Eichhornia crassipes*) from Lake Victoria, Kenya. In *Proceedings of the Sustainable Research and Innovation Conference* (pp. 196-199).
- Mathiyalagan, S., and Mandal, B. K. (2020). Stability Comparison of Quercetin and its Metal Complexes and their Biological Activity.
- Medhi, H., Chowdhury, P. R., Baruah, P. D., and Bhattacharyya, K. G. (2020). Kinetics of Aqueous Cu (II) Biosorption onto *Thevetia peruviana* Leaf Powder. *ACS*, **5**, 13489–13502.
- Mehes-Smith, M., Nkongolo, K., and Cholewa, E. (2013). Coping mechanisms of plants to metal contaminated soil. *Environmental change and sustainability*, **54**, 53-90.
- Melčáková, I., and Růžovič, T. O. (2010). Biosorption of zinc from aqueous solution using algae and plant biomass. *Nova Biotechnologica*, **10**(1), 33-43.
- Mocanu, V., Zhang, Z., Deehan, E. C., Kao, D. H., Hotte, N., Karmali, S., and Madsen, K. L. (2021). Fecal microbial transplantation and fiber supplementation in patients with severe obesity and metabolic syndrome: a randomized double-blind, placebo-controlled phase 2 trial. *Nature Medicine*, **27**(7), 1272-1279.
- Mojiri, A., Aziz, H. A., Zahed, M. A., Aziz, S. Q., and Selamat, R. B. (2013). Phytoremediation of heavy metals from urban waste leachate by southern cattail (*Typha domingensis*). *International Journal of Scientific Research in Environmental Sciences*, **1**(4), 63-70.
- Mus, A. A., Goh, L. P. W., Marbawi, H., and Gansau, J. A. (2022). The Biosynthesis and Medicinal Properties of Taraxerol. *Biomedicines*, **10**(4), 807.

- Muszynska, E., and Hanus-Fajerska, E. (2015). Why are heavy metal hyperaccumulating plants so amazing? *BioTechnologia. Journal of Biotechnology Computational Biology and Bionanotechnology*, **96**(4)..
- Muthusaravanan, S., Sivarajasekar, N., Vivek, J. S., Paramasivan, T., Naushad, M., Prakashmaran, J., and Al-Duaij, O. K. (2018). Phytoremediation of heavy metals: mechanisms, methods and enhancements. *Environmental chemistry letters*, **16**(4), 1339-1359.
- Mwandira, W., Nakashima, K., Togo, Y., Sato, T., and Kawasaki, S. (2020). Cellulose-metallothionein biosorbent for removal of Pb (II) and Zn (II) from polluted water. *Chemosphere* **246**, 125733.
- Mwegoha, W. J. (2008). The use of phytoremediation technology for abatement soil and groundwater pollution in Tanzania: opportunities and challenges. *Journal of sustainable development in Africa*, **10**(1), 140-156.
- Nayak, S. N., Aravind, B., Malavalli, S. S., Sukanth, B. S., Poornima, R., Bharati, P., and Puppala, N. (2021). Omics Technologies to Enhance Plant Based Functional Foods: An Overview. *Frontiers in Genetics*, **12**, 742095-742095.
- Novakova, V., Donzello, M. P., Ercolani, C., Zimcik, P., and Stuzhin, P. A. (2018). Tetrapyrazinoporphyrazines and their metal derivatives. Part II: Electronic structure, electrochemical, spectral, photophysical and other application related properties. *Coordination Chemistry Reviews*, **361**, 1-73.
- Ndeda, L. A., and Manohar, S. (2014). Bio concentration factor and translocation ability of heavy metals within different habitats of hydrophytes in Nairobi Dam, Kenya. *J Environ Sci Toxicol Food Technol*, **8**(5), 42-45.
- Ngabura, M., Hussain, S. A., Ghani, W. A. W., Jami, M. S., and Tan, Y. P. (2018). Utilization of renewable durian peels for biosorption of zinc from wastewater. *Journal of Environmental Chemical Engineering*, **6**(2), 2528-2539.
- Nzeve, J. K., Kitur, E. C., and Njuguna, S. G. (2018). Determination of heavy metals in sediments of Masinga Reservoir, Kenya.
- Ofudje, E. A., Adedapo, A. E., Oladeji, O. B., Sodiya, E. F., Ibadin, F. H., and Zhang, D. (2021). Nano-Rod Hydroxyapatite for the uptake of Nickel Ions: Effect of Sintering Behaviour on Adsorption Parameters. *J. Environ. Chem. Eng.* **9**, 105931.

- Olaniran, A. O., Balgobind, A., and Pillay, B. (2013). Bioavailability of heavy metals in soil: impact on microbial biodegradation of organic compounds and possible improvement strategies. *International journal of molecular sciences*, **14**(5), 10197-10228.
- Oleksińska, Z. (2015). Plants on duty—phytotechnologies and phytoremediation at a glance. *Acta Universitatis Lodzianensis. Folia Biologica et Oecologica*, **11**, 23-29.
- Oluoch, J. O. (2018). Phytoremediation Potential of *Cyperus Alternifolius*, *Cyperus Dives* and *Canna Indica* in Flamingo Farm Constructed Wetland, Naivasha Sub-County, Kenya (Doctoral dissertation, School of Environmental Studies, Kenyatta University).
- Orao, L. A. (2020). Diversity, Heavy Metal Concentration and Phytoremediation Potential of Wild Plants Species Naturally Growing on Kang’oki Dumpsite, Thika, Kenya (Doctoral dissertation, Chuka University).
- Park, H. L., Xuexian, O. Y., Seon, H. C., Roza, N., Yi-Hong, W., Ying, W., Leroy, H.Z., and Qiang, T. (2005). ‘A Distinct Lineage of CD4 T Cells Regulates Tissue Inflammation by Producing Interleukin 17’. *Nature Immunology***6**(11):1133–41.
- Parmar, S., and Singh, V. (2015). Phytoremediation approaches for heavy metal pollution: a review. *J Plant Sci Res*, **2**(2), 135
- Paul, J. M., Jimmy, J., Therattil, J. M., Regi, L., and Shahana, S. (2017). Removal of heavy Metals Using Low-Cost Adsorbents. *IOSR J Mech Civ Eng*, **14**(03), 48-50
- Petruzzelli, G., Pedron, F., Rosellini, I., and Barbaferi, M. (2013). Phytoremediation towards the future: focus on bioavailable contaminants. In *Plant-based remediation processes* (pp. 273-289). Springer, Berlin, Heidelberg.
- Piccin, J. S., Vieira, M. L. G., Gonçalves, J. O., Dotto, G. L., and Pinto, L. A. D. A. (2009). Adsorption of FD&C Red No. 40 by chitosan: Isotherms analysis. *Journal of Food Engineering*, **95**(1), 16-20.
- Pinter, B., Fievez, T., Bickelhaupt, F. M., Geerlings, P., and De- Proft, F. (2012). On the origin of the steric effect. *Physical Chemistry Chemical Physics*, **14**(28), 9846-9854.

- Porter, S. K., Scheckel, K. G., Impellitteri, C. A., and Ryan, J. A. (2004). Toxic metals in the environment: thermodynamic considerations for possible immobilization strategies for Pb, Cd, As, and Hg. *Critical reviews in environmental science and technology*, **34**(6), 495-604.
- Prakash, J. (2021). Potential application of endophytes in bioremediation of heavy metals and organic pollutants and growth promotion: mechanism, challenges, and future prospects. In *Bioremediation for Environmental Sustainability* (pp. 91-121). Elsevier.
- Priya, S. V., and Arulmozhi, M. (2012). Biosorbents for toxic heavy metals-A review. In *IEEE-International Conference on Advances in Engineering, Science and Management (ICAESM-2012)* (pp. 221-230). IEEE.
- Qasem, N. A., Ramy, H. M., and Dahiru, U. L. (2021). 'Removal of Heavy Metal Ions from Wastewater: A Comprehensive and Critical Review'. *Npj Clean Water***4**(1):1–15.
- Qureshi, S. A., Asad, W., and Sultana, V. (2009). The effect of *Phyllanthus emblica* Linn on type-II diabetes, triglycerides and liver-specific enzyme. *Pakistan Journal of Nutrition*, **8**(2), 125-128.
- Rajendran, S., Priya, T. K., Khoo, K. S., Hoang, T. K., Ngu, H. S., Munawaroh, S. H., and Show, P. L. (2022). A critical review on various remediation approaches for heavy metal contaminants removal from contaminated soils. *Chemosphere*, **287**, 132369.
- Rahimzadeh, Z., Naghib, S. M., Zare, Y., and Rhee, K. Y. (2020). An overview on the synthesis and recent applications of conducting poly (3, 4-ethylenedioxythiophene) (PEDOT) in industry and biomedicine. *Journal of materials science*, **55**, 7575-7611.
- Rasheed, T., and Nabeel, F. (2019). Luminescent metal-organic frameworks as potential sensory materials for various environmental toxic agents. *Coordination Chemistry Reviews*, **401**, 213065.
- Rathna, R., Varjani, S., and Nakkeeran, E. (2019). Sequestration of heavy metals from industrial wastewater using composite ion exchangers. In *Applications of Ion Exchange Materials in the Environment* (pp. 187-204). Springer, Cham.

- Rathore, S. S., Shekhawat, K., Dass, A., Kandpal, B. K., and Singh, V. K. (2019). Phytoremediation mechanism in Indian mustard (*Brassica juncea*) and its enhancement through agronomic interventions. *Proceedings of the National Academy of Sciences, India Section B: Biological Sciences*, **89**(2), 419-427.
- Ratié, G., Chrastny, V., Guinoiseau, D., Marsac, R., Vaňková, Z., and Komárek, M. (2021). Cadmium isotope fractionation during complexation with humic acid. *Environmental Science & technology*, **55**(11), 7430-7444.
- Reddy, D. H., Sessaiah, K., Reddy, A. V., Rao, M. M., and Wang, M. C. (2010). Biosorption of Pb^{2+} from aqueous solutions by *Moringa oleifera* bark: equilibrium and kinetic studies. *J. Hazard. Mater.* **174**, 831– 838.
- Rehman, K., Fatima, F., Waheed, I., and Akash, M. H. (2018). Prevalence of exposure of heavy metals and their impact on health consequences. *Journal of cellular biochemistry*, **119**(1), 157-184.
- Rioux, R. M. (2017). Influence of Multi-Valency, Electrostatics and Molecular Recognition on the Adsorption of Transition Metal Complexes on Metal Oxides: A Molecular Approach to Catalyst Synthesis (No. DOE-PSU-16364-3). Pennsylvania State Univ., University Park, PA (United States).
- Safford, H. D., and Vallejo, V. R. (2019). Ecosystem management and ecological restoration in the Anthropocene: integrating global change, soils, and disturbance in boreal and Mediterranean forests. In *Developments in Soil Science* (Vol. **36**, pp. 259-308).
- Saif, S., Tahir, A., Asim, T., and Chen, Y. (2016). Plant mediated green synthesis of CuO nanoparticles: comparison of toxicity of engineered and plant mediated CuO nanoparticles towards *Daphnia magna*. *Nanomaterials* **6**, 1–15.
- Sajidu, S. M., Henry, E. M. T., Kwamdera, G., and Mataka, L. (2005). Removal of lead, iron and cadmium ions by means of polyelectrolytes of the *Moringa oleifera* whole seed kernel. *WIT Trans. Ecol. Environ.* **80**, 251–258.
- Sajidu, S. M., Persson, I.I., Masamba, W.R.L., Henry, E.M.T., and Kayambazinthu, D.D. (2006). 'Removal of Cd^{2+} , Cr^{3+} , Cu^{2+} , Hg^{2+} , Pb^{2+} and Zn^{2+} Cations and AS_4O_3 -Anions from Aqueous Solutions by Mixed Clay from Tundulu in Malawi and Characterizations of the Clay'. *Water Sa***32**(4):519–26.

- Sao, K., Khan, F., Pandey, P. K., and Pandey, M. (2016). Equilibrium isotherm study for removal of Mn (II) from aqueous solutions by using novel bioadsorbent *Tinospora cordifolia*. *Advances in Research*, **6**(4), 1-11.
- Sari, A. and Tuzen M. (2009). “Kinetic and equilibrium studies of biosorption of Pb (II) and Cd (II) from aqueous solution by macrofungus (*Amanita rubescens*) biomass” *Journal of Hazardous Materials*, **164**, 1004–1011.
- Sarvalingam, A., Dhaarani, V., Pavithra, C., Sharmila, S., and Rajendran, A. (2017). Inventory and ethnomedicinal plants used by rural people of Eastern Ghats of Tamil Nadu, India. *Journal of Ecobiotechnology*, **9**.
- Sarwar, N., Imran, M., Shaheen, M.R., Ishaque, W., Kamran, M.A., Matloob, A., Rehim, A., and Hussain, S. (2017). Phytoremediation strategies for soils contaminated with heavy metals: modifications and future perspectives. *Chemosphere*, **171**, pp.710-721.
- Scerri, E. R. (2011). The periodic table: A very short introduction (Vol. **289**). Oxford University Press.
- Senthikumar, S. R., and Sivakumar, T. (2014). Green tea (*Camellia sinensis*) mediated synthesis of zinc oxide (ZnO) nanoparticles and studies on their antimicrobial activities. *Int. J. Pharm. Pharm. Sci*, **6**(6), 461-465.
- Shinde, A. B., and Mulay, Y. R. (2015). ‘Phytochemical Analysis and Antibacterial Properties of Some Selected Indian Medicinal Plants’. *International Journal of Current Microbiology and Applied Sciences* **4**(3):228–35.
- Shoaib, A., Badar, T., and Aslam, N. (2011). Removal of Pb (II), Cu (II) and Cd (II) from aqueous solution by some fungi and natural adsorbents in single and multiple metal systems. *Pak J Bot*, **43**, 2997-3000.
- Shrivastava, S. (2010). ‘Evaluation of Ethno Pharmacologically Important Plants *Catunaregum Spinosa* Thunb and *Pavonia Zeylanica* Cav for Antioxidant and Anticancer Activity’.
- Shtangeeva, I. (2010). Uptake of uranium and thorium by native and cultivated plants. *Journal of environmental radioactivity*, **101**(6), 458-463.

- Shuaib, M., Azam, N., Bahadur, S., Romman, M., Yu, Q., and Xuexiu, C. (2021). Variation and succession of microbial communities under the conditions of persistent heavy metal and their survival mechanism. *Microbial Pathogenesis*, **150**, 104713.
- Shukla, A. K., Behera, S. K., Pakhre, A., and Chaudhari, S. K. (2018). Micronutrients in soils, plants, animals and humans. *Indian Journal of Fertilisers*, **14**(3), 30-54.
- Shukla, S. R., Pai, R. S., and Shendarkar, A. D. (2006). Adsorption of Ni (II), Zn (II) and Fe (II) on modified coir fibres. *Separation and purification technology*, **47**(3), 141-147
- Singh, J., and Kalamdhad, A. S. (2011). Effects of heavy metals on soil, plants, human health and aquatic life. *International journal of Research in Chemistry and Environment*, **1**(2), 15-21
- Sonone, S. S., Jadhav, S., Sankhla, M. S., and Kumar, R. (2020). Water contamination by heavy metals and their toxic effect on aquaculture and human health through food Chain. *Letters in applied NanoBioScience*, **10**(2), 2148-2166.
- Sseruwagi, P., Legg, J. P., Maruthi, M. N., Colvin, J., Rey, M. C., and Brown, J. K. (2005). Genetic diversity of *Bemisia tabaci* (Gennadius) (Hemiptera: Aleyrodidae) populations and presence of the B biotype and a non-B biotype that can induce silverleaf symptoms in squash, in Uganda. *Annals of Applied Biology*, **147**(3), 253-265.
- Tangahu, B. V., Sheikh Abdullah, S. R., Basri, H., Idris, M., Anuar, N., and Mukhlisin, M. (2011). A review on heavy metals (As, Pb, and Hg) uptake by plants through phytoremediation. *International Journal of Chemical Engineering*, 2011.
- Tavares, F. O., Pinto, L. M., Bassetti, F. J., Vieira, M. F., Bergamasco, R., and Vieira, A. S. (2017) Environmentally friendly biosorbents (husks, pods and seeds) from *Moringa oleifera* for Pb (II) removal from contaminated water. *Environ. Technol.* **38**, 3145–3155.
- Tchounwou, P. B., Yedjou, C. G., Patlolla, A. K., and Sutton, D. J. (2012). Heavy metal toxicity and the environment. *Molecular, clinical and environmental toxicology*, 133-164.

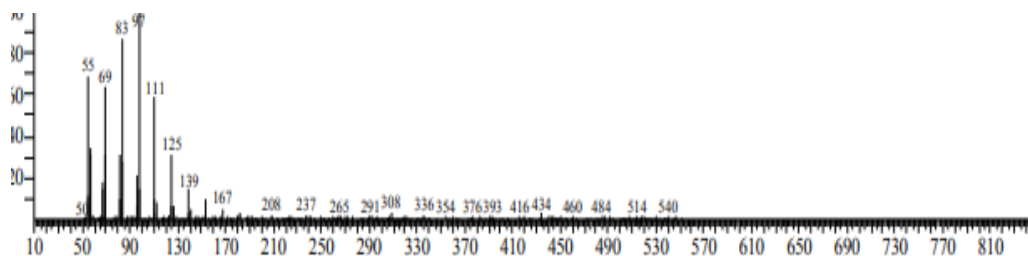
- Todde, G., Carboni, G., Marras, S., Caria, M., and Sirca, C. (2022). Industrial hemp (*Cannabis sativa* L.) for phytoremediation: Energy and environmental life cycle assessment of using contaminated biomass as an energy resource. *Sustainable Energy Technologies and Assessments*, **52**, 102081.
- Ukaogo, P. O., Ewuzie, U., and Onwuka, C. V. (2020). Environmental pollution: causes, effects, and the remedies. In *Microorganisms for sustainable environment and health* (pp. 419-429). Elsevier.
- Understanding the factors affecting the adsorption of lanthanum using different
- Valavanidis, A., and Vlachogianni, T. (2010). Metal pollution in ecosystems. Ecotoxicology studies and risk assessment in the marine environment. *Dept. of Chemistry, University of Athens University Campus Zografou, 15784*.
- Van- der E, A., Baker, A. J., Reeves, R. D., Pollard, A. J., and Schat, H. (2013). Hyperaccumulators of metal and metalloid trace elements: facts and fiction. *Plant and soil*, **362**(1), 319-334.
- Vardhan, K. H., Kumar, P. S., and Panda, R. C. (2019). A review on heavy metal pollution, toxicity and remedial measures: Current trends and future perspectives. *Journal of Molecular Liquids*, **290**, 111197.
- Vetrimurugan, E., Brindha, K., Elango, L., and Ndwandwe, O. M. (2017). Human exposure risk to heavy metals through groundwater used for drinking in an intensively irrigated river delta. *Applied Water Science*, **7**(6), 3267-3280.
- Vigneri, R., Malandrino, P., Gianì, F., Russo, M., and Vigneri, P. (2017). Heavy metals in the volcanic environment and thyroid cancer. *Molecular and cellular endocrinology*, **457**, 73-80.
- Vijayaraghavan, K., Rangabhashiyam, S., Ashokkumar, T., and Arockiaraj, J. (2016). Mono- and multi-component biosorption of lead (II), cadmium (II), copper (II) and nickel (II) ions onto coco-peat biomass. *Separation Science and Technology*, **51**(17), 2725-2733.
- wastewater using a novel biocarbon technology. *Journal of Environmental*
- Wei, S., da-Silva, J.T., and Zhou, Q. (2008). Agro-improving method of phytoextracting heavy metal contaminated soil. *Journal of Hazardous Materials*, **150**(3), 662-668.

- Wisniewska, J., Sobczak, I., and Ziolek, M. (2021). Gold based on SBA-15 supports— Promising catalysts in base-free glucose oxidation. *Chemical Engineering Journal*, **413**, 127548.
- Wong, M. H. (2003). Ecological restoration of mine degraded soils, with emphasis on metal contaminated soils. *Chemosphere*, *50*(6), 775-780.
- Wu, C., Zhang, W. J., Zeng, X., Mu, L., Xue, S. F., Tao, Z., and Yamato, T. (2010). New fluorescent sensor for antimony and transition metal cations based on rhodamine amide-arm homotrioxacalix [3] arene. *Journal of Inclusion Phenomena and Macrocyclic Chemistry*, **66**(1), 125-131.
- Xiaomei, L., Qitang, W., and Banks, M. K. (2005). Effect of simultaneous establishment of *Sedum alfredii* and *Zea mays* on heavy metal accumulation in plants. *International journal of Phytoremediation*, *7*(1), 43-53.
- Yan, A., Wang, Y., Tan, S. N., Mohd Yusof, M. L., Ghosh, S., and Chen, Z. (2020). Phytoremediation: a promising approach for revegetation of heavy metal-polluted land. *Frontiers in Plant Science*, **11**, 359.
- Younas, F., Mustafa, A., Farooqi, Z. U. R., Wang, X., Younas, S., Mohy-Ud-Din, W., and Hussain, M. M. (2021). Current and emerging adsorbent technologies for wastewater treatment: trends, limitations, and environmental implications. *Water*, **13**(2), 215.
- Zabiszak, M., Frymark, J., Nowak, M., Grajewski, J., Stachowiak, K., Kaczmarek, M. T., and Jastrzab, R. (2021). Influence of d-Electron Divalent Metal Ions in Complex Formation with L-Tartaric and L-Malic Acids. *Molecules*, **26**(17), 5290.
- Zhang, C., Korshin, G.V., Kuznetsov, A.M., and Yan, M. (2019). Experimental and quantum-chemical study of differential absorbance spectra of environmentally relevant species: A study of quercetin deprotonation and its interactions with copper (II) ions. *Science of The Total Environment*, **679**, 229-236, <https://doi.org/10.1016/j.scitotenv.2019.04.370>.
- Zhang, W., Jiang, F., and Ou, J. (2011). Global pesticide consumption and pollution: with China as a focus. *Proceedings of the international academy of ecology and environmental sciences*, **1**(2), 125.

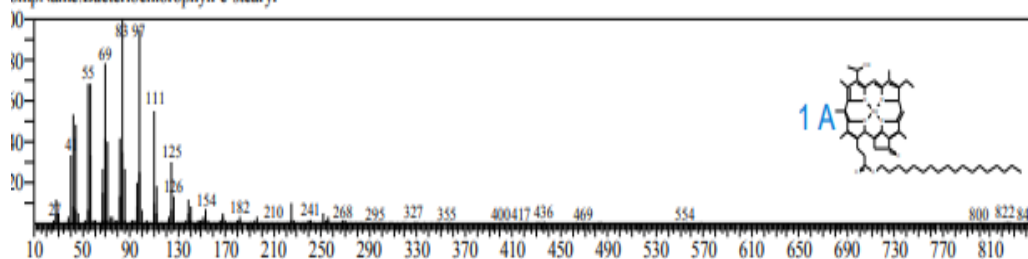
- Zhao, X., Joo, J. C., Lee, J. K., and Kim, J. Y. (2019). Mathematical estimation of heavy metal accumulations in *Helianthus annuus* L. with a sigmoid heavy metal uptake model. *Chemosphere*, **220**, 965-973.
- Zhao, X., Castka, P., & Searcy, C. (2020). Iso standards: A platform for achieving sustainable development goal 2. *Sustainability*, *12*(22), 9332.
- Zhou, H., Shi, X., Wu, W., An, X., Tian, Y., and Qiao, Y. (2020). Facile preparation of lignosulfonate/N-methylaniline composite and its application in efficient removal of Cr (VI) from aqueous solutions. *Int. J. Biol. Macromol.* **154**, 1194–1204.
- Zhou, J. D., Cui-Xue, W. J., Atsushi, F., Zu-Sheng, C., Jin-Quan, W., Akira, Y., Junji, Y., and Hai, T. (2020). ‘Anti-Allergic and Anti-Inflammatory Effects and Molecular Mechanisms of Thioredoxin on Respiratory System Diseases’. *Antioxidants & Redox Signaling***32**(11):785–801.
- Ziarati, P., Moradi, D., and Vambol, V. (2020). Bioadsorption of heavy metals from the pharmaceutical effluents, contaminated soils and water by food and agricultural waste: a short review. *Labour protection problems in Ukraine*, **36**(2), 3-7.
- Zofkova, I., Davis, M., and Blahos, J. (2017). ‘Trace Elements Have Beneficial, as Well as Detrimental Effects on Bone Homeostasis’. *Physiological Research***66**(3):391.
- Zvinowanda, C. M., Okonkwo, J. O., Shabalala, P. N., and Nana, M. A. (2009). ‘A Novel Adsorbent for Heavy Metal Remediation in Aqueous Environments’. *International Journal of Environmental Science & Technology* **6** (3):425

APPENDICES

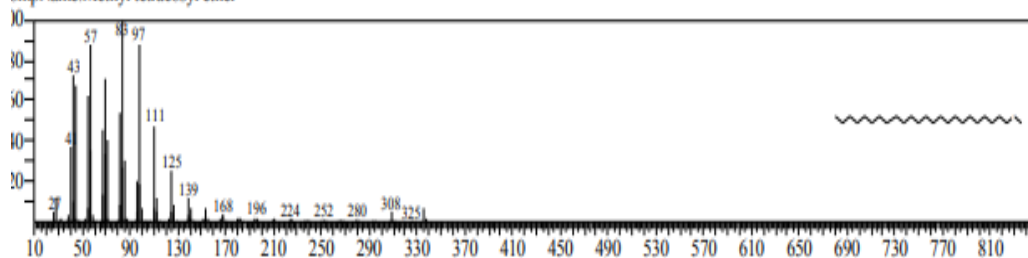
Appendix I: GC-MS Analysis of Fraction 1A



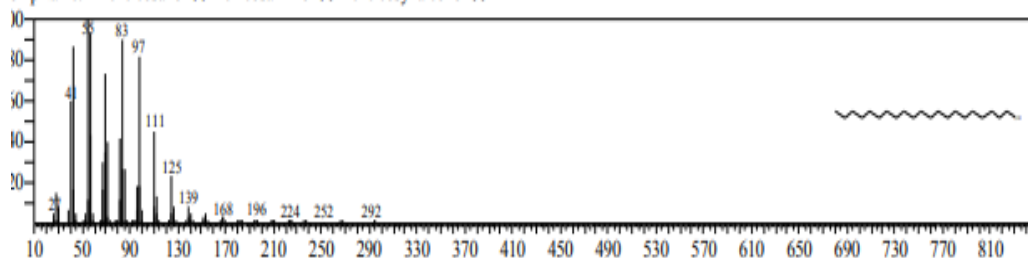
it#:1 Entry:242193 Library:NIST14.lib
 I:86 Formula:C52H72MgN4O4 CAS:0-00-0 MolWeight:840 RetIndex:0
 ompName:Bacteriochlorophyll-c-stearyl



it#:2 Entry:187890 Library:NIST14.lib
 I:86 Formula:C25H52O CAS:0-00-0 MolWeight:368 RetIndex:0
 ompName:Methyl tetracosyl ether



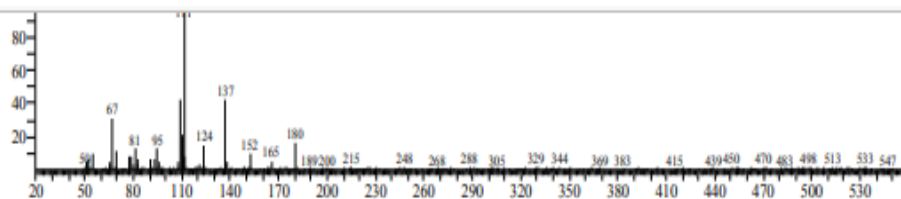
it#:3 Entry:142415 Library:NIST14.lib
 I:86 Formula:C21H44O CAS:15594-90-8 MolWeight:312 RetIndex:2351
 ompName:1-Heneicosanol \$\$ Heneicosan-1-ol \$\$ Heneicosyl alcohol \$\$



it#:4 Entry:117199 Library:NIST14.lib
 I:86 Formula:C19H40O CAS:0-00-0 MolWeight:284 RetIndex:1986
 ompName:1-Octadecanol, methyl ether



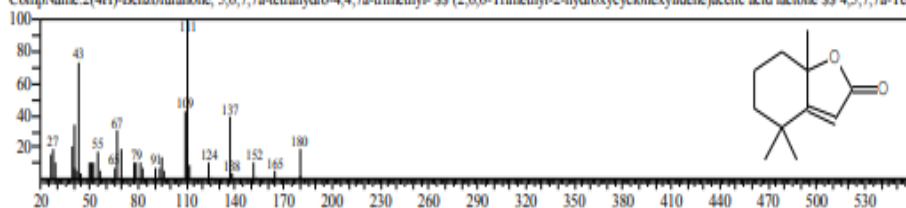
Appendix II: GC-MS Analysis of Fraction 2A



Hit#1 Entry:33222 Library:NIST14.lib

SI:90 Formula:C₁₁H₁₆O₂ CAS:15356-74-8 MolWeight:180 RetIndex:1426

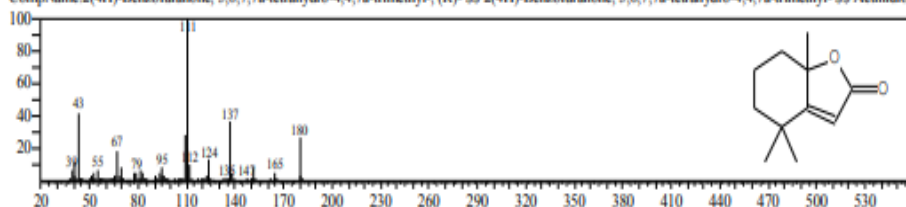
CompName:2(4H)-Benzofuranone, 5,6,7,7a-tetrahydro-4,4,7a-trimethyl- SS (2,6,6-Trimethyl-2-hydroxycyclohexylidene)acetic acid lactone SS 4,5,7,7a-Tetr



Hit#2 Entry:33223 Library:NIST14.lib

SI:89 Formula:C₁₁H₁₆O₂ CAS:17092-92-1 MolWeight:180 RetIndex:1426

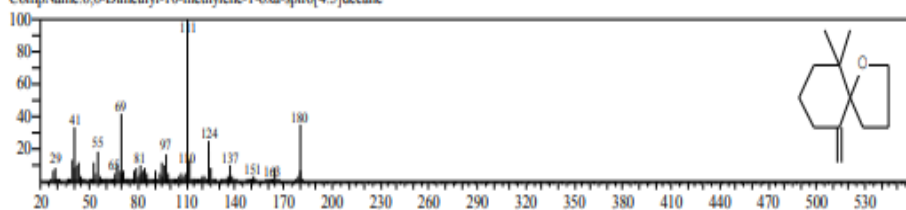
CompName:2(4H)-Benzofuranone, 5,6,7,7a-tetrahydro-4,4,7a-trimethyl-, (R)- SS 2(4H)-Benzofuranone, 5,6,7,7a-tetrahydro-4,4,7a-trimethyl- SS Actinidioli



Hit#3 Entry:33408 Library:NIST14.lib

SI:77 Formula:C₁₂H₂₀O CAS:43125-87-7 MolWeight:180 RetIndex:1304

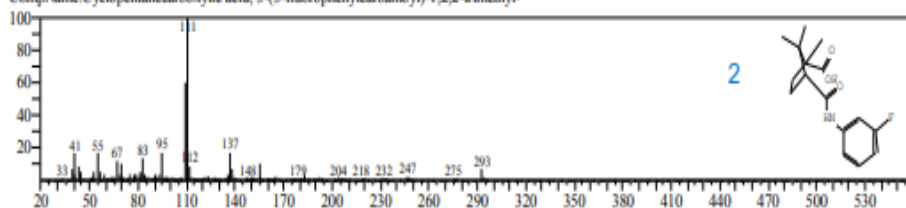
CompName:6,6-Dimethyl-10-methylene-1-oxa-spiro[4.5]decane



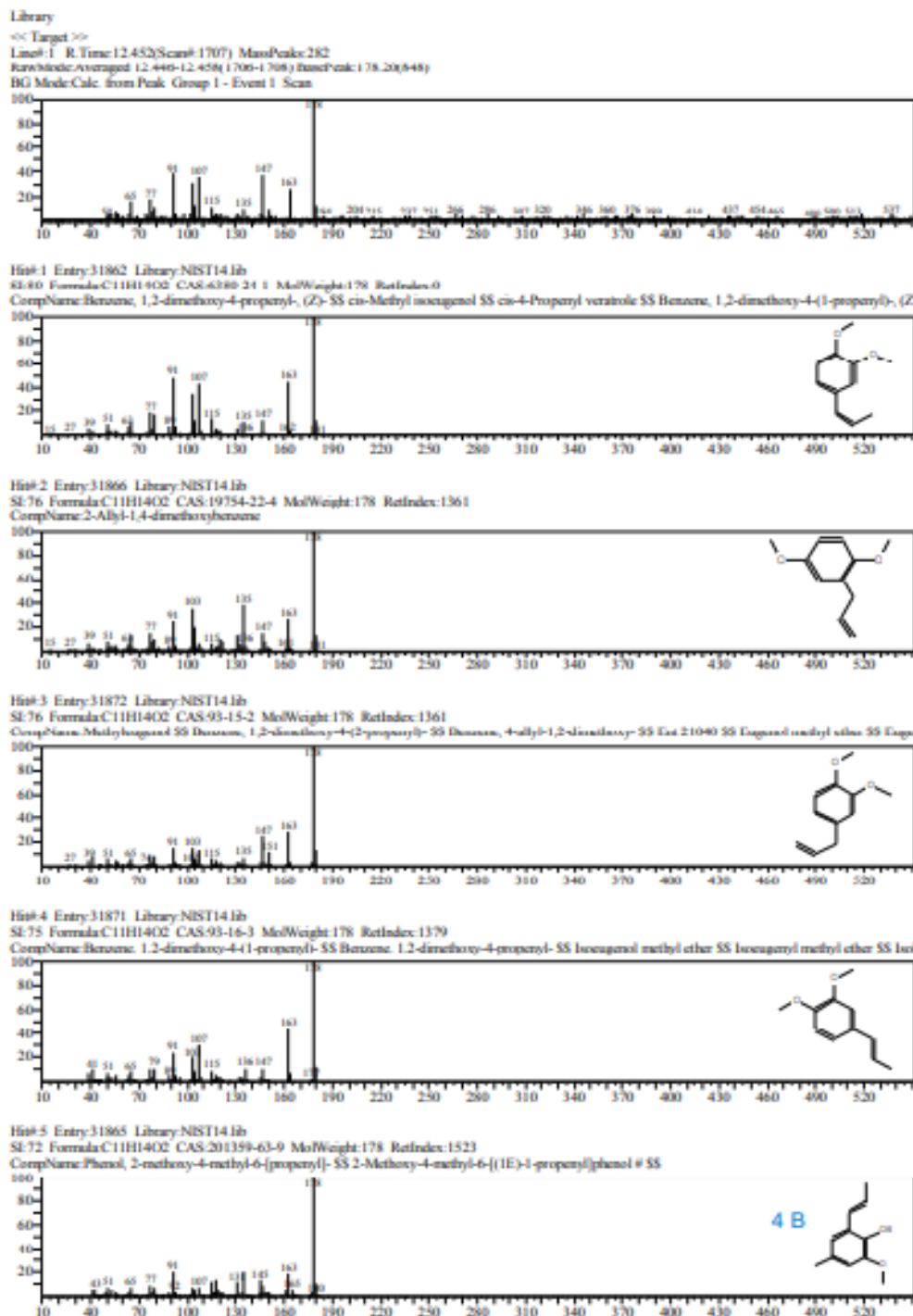
Hit#4 Entry:124708 Library:NIST14.lib

SI:76 Formula:C₁₆H₂₀FNO₃ CAS:0-00-0 MolWeight:293 RetIndex:2334

CompName:Cyclopentanecarboxylic acid, 3-(3-fluorophenylcarbamoyl)-1,2,2-trimethyl-



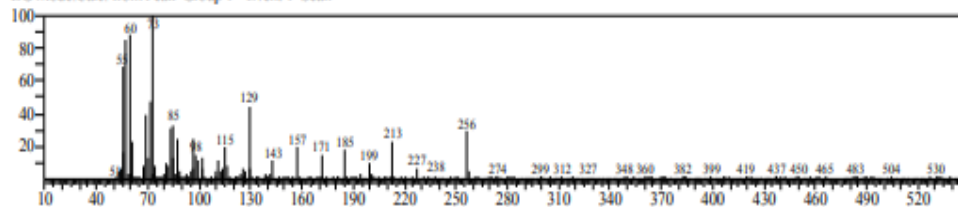
Appendix III: GC-MS Analysis of Fraction3A



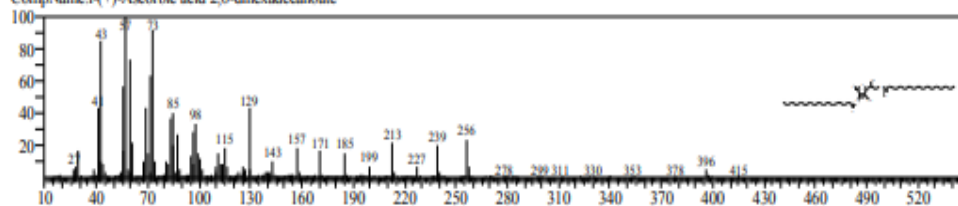
Appendix IV: GC-MS analysis of Fraction 4A

<< Target >>

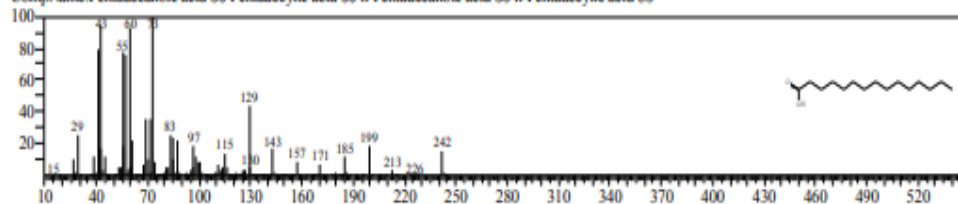
Line#:4 R.Time:19.178(Scan#:2860) MassPeaks:345
RawMode:Averaged 19.172-19.183(2859-2861) BasePeak:73.10(2218)
BG Mode:Calc. from Peak Group 1 - Event 1 Scan



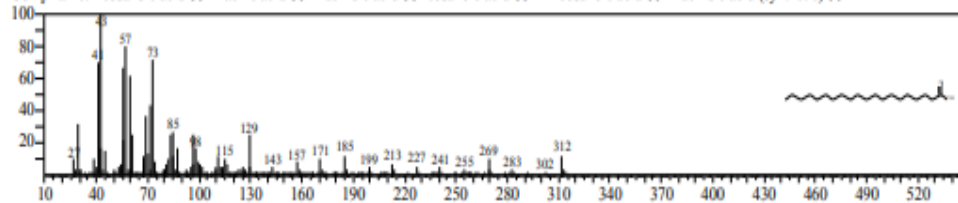
Hit#:1 Entry:240687 Library:NIST14.lib
SI:92 Formula:C38H68O8 CAS:28474-90-0 MolWeight:652 RetIndex:4765
CompName:1-(+)-Ascorbic acid 2,6-dihexadecanoate



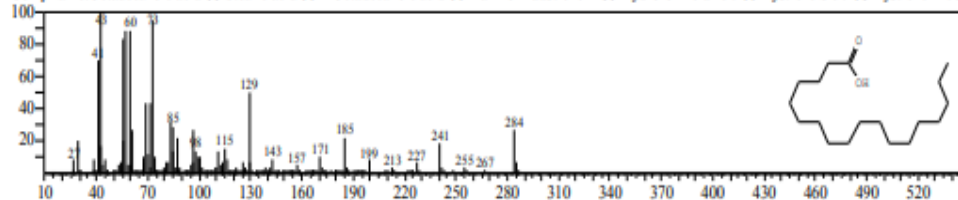
Hit#:2 Entry:80643 Library:NIST14.lib
SI:90 Formula:C15H30O2 CAS:1002-84-2 MolWeight:242 RetIndex:1869
CompName:1-Pentadecanoic acid SS Pentadecylic acid SS n-Pentadecanoic acid SS n-Pentadecylic acid SS



Hit#:3 Entry:142298 Library:NIST14.lib
SI:89 Formula:C20H40O2 CAS:506-30-9 MolWeight:312 RetIndex:2366
CompName:Eicosanoic acid SS Arachidic acid SS Arachidic acid SS Icosanoic acid SS n-Eicosanoic acid SS Arachidic acid (synthetic) SS



Hit#:4 Entry:117078 Library:NIST14.lib
SI:89 Formula:C18H36O2 CAS:57-11-4 MolWeight:284 RetIndex:2167
CompName:Octadecanoic acid SS Stearic acid SS n-Octadecanoic acid SS Humko Industrene R SS Hydrofol Acid 150 SS Hystrene S-97 SS Hystrene T-70 SS



Appendix V: Metal uptake

Time	Cu	Ni	Zn
0	0	0	0
20	50	20	18
40	64	45	32
60	65	54	40
80	75	67	50
100	78	70	55
120	86	72	60

Appendix VI: Temperature on adsorption of (a) copper (b) nickel and (c) zinc on *Pavonia urens* leaves

Ce	298k		27	300k		25	298k	300k	
Cu	Ni	Zn	Cu	Ni	Zn	Zn Ce	qe	Ce	qe
0	0	0	0	0	0	0	0	0	0
1.5	1.3	0.2	0.8	2	1	0.5	25	1	20
2.6	1.8	0.5	2	2.6	1.6	1	35	1.6	35
3.2	2.2	1	3	3.7	2	1.5	45	2	40
4	3	1.4	4	4.6	3.2	2.5	58	3.2	55
5	3.5	1.6	5	5	3.8	3	60	3.8	58
6	4.2	2	6	5.5	4.2	3.8	65	4.2	60

Appendix VII: Adsorption equilibrium isotherms of Langmuir of Cu (II), Ni (II) and Zn (II) ions on *Pavonia urens*

AT 25 Time	q _e			C _e			C _e /q _e		
	Cu	Ni	Zn	Cu	Ni	Zn	Cu	Ni	Zn
0	0	0	0						
20	53	20	19	3.7	1.7	0.2	6	7.1	0.3
40	64	45	32	3.9	3	0.3	6.4	8	0.4
60	65	54	50	4	3.6	0.6	7.3	9	0.9
80	75	67	65	4.5	4	0.8	7.7	10.8	1.1
100	78	70	68	5	4.2	0.8	8	11	1.2
120	86	72	70	5.2	4.6	0.9	8.3	12	1.6

Appendix VIII: Experimental data's adsorption equilibrium isotherms

q _e			C _e			C _e		q _e
Cu	Ni	Zn	Cu	Ni	Zn	Ce		
0	0	0	0	0	0	0	0	
53	25	10	1.5	1.3	0.8	1.5	53	
64	35	23	2.6	1.8	1.5	2.6	64	
68	40	28	2.8	2.2	1.9	2.8	68	
75	50	30	4	3	2	4	75	
78	52	45	5	3.2	2.8	5	78	
86	60	56	6.2	4.2	4	6.2	86	

Appendix IX: Adsorption equilibrium isotherms of Langmuir of Cu (II), Ni (II) and Zn (II) ions on *Pavonia urens*

q _e			C _e			C _e			C _e /q _e		
Cu	Ni	Zn	Cu	Ni	Zn	Cu	Cu	Ni	Zn		
0	0	0	0	0	0	0	0	0	0		
50	25	10	1.5	1.3	1	1.5	3	3	3.5		
64	35	23	2.6	1.8	1.3	2.6	4	3.8	4		
68	40	28	2.8	2.2	2.5	3.2	5	4.5	6.2		
75	50	30	4	3	2.8	4	6	5.5	7		
78	52	45	5	3.5	3.3	5	7	6	8		
86	60	56	6.2	4.2	4	6.2	8	7	9		


Appendix X: Adsorption equilibrium isotherms of Freundlich

C _e			Log q _e			Log C _e			Log C _e		Log q _e
Cu	Ni	Zn	Cu	Ni	Zn	Cu	Ni	Zn	Cu	Cu	
0	0	0									
1.5	1.3	1	1.7	1.4	1	0.2	0.11	0.1	0.2	1.7	
2.6	1.8	1.3	1.8	1.5	1.3	0.4	0.26	0.3	0.4	1.8	
2.8	2.2	2.5	1.85	1.6	1.4	0.45	0.34	0.4	0.5	1.85	
4	3	2.8	1.9	1.7	1.5	0.6	0.48	0.5	0.6	1.9	
5	3.5	3.3	1.95	1.72	1.55	0.7	0.54	0.55	0.7	1.95	
6.2	4.2	4	2	1.8	1.6	0.8	0.62	0.6	0.8	2	

Appendix XI: Isotherm of Temkin for biosorption of Cu (II), Ni (II) and Zn (II) ions onto *Pavonia urens* leaves

Ce			Log Ce			Log Ce		qe
Cu	Ni	Zn	Cu	Ni	Zn	Cu		
0	0	0						
1.5	1.3	1	0.18	0.1	0.05	0.2	50	
2.6	1.8	1.3	0.41	0.26	0.11	0.4	63	
2.8	2.2	2.5	0.45	0.34	0.4	0.5	68	
4	3	2.8	0.6	0.48	0.45	0.6	75	
5	3.5	3.3	0.7	0.54	0.52	0.7	78	
6.2	4.2	4	0.8	0.62	0.6	0.8	86	

Appendix XII: Similarity Report

University of Eldoret	
Certificate of Plagiarism Check for Synopsis	
Author Name	Salina Rutto PSG/SC/037/13
Course of Study	Type here...
Name of Guide	Type here...
Department	Type here...
Acceptable Maximum Limit	Type here...
Submitted By	stuttoo@uoeld.ac.ke
Paper Title	INVESTIGATION OF Pavonia urens AS A POTENTIAL BIOSORBENT IN HEAVY METAL REMOVAL THROUGH COMPLEXATION
Similarity	9%
Paper ID	987323
Submission Date	2023-09-28 11:50:25
Signature of Student	Signature of Guide
	
Head of the Department	
* This report has been generated by Drift Anti-Plagiarism Software	